AUS DEM ZENTRUM ANATOMIE
DER UNIVERSITÄT ZU KÖLN

INSTITUT I FÜR ANATOMIE

Geschäftsführender Direktor: Universitätsprofessor Dr. med. K. Addicks

EFFEKTE DER MIT DER FAMILIÄREN HYPERTROPHEN KARDIOMYOPA-
THIE ASSOZIIERTEN MUTATION cTnI$^{\Delta K184}$ AUF DIE MORPHOLOGIE UND
ULTRASTRUKTUR DES HERZENS IN MÄUSEN

Inaugural-Dissertation

zur Erlangung der Würde eines Doktor rerum medicinalium

der Hohen Medizinischen Fakultät

der Universität zu Köln

vorgelegt von
Jutta Biskup geb. Reher
aus Salzgitter

Promoviert am 03. Februar 2010

Dekan: Universitätsprofessor Dr. med. J. Klosterkötter

1. Berichterstatter: Universitätsprofessor Dr. med. K. Addicks

2. Berichterstatterin: Frau Universitätsprofessor Dr. med. G. Pfitzer

Erklärung:

Ich erkläre hiermit, dass ich die vorliegende Arbeit ohne unzulässige Hilfe Dritter und ohne Benutzung anderer als der angegebenen Hilfsmittel angefertigt habe; die aus fremden Quellen direkt oder indirekt übernommenen Gedanken sind als solche kenntlich gemacht.

Bei der Auswahl und Auswertung des Materials habe ich keine Unterstützungs-leistungen erhalten.

Weitere Personen waren an der geistigen Herstellung der vorliegenden Arbeit nicht beteiligt. Insbesondere habe ich nicht die Hilfe eines Promotionsberaters in Anspruch genommen. Dritte haben von mir weder unmittelbar noch mittelbar geldwerte Leistungen für Arbeiten erhalten, die im Zusammenhang mit dem In-halt der vorliegenden Dissertation stehen.

Die Arbeit wurde von mir bisher weder im Inland noch im Ausland in gleicher oder ähnlicher Form einer anderen Prüfungsbehörde vorgelegt und ist auch noch nicht veröffentlicht.

Köln, den 21. September 2008

Die dieser Arbeit zugrunde liegenden Experimente sind nach entsprechender Anleitung durch Herrn Prof. Dr. med. Addicks von mir selbst durchgeführt worden; die Operationen an den Versuchstieren (Perfusionen) und die Erstellung der Semidünnschnitte sind von mir mit Unterstützung der medizinisch-technischen Assistentin Frau E. Janßen durchgeführt worden.

Acknowledgements

Table of contents

Glossary

ATP	Adenosine triphosphate
BDM	2,3-butanedione monoxime
C57BL/6	Common inbred mouse strain
c_m	Midwall circumference
cSR	Corbular sarcoplasmic reticulum
cTnC	Cardiac calcium-binding troponin subunit
cTnI	Cardiac inhibitory troponin subunit
cTnI$^{\Delta K183}$	Cardiac troponin I with a deletion on amino acid position 183
cTnT	Cardiac tropomyosin-binding troponin subunit
DCM	Dilated cardiomyopathy
F-actin	Filamentous actin
FHC	Familial hypertrophic cardiomyopathy
fTnI	Fast skeletal inhibitory troponin subunit
HCM	Hypertrophic cardiomyopathy
jSR	Junctional SR
LV	Left ventricle
MRI	Magnetic resonance imaging
MyBP-C	Myosin binding protein C
nSR	Network sarcoplasmic reticulum
nTG	Non-transgenic
PCr	Phosphocreatine
PKA	Protein kinase A
PKC	Protein kinase C
RCM	Restrictive cardiomyopathy
$r_{m, o, i}$	Midwall, outer, inner radius
RV	Right ventricle
SERCA	Sarcoplasmic/endoplasmic reticulum ATPase
SR	Sarcoplasmic reticulum
sTnI	Slow skeletal inhibitory troponin subunit
TG	transgenic
Tm	Tropomyosin
Tn	Troponin complex
TNNI	Gene coding for inhibitory troponin
β-MHC	β myosin heavy chain

1 Introduction

1.1 Overview

Mutations in proteins of the contractile apparatus from heart muscle cells may lead to aberrations in their conformation and binding properties. Subtle as these changes might be, they may affect the mechanics and/or timing of contraction, relaxation and phase transition between these two. Even under thorough medical examination a heart misconstructed in this sense may remain deceivingly inconspicuous. Then suddenly and without warning, it may stop beating.

In fact, sarcomere mutation-based cardiomyopathies are the main cause for sudden cardiac death in the young and physically active (Richardson et al., 1996). In addition to such catastrophic events, the course of disease is highly variable, often leading to (mal-)adaptive heart hypertrophy and diastolic and/or systolic dysfunction, among other symptoms and secondary effects. This irregularity of phenotypic presentation follows, in part, from the multitude of different sarcomere protein mutations accounting for inherited cardiomyopathies, but also depends on factors such as environment, gender and other genetic modifiers.

Representative outpatient studies and studies in the general population are scarce and difficult to carry out, as genetic screening alone is time and money consuming in a syndrome caused by more than 450 different, mostly missense, mutations in at least 12 genes (http://cardiogenomics.med.harvard.edu/mutation-db.tcl). Therefore, several groups have generated animal models for inherited sarcomere–based cardiomyopathies and from their basic research, they try to deduce disease mechanisms and prognostic criteria.

It is most astonishing though, that over 10 years after the publication of the first transgenic mouse model for sarcomere mutation-based cardiomyopathy, there exists not a single comprehensive ultrastructural study on any given sarcomere protein mutation. This may be due to the fact that coincident with the discovery that certain idiopathic, inherited cardiomyopathies are related to sarcomere protein mutations, the use of electron microscopy declined. Thus, the older literature provides us with comprehensive and detailed descriptions of e. g., the hypertrophic phenotype but does not relate it to specific mutations, i.e. to the underlying cause of the disease.

More recent studies, on the other hand, often neglect electron microscopy, although it would offer an excellent chance to systematically re–evaluate earlier studies and to identify structural alterations that precede the clinical stage of the disease.

Especially cardiac Troponin I (cTnI) mutations are exciting to study: The majority of TnI mutations has been related to hypertrophic cardiomyopathy (HCM), but several restrictive (RCM) and one dilated (DCM) cardiomyopathy mutations have been identified as well. The assignment of some of these cTnI cardiomyopathies (and other thin filament mutations) to HCM is somewhat problematic, as patient cohorts and families investigated are usually small and one disease may progress into another. For example, heart dilation may represent the burned-out phase of HCM; and RCM and HCM may coexist within the same family. These facts make it likely, that for TnI mutations, the least common ultrastructural denominator has not been identified to date.

The TnI lysine deletion mutation ΔK183 has been associated to HCM and a transgenic mouse model (cTnI$^{\Delta K184}$) for this mutation has been generated by N. Blaudeck. It displays classic features of a sarcomere cardiomyopathy like an increased Ca^{2+}-sensitivity of force production at the myofibrillar and skinned fiber level and an enhanced systolic function but diastolic dysfunction. In the present study, the cTnI$^{\Delta K184}$ mouse model was structurally characterized from the macroscopic to the ultrastructural level.

1.2 The misconstructed pump: inherited sarcomere cardiomyopathies

Subordinated to usability in clinical practice, inherited cardiomyopathies are basically classified according to morphological features in the case of HCM and DCM, and according to functional features in the case of RCM.

Nevertheless, there has been a shift in disease perception in the past years, that is based on numerous studies investigating the primary effects of single sarcomere protein mutations. From these studies, it became increasingly clear that there is an interrelation between all sarcomere cardiomyopathies, whether they are assigned to HCM, RCM or DCM, namely an altered Ca^{2+}-sensitivity of force development and an impaired energy metabolism (summarized in Gomes & Potter, 2004; Tardiff, 2005). While HCM and RCM mutations have been shown to increase Ca^{2+}-sensitivity of force generation, in DCM, Ca^{2+}-sensitivity is slightly

decreased (Venkatraman et al., 2005; Venkatraman et al., 2003). Besides, sarcomere protein mutations associated to HCM develop dilated ventricles in 5–10 % of cases (so-called burned-out phase), mimicking DCM (Maron, 2002).

1.2.1 Hypertrophic cardiomyopathies

Familial hypertrophic cardiomyopathies (HCM) make up the majority of inherited cardiomyopathies. Their estimated prevalence is about 1 individual in 500 in the general population (Maron, 2002). HCM is inherited by an autosomal-dominant trait, but spontaneous mutations have been reported as well. Since the first assigment of a sarcomere gene defect to HCM in a french-canadian family (Geisterfer-Lowrance et al., 1990], evidence provided by a multitude of research groups established a relationship between a hypertrophic phenotype and sarcomere protein mutations (Binder et al., 2006). To date, approximately 70% of unexplained hypertrophic cardiomyopathies can be assigned to a specific sarcomere protein mutation by genetic analysis (Ahmad et al., 2005).

Three mutated genes account for most diagnosed HCM cases: β-myosin heavy chain (β-MHC, ~ 30-40%), myosin-binding protein C (MyB-C, ~ 30-40%) and cardiac troponin T (cTnT, ~ 15- 20%). Troponin I mutations cause ~3% of all HCM cases. Screening for an HCM causing disease in the general public is currently difficult due to the multitude of possible mutations in a given gene and to the infrequency of most mutations, so that a large bias in the above stated numbers is likely. To complicate matters further, disease penetrance varies greatly between different mutations, between individuals, genders and age.

Currently, diagnosis is usually carried out by 2D echocardiography and/or MRI. Hypertrophy mostly presents as an asymmetric thickening of the left (LV) or right (RV) ventricle or both (LV > 15 mm), that is non-dilated and hyperdynamic, often with chamber obliteration. Diagnosis requires the absence of other heart or systemic diseases (Richardson et al., 1996). Recently, the importance of sarcomere mutations has been upvalued, as the contemporary diagnostic criteria established by the American Heart Association and European Society of Cardiology now allow wall thicknesses within the normal range if they cosegregate with an FHC-related gene mutation (Maron et al., 2003; Maron et al., 2006).

Clearly, there is a discrepancy between practice of diagnosis and spectrum of disease presentation to date, as genetic screening often is not routinely applied

in clinical practice and besides, may not identify all of the growing number of mutations. For these reasons, it is likely that some more rare sarcomere-based cardiomyopathies that do not tend to produce hypertrophy are under-diagnosed.

Other features of HCM include systolic gradients. In a recent study by Maron et al., 70 % of HCM patients had a LV outflow gradient under resting and/or provoking conditions (persistent vs. latent/labile) (Maron et al., 2006). In presence of outflow gradients, prognosis is clearly worsened, especially if the outflow gradient is larger than 30 mm Hg (Maron et al., 2003). Outflow gradients may be produced by mitral valve anterior motion and septal contact during systole, producing a loud systolic murmur (Maron, 2002).

Morphological changes include myocyte hypertrophy and myocyte disarray, accompanied by an increase of interstitial loose connective tissue (Ho & Seidman, 2006). Abnormal ECG-patterns, LV overcontraction and diastolic dysfunction (impaired ventricular relaxation) likewise occur in HCM (Huang & Du, 2004; Mogensen et al., 2003). Common complications of the disease are arrhythmias, progressive heart failure and sudden cardiac death (Richardson et al., 1996).

1.2.2 Restrictive cardiomyopathy

Restrictive cardiomyopathy is a rare disease (estimated prevalence ≤ 5 % of all cardiomyopathies) that may result from a variety of causes and can be familial and inherited by an autosomal-dominat trait (Maron et al., 2006; reviewed in Kushwaha et al, 1997) To date, of all sarcomere proteins only cTnI mutations have been associated with RCM.

Interestingly, cardiomyopathies with variable hypertrophic and restrictive features have been reported (Feld & Caspi, 1992), and more recently, Mogensen et al. identified a family in which both HCM and RCM ocurred. Linkage analysis to sarcomere genes identified a novel cardiac Troponin I mutation as the likely disease gene. Subsequent analysis of nine unrelated RCM patients revealed that six of them had cTnI mutations (Mogensen et al., 2003). All of these mutations were located in the actomyosin ATPase inhibitory domain of cTnI.

Restrictive cardiomyopathy is classically defined as a disease based on a reduced ventricular compliance that leads to an impaired filling of either or both ventricles. Ventricular volume is normal or reduced. Cardinal symptom of restric-

tive cardiomyopathy is an increased ventricular pressure that results from the increase in myocardial stiffness. Diagnosis requires pressure measurents accomplishable with catheterization only. Therefore, this inherently rare disease may be additionally under-diagnosed.

On Doppler echocardiography, an increased early diastolic filling velocity and decreased atrial filling velocity is detectable, resulting in an increased ratio of early diastolic to atrial filling ($\geq$ 2). Deceleration time and isovolumic relaxation are decreased. Thus, diastolic dysfunction is characteristic for restrictive cardiomyopathy that may result in atrial fibrillation or diastolic heart failure (Hamlin et al., 2004). Biatrial enlargement is common, and ventricles may show a mild to moderate weight increase. Peripheral edema, ascites and/or pulmonary congestion and interstitial edema occur in advanced cases. A third heart sound originating from either of the ventricles is usual (Kushwaha et al., 1997). One of the first manifestations of the disease is exercise intolerance followed by fatigue and chest pain, but sudden cardiac death has been reported as well (Gomes & Potter, 2004).

As both diastolic dysfunction, atrial enlargement and wall thickness may be equal in RCM and HCM, the differences between the two are blurred and simultaneous classification of a cardiomyopathy as restrictive and hypertrophic is not contradictory.

1.2.3 Dilated cardiomyopathy

Dilated cardiomyopathy (DCM) is defined as left- or biventricular dilatation accompanied by decreased myocardial contractility and affects 1 in ~ 2700 persons. In 25 – 30% of cases the disease is familial. Inheritance is mainly autosomal-dominant (56% of cases), but autosomal-recessive, x-linked or matrilineal cases also occur. Several sarcomere mutations account for primary DCM, although mutations in cytoskeletal proteins predominate. In other words, DCM is at least in part, a sarcomere cardiomyopathy as well.

DCM is characterized by an increase in myocardial mass and a reduction in myocardial wall thickness. Atrial enlargement is frequent, with thrombi in the appendages. Myocytes may be non-specifically hypertrophied or degenerated, which may be accompanied by interstitial fibrosis. Prognosis is poor, as patients gradually develop heart failure that is often accompanied by atrial or ventricular

arrhythmia, leading to a five year survival rate of only 50 %. The mutations with the highest prevalence occur in the β-myosin heavy chain, myosin binding protein C, Troponin T, C and I, tropomyosin and actin.

1.2.4 At the crossroads of hypertrophy, restriction and dilatation

It is currently not well understood why some sarcomere mutations cause a hypertrophic phenotype and others fail to do so. Hypertrophy (and fibrosis) very likely are secondary effects that may be caused by different intracellular signaling pathways (summarized in Heineke & Molkentin, 2006).

The variability between different carriers of the *same* mutation that is common in sarcomere cardiomyopathies is most likely a consequence of genetic modifying factors and lifestyle. There are some mutations in sarcomere proteins, however, which are clearly linked to a hypertrophic phenotype: The β-MHC missense mutations R403Q and R435C, for example, usually cause more hypertrophy than other disease genes, hypertrophy onset takes place in the first two decades of life and the high degree of hypertrophy correlates with a poor prognosis (Watkins et al; 1992). In other mutations, the development of left ventricular hypertrophy later in life (5th to 6th decade) coincides with a better prognosis, as is the case in several MyBP-C mutations (Charron et al, 1998; Niimura et al., 1998).

Troponin mutations are different from thick filament mutations in that they often fail to produce much hypertrophy, but show an overall higher incidence of cellular disarray and sudden cardiac death (Moolman et al., 1997; Watkins et al., 1995). This has led to the assumption that cellular disarray may in fact, be causative of sudden death by disturbing the intramyocardial excitation transmission (Wolf et al., 2005). It is unknown what causes the cellular disarray.

HCM and RCM share an increase in Ca^{2+}-sensitivity of force development in the sarcomere. On one hand, the increase of Ca^{2+} sensitivity may increase cardiac contractility, producing a hypercontractile heart, as several studies suggest (Sweeney et al., 1998) and as is common in HCM and occurs in RCM. On the other hand, it may inhibit full relaxation of the sarcomere at physiologic $[Ca^{2+}]$ (see below), leading to diastolic dysfunction.

Yumoto et al. (2005), measured the Ca^{2+}-sensitivity of force development on rabbit skinned fibres in which the native cTnI had been exchanged with human

wild type or mutant cTnI. Mutations, that had been associated to RCM showed a larger mean increase of Ca^{2+}-sensitivity than those that had been linked to HCM. Nevertheless, the largest pCa at half-maximum force (pCa_{50}) in HCM mutations did not differ much from the smallest pCa_{50} in RCM mutations (5.90 ± 0.03 and 5.95 ± 0.01), suggesting a gradual transition between HCM and RCM. In this sense, sarcomere protein-based RCM could be only a special case of HCM with an extreme diastolic dysfunction.

The side-effect of hypercontractility caused by the increased Ca^{2+}-sensitivity could be an increase of ATP-consumption, making cardiac contraction energetically less efficient, possibly reducing phosphocreatine (PCr) levels (Kalsi et al., 1999; Spindler et al, 1999; Jung et al, 1998). Although the ATP-level is known to remain relatively constant in cardiomyocytes, reduced PCr level could alter the equilibrium constants of various reactions involving ATP (summarized in Ingwall & Weiss, 2004) including contraction. Decreased PCr-ATP-ratios have been related to heart failure (Wallis et al., 2005; Ashrafian et al., 2007) and they are a good predictor of mortality in patients with DCM (Neubauer et al., 1997). Interestingly in HCM, the impairment of energy metabolism has been shown to be independent of the degree of hypertrophy in three different mutations in β-MHC, MyBP-C and TnT (Crilley et al., 2003). In addition, the metabolic changes found in HCM and DCM were similar despite the different clinical phenotypes.

The question is whether there exists, at least in the Troponin I mutations that cause a Ca^{2+}- sensitization, an early (ultra-) structural correlate that characterizes these cardiomyopathies in advance to hypertrophy, fibrosis and/or dilatation.

1.3 A broken switch between heart contraction and relaxation: TnI dysfunction

Heart pumping is mediated by the constant succession of contraction and relaxation of heart muscle cells, of systole and diastole, both heart phases being equally important for proper heart function.

The functional units of contraction and relaxation are the sarcomeres (fig. 1.1 A and B). Sarcomeres are highly organized force-generating protein machines that are serially aligned in direction of the longitudinal axis of the cell, making up the greatest part of cellular mass and volume. The motor protein myosin and F-actin have the leading parts in contraction (fig. 1.1 A–C). During contraction, myosin filaments (A-band) move in between actin filaments (I-band), producing force. Each sarcomere is spanned between two intricate protein webs, the Z-discs.

A

B
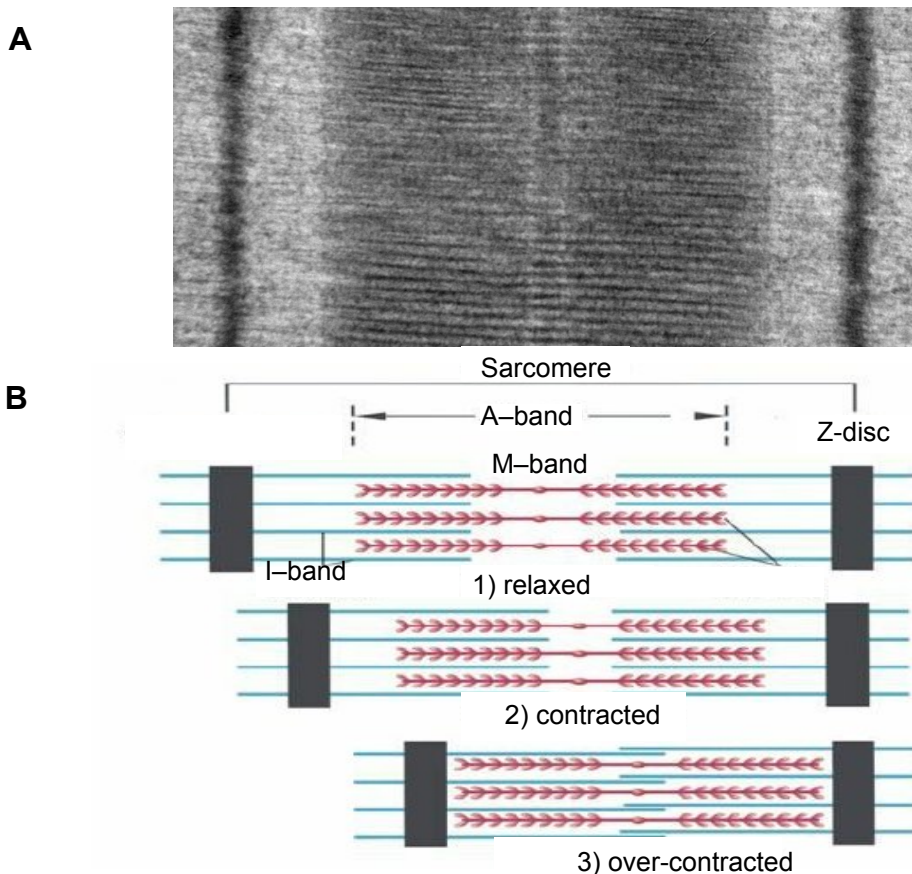
Fig.: 1.1: Structure of the sarcomere. A: electron micrograph of sarcomere. **B:** scheme of sarcomere at different contractile states. A, A–band; I, I–band; Z, Z–disc; M, M–band; C: thin and thick filament structure.

Another flexible protein web, the M-band, divides each sarcomere into two mirror-inverted half-sarcomeres. Both M-bands and Z-discs stabilize the sarcomere and more importantly, transmit the force generated by actinomyosin, as they are connected with one another by the elastic bidirectional spring titin ($\sim$ 3.3 Mda) and the costameres of the plasma membrane by the desmin cytoskeleton. Z-discs are pulled toward the M-band of each sarcomere, as the actin filaments slide past the myosin filaments. At the longitudinal ends of cardiomyocytes, the terminal actin filaments of the myofibrils are bound to desmosomes of the intercalated discs between neighboring cardiomyocytes. Thus, the $\sim$ 15 % sarcomere shortening results in cellular contraction.
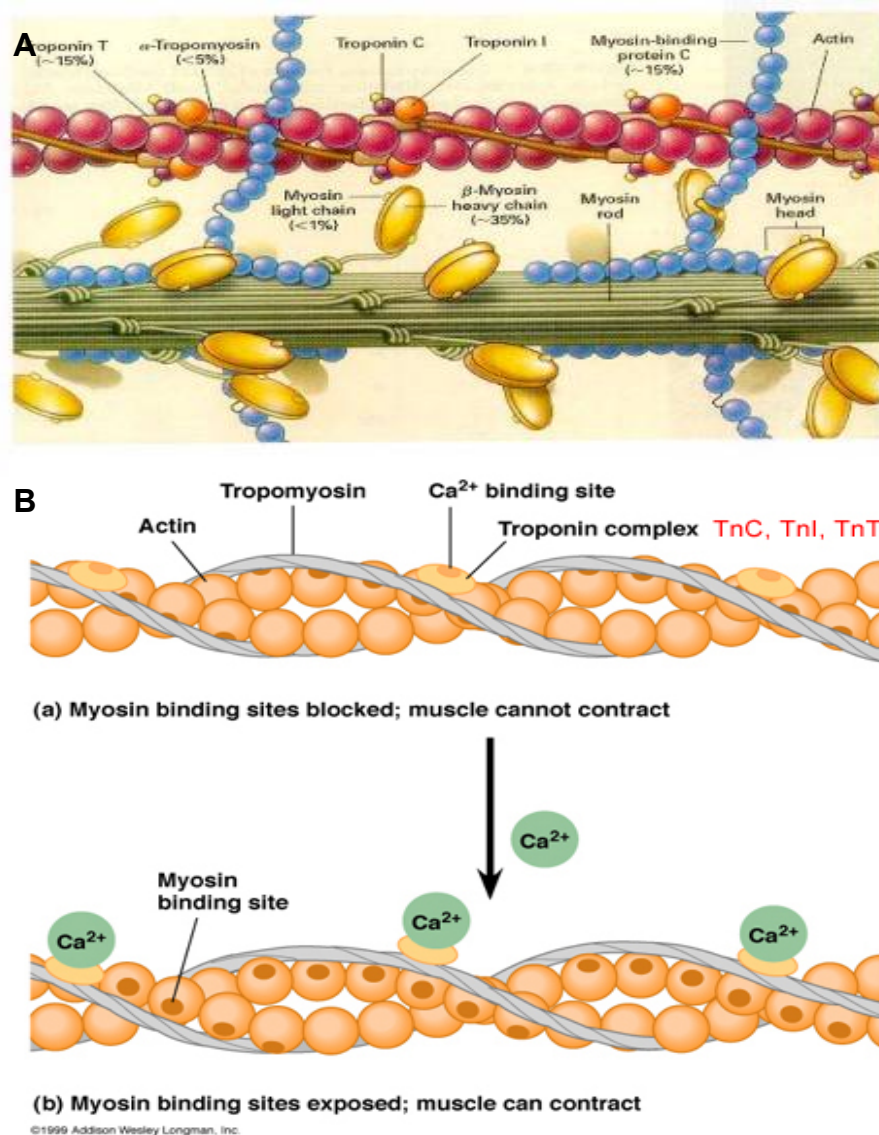
Fig. 1.2: **A:** Sarcomer, detail of the region of interaction of myosin with actin. Figure taken from http://www.edcenter.sdsu.edu/cso/paper.html
B: Changes at the thin filament upon Ca^{2+}-binding to TnC. Figure taken from http://fig.cox.miami.edu/~cmallery/150/neuro/49x29.jpg, © 1999 Addison Wesley Longman

1.3.1 Troponin function in the heart cycle

The molecular switch between diastole/relaxation and systole/contraction is the troponin complex (Tn) (see fig. 1.2). In cooperation with tropomyosin (Tm), Tn translates the intracellular oscillation of [Ca^{2+}] into an alteration in relative position and interaction of actin and myosin (Chalovich & Eisenberg, 1982; Chalovich, 2002; Mc Killop & Geeves, 1993).

Tn consists of a Ca^{2+}-binding subunit (TnC, 18 kD), a tropomyosin-binding subunit (TnT) and an inhibitory subunit (TnI) (Greaser et al., 1971;1972; 1973). CTnT (~35 kD) has the shape of a ~185–205 Å long rod or comma as indicated by electron microscopic data and is located in the groove of the actin helix (Flicker et al., 1982; Perry, 1998). The Tn complex is strategically positioned at every 7th of actin monomers that build each of the two actin filaments that are intertwined in a helical fashion. A sequence of 7 actin monomers has a periodicity of 37.8 nm which is close to the 42.9 nm distance of myosin heads. That is, the Tn switch is located at each interaction point of actin with myosin.

In diastole, the Ca^{2+}-binding sites of TnC are not occupied. The Tn complex is in a conformation where the key Troponin I inhibitory site (amino acid residues 137–148, see below) is bound to actin, preventing actomyosin ATPase activity (Tripet et al., 1997; Takeda, 2003). In this configuration of the complex, TnT positions tropomyosin (Tm) to the rim of the helical actin filament. Tm functions as a bar that sterically blocks the actomyosin interaction. Tm spans 7 actin monomers (cooperative unit), again repeating the myosin head periodicity.

Elicited by an action potential at the plasma membrane that leads to Ca^{2+}- induced Ca^{2+}-release from the sarcoplasmic reticulum (SR), the switch between diastole and systole is achieved in three steps:

1. Ca^{2+} binds to troponin C followed by a conformation change of the entire Tn complex,

2. TnT pulls Tm from the rim of the actin helix into its groove, thereby exposing its myosin binding sites (see fig. 1.2B),

3. The flexible C-terminal half of cTnI toggles from actin-Tm to cTnC and the inhibitory segment is then bound by the rigid central helix of cTnC (Vino-

gradova et al., 2005]. This facilitates the tight hydrophobic binding of actin to myosin (open state) that is necessary for crossbridge cycling and cellular contraction.

The backlash to relaxation during diastole is achieved by re-uptake of Ca^{2+} into the SR via the sarcoplasmic/endoplasmic reticulum ATPase (SERCA), release of Ca^{2+} from TnC and subsequent reversal of reactions at the thin filament, that restores the steric blockade of strong crossbridges.

It is important to bring to mind, that the contractile apparatus is constructed in a way that once actin is properly positioned, it is spontaneously pulled in between myosin filaments by the myosin lever arms ("fishing rod" model) in a series of ATP-consuming processes termed crossbridge cycles (reviewed in Maughan, 2005; Gordon et al., 20009). If Troponin did not exist, crossbridge cycling and cell contraction would continue until all ATP would be consumed, producing rigor. Excitation and contraction would be decoupled.

Interestingly, *in vitro* experiments have shown, that up to 30 % of crossbridge cycling is present even at very low $[Ca^{2+}]$ in the heart, contributing to the resting tension in the heart muscle (Maughan, 2005), which means that inhibition by Tn-Tm is incomplete. This fraction might be altered in sarcomere cardiomyopathies The Troponin Complex very likely also participates in the molecular implementation of the Frank-Starling relation (Allen & Kentish, 1985), that is based on the length-tension relation of the sarcomere. Thereby, the increase in sarcomere length increases maximum tension and myofilament Ca^{2+}-sensitivity. According to one hypothesis, interfilament spacing decreases during stretch applied on the sarcomere, making a force-generating interaction of actin and myosin more likely. The resulting increase in strong crossbridges could excert a feedback effect on the affinity of TnC for Ca^{2+} within a cooperative unit (see above), leading to the cooperativity of actin activation within this unit (Konhilas et al., 2002). Tn isoform shifts during development or disease as well as mutations of Tn subunits might alter this length-dependency of cooperative Ca^{2+}-binding to TnC (Akella et al., 1995; Chandra et al., 2001; Arteaga et al., 2000).

1.3.2 Troponin I

TnI (~ 24 kD) (see fig. 1.2) is the inhibitory subunit of the Troponin complex. TnI has three isoforms, one fast skeletal (fTnI), one slow skeletal (sTnI) and one cardiac (cTnI) that are products of three different genes: fTNI is a product of *TNNI2*, sTnI of *TNNI1* (1q32), and cTnI of *TNNI3* (19p13.2) that contains eight exons. In the fetal period, sTnI is exclusively expressed in the myocardium and after birth, becomes substituted by cTnI within 9 months (human) or 3 weeks (mouse) (Bhavsar et al., 1991; Hunkeler et al., 1991; Siedner et al, 2003). There is no evidence for re-expression of the slow skeletal isoform during pathological processes. Progressive depletion of sTnI even took place in cTnI knockout mice so that mice died ~19 days postnatally of acute heart failure (Huang et al., 1999). CTnI differs from sTnI in that it has an N-terminal extension (33 residues) containing protein kinase A (PKA) phoshorylation sites on serine residues 23 and 24 (see below). Besides, expression of sTnI in fetal myocardium correlates with a higher Ca^{2+} sensitivity compared to adult hearts (Fentzke et al., 1999;
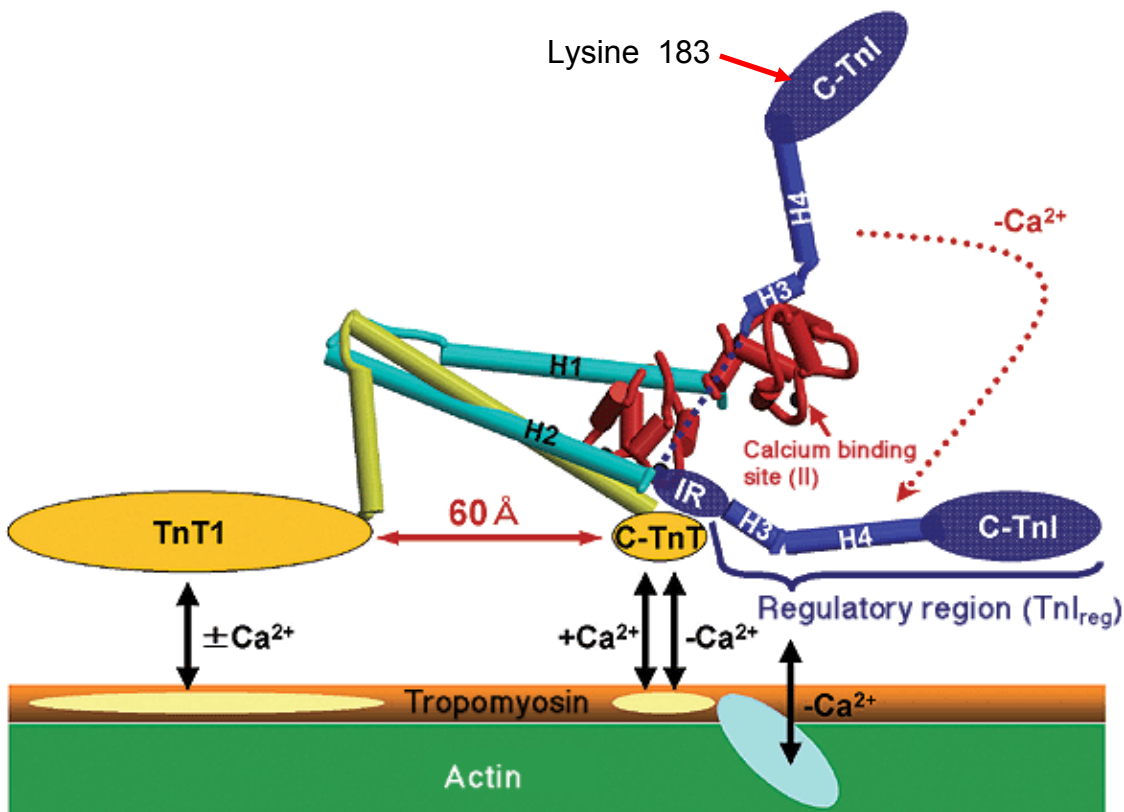
Fig.: 1.2: Troponin changes its structure and interaction with other protein upon Ca^{2+}-binding to TnC. In absence of Ca^{2+}, TnI (blue) binds to actin–Tm. When Ca^{2+} is bound to TnC, TnI releases actin–Tm and binds to TnC instead. Lysine 183 is located in The C-terminal region that binds to actin. The figure is by Takeda et al., 2003).

Westfall et al., 1997). The decrease of Ca^{2+}-sensitivity due to sTnI replacement by cTnI dominates the effects of developmentally regulated TnT and Tm replacement in mice (Metzger et al., 2003). Furthermore, cellular acidosis as induced by ischemia decreases Ca^{2+}-sensitivity of tension development in adult myocardium to a greater extend than in fetal cardiomyocytes (Westfall et al., 1997). The isoform specific, pH-sensitive domain probably lies in the C-Terminus of cTnI as indicated by experiments with cardiomyocytes expressing chimeras of sTnI and cTnI (Solaro et al, 1988; for a comprehensive review see Westfall & Metzger, 2001). Various studies have identified other functional regions of TnI in skeletal and cardiac tissue. These are summarized in (fig. 1.3). Briefly, cTnI N-terminal residues 34-71 bind to the C-terminus of cTnC, residues 80–136 account for TnT binding, residues 128–147 form the inhibitory region that binds both TnC and actin-Tm, $TnI_{147-163}$ comprise the switch or triggering region that binds to the N-terminal domain of TnC, and the C-terminal region (residues 164–210) binds actin-Tm (reviewed in Li et al., 2004; Perry, 1999].

1.3.3 Regulation of cTnI by phosphorylation

Several kinases regulate TnI function. Residues S22 and S23 in the N-terminal extension of cTnI are substrate of **protein kinase A** (PKA). Phosphorylation at these sites leads to a reduction in myofilament Ca^{2+}-sensitivity, an increase in cross bridge cycle kinetics and an increased relaxation (Solaro & Rarick, 1998; Rarick et al., 1999). Structurally, TnI phosphorylation by PKA may lead to prevention of C-terminal TnI binding to cTnC which may result in a reduced Ca^{2+}-affinity of cTnC (Solaro et al., 2003; and references therein). This response may be essential in the enhanced relaxation after β-adrenergic stimulation, which leads to an increase in cAMP generation and subsequent activation of PKA (Chandra et al, 1997; Westfall & Metzger, 2004; Solaro, 2003]. A decrease of PKA-mediated phosphorylation of TnI has been related to heart failure (Zakhary et al, 1999; Messer et al., 2007; Bilchick et al., 2007). TnI phosphorylation by **protein kinase C** (PKC) is less well understood. Three residues are subject to PKC phosphorylation, S43, S45 and Thr144 (Thr143 in

the human protein, Noland et al., 1996). There is a minimum of 12 PKC isoforms (Steinberg et al., 1995); PKCα, PKCδ and PKCε are myocardial isoforms in most species; in mice and rabbits, the PKCβ isoform is also expressed, PKCβ expression in human myocardium is elevated during heart hypertrophy and failure (Bowling et al., 1999; Takeishi et al., 1998; Wakashi et al., 1997). Other PKC isoforms may be present as well (Erdbrügger et al, 1997; Bogoyevitch et al., 1993; Schreiber et al., 2001; Rouet-Benzineb, 1996). Biochemical studies revealed that phosphorylation of TnI with either PKCα or PKCδ decreased maximum acto-S1 MgATPase activity and Ca^{2+}-sensitivity (Noland et al., 1996). PKCε phosphorylation of TnI inhibits the actin-myosin-interaction by decreasing maximum tension, Mg^{2+}-ATPase activity, Ca^{2+}-sensitivity and thin filament sliding speed in studies that used skinned cardiac mouse fibers in which endogenous TnI was replaced with mutated or PKCε-phosphorylated TnI (Burkart et al, 2003). Complicating matters further, there are different elicitors of PKC action (endothelin, arachidonic acid, adenosine, κ-opoids, diacylglycerol analogs) that may even have opposite effects on contractile function of intact myocytes and protein kinases downstream from PKC may modulate its effects (summarized in Metzger and Westfall, 2004).

1.3.4 Troponin I cardiomyopathies

All of the 27 HCM-and of the 6 RCM-related mutations are located in exons 7 and 8 of cTNI, comprising the inhibitory (actin binding) and C-terminal TnC binding domains and the switch region (second TnC binding region) (Gomes & Potter, 2004) except for R21C which is directly adjacent to one of the PKA phosphorylation sites at is encoded by exon 3. By contrast, the only DCM-mutation identified so far is located in exon 1 (Murphy et al., 2004). For an overview of cTnI mutations please refer to fig. 1.3.

Morphological features have not been extensively investigated. Hypertrophy may be typical, apical or absent, but caution is necessary as most studies were carried out with only very few patients. Atrial enlargement and ventricular obstruction have been reported in some cases.

CTnI HCM and RCM mutations have been shown to cause an increase in Ca^{2+}-sensitivity of force development (see above). To date, three different cTnI mutations associated to sarcomere cardiomyopathy in humans have been studied in mouse models: Two are associated to HCM: $cTnI^{R145G}$ (James et al., 2000) is located in the inhibitory region and $cTnI^{G203S}$ (Tsoutsman et al., 2006) in the extreme C-terminus. $cTnI^{R192H}$ has been related to RCM and is located in the C-terminus as well (Zhang et al., 2006).

Both HCM mouse models ($cTnI^{R146G}$ and $cTnI^{G203S}$) present morphological myocyte disarray, interstitial fibrosis and elevation of some RNA markers of hypertrophy. Myocyte hypertrophy and thickening of the LV wall associated with a reduction in LV end-diastolic dimension, however, is prominent only in $cTnI^{G203S}$ mice. By contrast, ventricular weight is even slightly *decreased* in $cTnI^{R146G}$ mice, and atrial mass is increased. In a corresponding $cTnI^{R146G}$ rabbit model, hypertrophy is only mild (Sanbe et al., 2005). Skinned fibers isolated from $cTnI^{R146G}$ mice show an increased Ca^{2+} sensitivity (as in *in vitro* studies with the recombinant human protein) but depressed maximum tension; at the whole organ level, contractile function is enhanced but relaxation is impaired. The RCM mouse model ($cTnI^{R193H}$) displays features that seem to be conform with RCM. LV wall thickness is normal and cardiac relaxation seems to be impaired, as shown by a decreased LV- and an increased atrial end diastolic dimension. Besides, the ejection fraction was significantly decreased in $cTnI^{R193H}$ mice at the age of nine months.

```
           A2V                        R21C
mcTnI    1  MADESSDAAGEPQPAPAPVRRRSSANYRAYATEPHAKKKSKISASRKLQLKTLMLQIAKQ
hcTnI    1  MADGSSDAAREPRPAPAPIRRRS-SNYRAYATEPHAKKKSKISASRKLQLKTLLLQIAKQ
mssTnI   1  ---------------------------MPEVERKSKITASRKLMLKSLMLAKAKE
hssTnI   1  ---------------------------MPEVERKPKITASRKLLLKSLMLAKAKE
```

cardiac specific N-terminus

```
mcTnI   61  EMEREAEERRGEKGRVLRTRCQPLELDGLGFEELQDLCRQLHARVDKVDEERYDVEAKVT
hcTnI   60  ELEREAEERRGEKGRALSTRCQPLELTGLGFAELQDLCRQLHARVDKVDEERYDIEAKVT
mssTnI  29  CWEQEHEEREAEKVRYLSERIPTLQTRGLSLSALQDLCRELHAKVEVVDEERYDIEAKCL
hssTnI  29  CWEQEHEEREAEKVRYLAERIPTLQTRGLSLSALQDLCRELHAKVEVVDEERYDIEAKCL
```

L144P L144Q   R162Q   K178del
R141G R145G/Q/W   A157V R162P S166F A171T K178E

```
mcTnI  121  KNITEIADLTQKIYDLRGKFKRPTLRRVRISADAMMQALLGTRAKESLDLRAHLKQVKKE
hcTnI  120  KNITEIADLTQKIFDLRGKFKRPTLRRVRISADAMMQALLGARAKESLDLRAHLKQVKKE
mssTnI  89  HNTREIKDLKLKVLDLRGKFKRPPLRRVRVSADAMLRALLGSKHKVSMDLRANLKSVKKE
hssTnI  89  HNTREIKDLKLKVMDLRGKFKRPPLRRVRVSADAMLRALLGSRHKVSMDLRANLKSVKKE
```
                                                  O OO   O O

K183del   I195M L198V/P   R204C
K183E   R204H
        R186Q   D196N S199G/N

```
mcTnI  181  DIEKEN-REVGDWRKNIDALSGMEGRKKKFEG-------
hcTnI  180  DTEKEN-REVGDWRKNIDALSGMEGRKKKFES-------
mssTnI 149  DTEKERPVEVGDWRKNVEAMSGMEGRKKMFDAAKSPTSQ
hssTnI 149  DTEKERPVEVGDWRKNVEAMSGMEGRKKMFDAAKSPTSQ           AS188
```
        O   O   O   O   O OOO
        +   +   - +   -   - + +
        D190H   E202G K206Q
        R192H   G203R
                               G203S

DCM HCM RCM Polymorphism, uncertain effect

▨ (first) TnC binding region (C-terminus of TnC): cTnI E34-E71 (sk 1-E40)
▥ TnT binding region: cTnI 80-136 (sk 50-106)

☐inhibitory region (actin binding): hcG137-R146 (sk105-114 Murakami et al.) (sk 96-115; Monica et al.)
▨switch region (second TnC binding region): (sk116-131; Murakami et al.) (sk 115-131; Monica et al.)
══ "second actin-tropomypsin-binding site": (sk140-148)
☐ mobile domain, C-Terminus (sk Lys131-Ser182)
── α-helix 4 (sk Val132-Leu140)
mini globular subdomain (Val143-Lys167)

o residues, that interact with actin (putative salt-bridges)

Fig. 1.3: Functional domains and mutations of cTnI. Figure by N. Blaudeck.

1.3.5 When lysine 183 is missing

The cTnI$^{\Delta K183}$ mutation has been related to hypertrophic cardiomyopathy in humans (Kimura *et al.*, 1997, Kokado *et al.*, 2000; Shimizu et al., 2002a, 2002b). The mutation has a high disease penetrance and is associated with sudden death at any age. Typical HCM has been reported of in only one patient, but three of 36 individuals showed an apical hypertrophy (Kimura *et al.*, 1997). In another study by Kokado *et al.* (2000), hypertrophy was regionally limited to different parts of the intraventricular septum in some patients, and in others, ventricles were not hypertrophied at all. Light and electron microscopic data are not available for the human cTnI$^{\Delta K183}$ mutation. In addition to the sometimes altered heart appearance, various patients aged >40 years had LV systolic dysfunction, and some displayed features of DCM (Shimizu et al 2002a). The diverse clinical expression of the cTnI$^{\Delta K183}$ mutation suggests, that the disease phenotype is influenced by additional genetic and environmental factors.

The transgenic cTnI$^{\Delta K184}$ mouse model for sarcomere cardiomyopathy corresponds to a deletion of lysine 183 in the human sequence. In mice from the lines with the highest expression levels of the transgene, ~ 98 % (line B) and 92 % (line E) of the native cTnI was replaced by the transgene (N. Blaudeck, personal communication). Heart chambers from transgenic mice (12 and 24 weeks old) had significantly reduced enddiastolic and even more reduced endsystolic volumes as determined with magnetic resonance imaging (MRI), resulting in an increased ejection fraction. In conclusion, systolic function of TnI$^{\Delta K184}$ mice was enhanced, while cardiac output and diastolic filling capacity were reduced. In skinned fibers from papillary muscle, the Ca^{2+} sensitivity of half-maximal force development was very high (ΔpCa_{50} = 0.225). In myofibrils from TnI$^{\Delta K184}$ mice, the maximal active force at saturating [Ca^{2+}] was significantly higher (+ 40 %). Passive tension was increased as well. This tension could be completely abrogated by administration of 2,3-butanedione monoxime, which points to an incomplete turning off of strong actin-myosin interaction in myofibrils containing cTnI$^{\Delta K184}$. Relaxation, by contrast, was delayed and proceeded slower in myofibrils from TG mice. However, it is questionable if these findings are directly causative for and sufficient to explain the observed *in vivo* aberrations. As in humans, the morphology of the TnI$^{\Delta K184}$ mice, however, was unknown.

1.4 Aim of the study

Cardiac Troponin I mutations may represent a missing link between HCM and RCM and their investigation especially, may eventually lead to a unifying theory of sarcomere cardiomyopathies beyond hypertrophy, restrictive ventricular filling pattern or dilatation. Morphological features of cTnI mutations have not been thoroughly investigated, especially in the preclinical stages of the disease, that nevertheless, are of special interest, as sudden cardiac death is a common feature of sarcomere cardiomyopathies even in the absence of hypertrophy or dilatation.

The aim of the study presented here is

- to establish the morphological phenotype of the $TnI^{\Delta K184}$ mouse model from the whole heart to the ultrastructural level

- to compare the structural effects of the $TnI^{\Delta K184}$ mutation between ventricles and atria.

2 Material and Methods

2.1 Mice

All animal procedures were conducted in accordance with the Institutional Animal Care and Use Committee. For the present study, male $TnI^{\Delta K184}$ mice (expressing murine cardiac TnI containing the $\Delta K184$ mutation) 12 weeks of age and their nTG littermates were provided by the Institute of Vegetative Physiology, Cologne. For our investigations, we exclusively used mice from lines B and E, which have a high expression level of $cTnI^{\Delta K184}$. The $TnI^{\Delta K184}$ mouse model has a C57BL/6 genetic background.

2.2 Body and heart weight determinations

Body weights were determined directly before perfusion fixation (living, anaesthetized animals). By contrast, total hearts, left and right ventricles, and atria were weighed after perfusion and postfixation with glutaraldehyde/formaline/picric acid (see below). Hearts were dissected from the large blood vessels, and separated into left and right ventricles and atria. These three weights were summed up to the total heart weight.

2.3 Magnetic resonance image analysis

Magnetic resonance images from hearts in end-systole and end-diastole from $cTnI^{\Delta K184}$ mice and their nTG littermates (24 weeks of age) were kindly provided by N. Blaudeck, Institute of Vegetative Physiology, Cologne. They had been generated at the Institut für Herz- und Kreislaufphysiologie, University of Düsseldorf, with a vertical Bruker DRX 9.4 Widebore NMR spectrometer. Mice had been anaesthetized with isoflurane and held at body temperature.

For comparability, the first three optical slices from the heart base were used. For the free left ventricular wall, the right ventricular wall and the septum three independent measurements were conducted and averaged. In addition, each the smallest and largest inner and outer caliper diameter of the left ventricles were determined and averaged to even out cavity irregularities. From the inner and outer diameter, circumferences were calculated which then were averaged to the midwall circumference.

2.4 Perfusion fixation

1 M cacodylate buffer stock, pH 7.35

Sodium cacodylate trihydrate	214.03 g
Aqua dest.	~ 800 ml
25% HCl	adjust to pH 7.35
Aqua dest.	to 1000 ml

1 M phosphate buffered saline (PBS) stock, pH 7.4

Na_2HPO_4 x 2 H_2O	14.4 g
NaH_2PO_4 x H_2O	2.6 g
NaCl	8.766 g

Ca^{2+}-free Krebs-Henseleit solution

	mM	g/l
NaCl	118	6.9
KCl	4,7	0.35
$NaHCO_3$	25	2.10
KH_2PO_4	1,2	0.16
$MgSO_4$	1,2	0.141
$CaCl_2$	—	—
Glucose		2
Procaine hydrochloride		5

Both glucose and procaine hydrochloride were added at day of experiment
Directly before the experiment, the pH solution of the solution was adjusted
to 7.35 by bubbling it with carbogen (95% (v/v) O_2; 5% (v/v) CO_2).

4% paraformaldehyde fixative (per liter)

Paraformaldehyde (PFA)   40 g

Aqua dest   ~ 500 ml

- PFA and Aqua dest were stirred and heated to max. 60°C,

then ~ 8 drops of 1 N NaOH were added

- the solution was cooled to 4°C in the refrigerator, then filtrated

- salts were added as required for 1 l PBS

- pH was adjusted to 7.4

- Aqua dest was filled up to 1 l

Glutaraldehyde fixative (per liter)

8 % aqueous paraformaldehyde solution	500 ml
25% glutardialdehyde (Merck, Darmstadt)	80 ml
1 M cacodylate buffer	70 ml
	pH was adjusted to 7.35
Aqua dest.	to 1000 ml

Heart arrest at well-defined stage of the cardiac cycle and fixation

As the heart is continuously changing its shape and size, it is necessary for any histological analysis to arrest the heart at a well-defined stage of the cardiac cycle. To this end, mice were pre-anesthetized with CO_2 followed by an intraperitoneal injection of 100 mg kg^{-1} ketamine and 5 mg kg^{-1} xylazine. To prevent blood coagulation, 5 I. E. /g heparin (Liquemin N 25000, Roche, Grenzach-Wyhlen) was added to the injection. The deeply anesthetized animals were transcardially perfused with a Ca^{2+}-free Krebs Henseleit solution (containing 5 g l^{-1} procainhydrochloride, adjusted to pH 7.35 by oxygenation with 95% O_2 and 5% CO_2) for 45 sec at a constant pressure of 80 mm Hg corresponding to the mean arterial pressure in mice.

Perfusion fixation

Then, for electron microscopy mice were perfused with fixative containing 2% paraformaldehyde, 2% glutardialdehyde and 0.07 % picric acid in 0.07 M caco-dylate buffer, pH 7.35 for 15 min. For light microscopy, mice were either fixated with the same fixative or alternatively, with 4% paraformaldehyde in 0.1 M pho-spate buffered saline (PBS), pH 7.4.

After the perfusion fixation, hearts were excised and postfixated over night in the same fixative as had been used during perfusion.

2.5 Light microscopy

2.5.1 Paraffin embedding and sectioning

For paraffin embedding whole hearts or heart heart halves were pro-ceeded as follows:

Wash

-   2 h wash under running tab water

Dehydration

-   20 min in each 30 %, 50 %, 70 % and 90 % ethanol (v/v) with smooth agitation on a shaker
-   2 x 1 h 96 % (v/v) ethanol
-   1 h pure isopropanol
-   a minimum of 2 h chloroform (or until probes sink to the bottom of the beaker)
-   2 x 15 min xylene

Embedding

-   3 x 2 h Paraplast plus (Fa. Covidien Kendall, Mansfield, MA, USA)
-   over night Paraplast plus

Casting in metal or silicone molds

-   Rapid cooling on cold metal plate

Paraffin blocks were sectioned (2-5 µm section thickness) on a rotation microtome (HM 355, Microm Laborgeräte GmbH, Walldorf) and were stretched in a warm paraffin stretch bath (TFB 45, Medite Medizintechnik, Burgdorf) before they were mounted on microscope slides.

2.5.2 Vibratome sectioning

For vibratome sections, a vibratome VT 1000 E (Leica, Wetzlar) was used. Glutaraldehyde/paraformaldehyde fixated heart ventricles were cross-sectioned with a razor blade directly beneath the valvular plane and glued on the probe holder with superglue, so that the heart longitudinal axis was oriented perpendicular to the section plane. Cross sections of either 50 µm or 100 µm thickness were prepared, beginning with the heart tip. 0.1 M PBS, pH 7.4 was used as probe/storage buffer. Every 10th of the 50 µm sections and every or 5th of the 100 µm sectons were collected and mounted on microscope slides. Total section number was documented for each heart.

2.6 Histological Staining procedures

2.6.1 Hematoxylin-eosin dye

Mayers hematoxylin solution:

Solve sequentially in 1000 ml Aqua dest:

Hematoxylin	1 g
$NaJO_3$ oder KJO_3	0.15 g
Chloralhydrat	50 g
Citric acid	1 g

Eosin

Eosin	1 g
96% alcohol	100 ml

Procedure:

- Paraffin sections were de-waxed in xylene and re-hydrated in a descending sequence of alcohol washes (96%, 90%, 70%, Aqua dest.), followed by a
- 10 min incubation in Meyer's Hematoxylin solution,
- brief rinse in Aqua dest
- 10 min blueing under running tab water
- 1 min incubation in eosin solution
- brief washes in Aqua dest,
- Then, sections were dehydrated in an ascending sequence of alcohol washes and
- Cleared in xylene and mounted in Entellan (Merck, Darmstadt)

2.6.2 Hematoxylin nuclear staining (Weigert, 1904)

Hematoxylin stock solution

Hematoxylin	1 g
96% undenatured alcohol	10 ml

requires maturation for several months

Solution A

Hematoxylin stock solution	10 ml
96% alcohol	90 ml

Solution B

$FeCl_3$	4 g
Aqua dest.	95 ml
25% hydrochloric acid	1 ml

Working solution

2 parts solution A + 1 part solution B

stable for 1 week

Procedure:

- sections were stained for 5 - 10 min (or as required), then
- rinsed with Aqua dest.
- Differenciated with 1% HCl in ethanol as required
- Rinsed with Aqua dest.
- Blued in running tab water for 10 min and
- Used as desired

2.6.3 Picrosirius red dye

This dye was used for selective staining of collagenous and reticular fibers.

Solution A

Sirius red F3B (C.I. 35782) (=Direct Red 80", Catalog # 36-554-8, Sigma-Aldrich, Munich)	0.5 g
Saturated aqueous solution of picric acid	500 ml
Solid picric acid	a small amount (to ensure saturation)

keeps for at least 3 years and can be used many times

Solution B

Acetic acid (glacial)	5 ml
Tap or distilled water	1 l

Procedure:

Paraffin sections were de-waxing and rehydrated as described above, then the nuclei were stained with hematoxylin after Weigert, followed by

- 10 min blueing in tab water

- a minimum of 1 h staining in solution A

- 2 x brief washes in two changes of solution B

- removal of most of the water from the slides by vigorous shaking or (for a few slides only) blotting with damp filter paper.

- Dehydration in three changes of 100% ethanol.

- Clearing in xylene and mounting in Entellan (Merck, Darmstadt)

- Alternatively, dyhydration was omitted and sections were directly mounted in liquified (37°C warm) Kaiser's glycerol gelatine (Merck, Darmstadt).

2.7 Tissue preparation for electron microscopy

2.7.1 En bloc staining and Epon embedding for electron microscopy

4 % OsO4 stock solution

OsO4	1 g
Aqua dest	25 ml
	storage at 4°C

For working solution: dilution with 1.14 M cacodylate buffer, pH 7.35

Maleate buffer

0.2 M maleate stock solution	**For 100 ml**
Maleic acid (MW 116.07)	2.32 g
1 N NaOH	20 ml
Aqua dest.	to 100 ml

0.05 M maleate rinse buffer	**For 100 ml**
0.2 M maleate stock	25 ml
0.2 N NaOH	~ 4.2 (to pH 5.15)
Aqua dest.	To 100 ml

0.05 M maleate buffer for uranyl acetate solution)	**For 100 ml**
0.2 M maleate stock	25 ml
0.2 N NaOH	To **pH 6.0**
Aqua dest.	to 100 ml

1.0% uranyl acetate (w/v)	
Uranyl acetate	1 g
0.05 M maleate buffer (pH 6.0)	to 100 ml
	storage at 4°C in the dark

Epon	For 100 g
Epicot	46.20 g
Dodecanyl succinic acid anhyride (DDSA)	28.50 g
Methylnodicanhydride (MNA)	23.10 g
2,4,6-triphenole (DMP-30)	1.50 g

Procedure:

Fixated specimen were washed in 0.07 M cacodylate buffer and cut into 1 mm^3 blocks. Tissue blocks were washed three times with 0.07 M cacodylate buffer. Then samples were post-fixed and *en bloc* contrasted in 2% osmiumtetroxide in 0.07 M cacodylate buffer for 3 h, 2 x washed twice with cacodylate buffer and once with maleate wash buffer, followed by *en bloc* staining with maleate buffered 1% uranyl acetate over night.

After a three time wash with maleate wash buffer, tissue blocks were dehydrated at 4°C as follows:

- 5 min of each 30%, 50%, 70%, 90% ethanol

- 3 x 20 min 96% ethanol

- 15 min ethanol-1,2-epoxypropane in a 1:1 ratio

- 15 min pure 1,2-epoxypropane and embedded in Epon: Epon:100% ethanol in a ratio of 1:1 for 45 min

and embedded in epon (all steps at 4°C):

- 45 min Epon-1,2-epoxypropane in a ratio of 3:1

- 45 min Epon-1,2-epoxypropane in a ratio of 3:1

- over night pure Epon (all at 4°C) (new vials).

The next day, specimen were embedded in fresh Epon and cured for 12 h at 45°C and then for three days at 60°C.

2.7.2 Semithin sectioning and dyeing with methylene blue/azure II

Methylen blue-azure

Solution A

1% methylene blue in Aqua dest

Solution B

1% azure II

1 % borax in Aqua dest.

Working solution

1 part solution A and 1 part solution B

For light microscopic observations, the Epon embedded specimen were trimmed with a rotation trimmer (Reichert, Wolfratshausen). Semithin sections (500 µm tickness) were prepared on an ultramicrotome (Leica, Wetzlar, Germany), heat-fixated on a household heating plate and stained with methylene blue + azure II. Excesseive stain was washed from the microscope slide. Slides were dried on the heating plate, and mounted with Entellan®.

2.4.3 Ultrathin sectioning and section contrasting

uranyl acetate solution

1 % uranyl acetate in Aqua bidest.

filtered through a syringe filter directly before use

stored at 4°C in the dark

Lead citrate stock solutions

Solution A

1.3 M Na^+-citrate   1.99 g Na^+-citrate in 5 ml Aqua bidest.

Solution B

1.0 M Pb-nitrate   1.66 g Pb-nitrate in 5 ml Aqua bidest.

Solution C

1 M NaOH   4 g in 100 ml Aqua bidest.

Working lead solution

Aqua dest.	800 µl
Solution A	155 µl
Solution B	100 µl
Solution C	200 µl

Air-tight storage in a syringe at 4°C

Ultrathin sections were prepared on the same microtome as the semithin sections, mounted on copper grids (mesh 150), contrasted with uranyl acetate for 17 min at 37°C in the dark, washed and contrasted with lead citrate for 6 min in an atmosphere saturated with NaOH at room temperature.

Specimen were examined on a 902A transmission electron microscope (Zeiss, Oberkochem, Germany) at 80 V.

2.8 Sampling procedure for morphometry

2.8.1 Random systematic sampling

To assure comparability of morphometric analyses between hearts nTG and TG mice (n=4, respectively) random systematic sampling procedure was pivotal. As heart tissue is highly anisotropic, which means that between given perspectives, tissue appearance differs greatly. For example, heart cells are much longer than they are wide and thick, and cardiomyocyte thickness varies considerably across the ventricular walls.

Random systematic sampling means that the spatial distance of the samples is defined in advance to the sampling procedure, and that it is uniform between all samples. Random systematic sampling is more potent than simple randomization in assuring a uniform coverage of the entire sampling area. Thus, local differences are compensated by this sampling method. We conducted random systematic sampling on every level of investigation to assure an unbiased estimation of geometric parameters of the heart muscle tissue:

a) Tissue sampling: ventricles were cut right beneath the valvular plane. Right ventricles were separated from the left ventricles, and the left ventricular free wall from the ventricle septum. The ventricles were cut into 1 mm^3 blocks with the help of two razor blades moved against each other without applying pressure to the tissue. From the left ventricles, every other sample was used. As the RV ventricle wall from mice is small, every sample was used. Samples were processed as described in section 2.4.

b) Microphotography: microphotographs were taken systematically, beginning at the upper left corner of the ventricle, leaving out every other field of view, and then meandering through the sample.

c) Morphometric analysis: For the morphometric analysis, we applied the point counting method (see below)

2.8.2 Isotropic sampling

Anisotropy of heart tissue was compensated by isotropic sampling: during embedding in epon, 2-3 samples per block were oriented at random, so that section planes were laid through every possible angle relative to tissue position. During photography, the camera orientation was turned clockwise for 45° between successive shots, respectively. Thus, morphometrically determined mean tissue parameters behave as if the tissue itself was isotropic, and it was not neccessary to use a cyclic arc or a similar grid. For morphometric measurements, a linear grid was used instead.

2.9 Light and electron microscopic morphometry

For light microscopic morphometry, microphotographs from semithin sections were taken with a 40 x objective and a digital camera (Leica, Solms) as decribed above, resulting in a final (screen) magnification of 1100 x.

The open source image analysis program ImageJ was used for morphometric analysis, and downloaded from http://rsb.info.nih.bov/ij/. Additionally, the plugins *Cell Counter* (Kurt De Vos) , Academic Neurology, University of Sheffield, Great Britain), *Measure and Label*, and *Grid* (both by Wayne Rasband, National Institute of Health, USA) were applied. Pictures were analysed without the observer's knowledge of the image origin from TG or nTG mice (blind experiments). All pictures were analysed by the same observer and on the same monitor (same image resolution).

Total area estimation

In order to estimate areas, a grid consisting of 30 fixed small rings of identical size, marked out at regular intervals was overlaid on the screen (point counting method). Each ring represented 1600 µm and was considered positive for a given structure if the structure was to be observed within the ring, and negative, if a structure was only touched by an edge of the ring.

Determination of area fraction

Area fractions were determined as fractions per cent from the contractile tissue, that consists of cardiomyocytes, capillaries and interstitial space or interstitium. Rings positive for structures other than the above mentioned (e.g. arteries, veins, epicard) were subtracted from the total area of 30 x 1600 µm = 48000 µm. Area fractions were calculated for each picture analysed and the mean of all pictures was calculated for each animal and ventricle.

Counting of cell and capillary number

A linear grid consisting of squares with a side length of 40 µm was overlaid on the screen to count structures. Per photo, 30 squares or points representing an area of 1600 µm each were evaluated, analysing 18-53 images per animal and ventricle. A structure was counted if it was entirely located within a square or if it intersected the upper or right edge of the square, but was not counted if it intersected the lower or left edge. Likewise, it was not counted if it both intersected upper or right *and* the lower or left edge. Thus, multiple counting of objects was avoided.

Cardiomyocyte size and diameter

Cell size was calculated from the estimated area covered by cardiomyocytes divided by the counted cell number. Cardiomyocyte diameter was determined for 10 images per mouse and ventricle, picked in a random systematic manner (that is, every third or every fifth image, depending on the total amount of images). The smallest diameter was measured for each cell, irrespective of cell orientation. A linear grid consisting of 30 squares with an area of each 1600 µm was laid over the image. Cardiomyocytes of the second and fourth square were usually measured. Only if these squares were devoid of cardiomyocytes, the next lower square was chosen.

Capillaries per cardiomyocyte, Capillary diameter, intercapillary distance and pericapillary space

The ratio of capillaries per cardiomyocytes was determined per image and then averaged for each mouse and ventricle. Capillary diameter was measured as the smallest diameter in 10 images per mouse and ventricle, analogous to the determination of cardiomyocyte diameter. For determination of the maximal intercapillary distance as a measure for the diffusion distance, it was proceeded as has been described previously (Tagarakis et al., 2000a, 2000b; Rakusan et al., 1986). First the capillary density was calculated as the number of capillaries per mm^2 cross sectional area of contractile tissue with the point counting method according to Gundersen (Gundersen, 1977) Then, the intercapillary distance was calculated according to the hexagonal model of tissue capillarization (R=10^3 $\sqrt{2/\sqrt{3}}$ CD $\sqrt{3,}$ CD= capillary density). From this, the capillary radius was substracted to yield the maximal intercapillary distance) as the average area supplied by a single capillary.

2.10 Electron microscopy

An EM 902 (Zeiss, Oberkochen) was utilized for electron microscopic imaging. The electron microscope was connected to a digital camera (Megaview III, Soft Imaging System, Münster) which was used in combination with the ITEM image analysis software (Soft Imaging System, Münster) installed on a personal computer.

For each mouse and ventricle, a minimum of 4 Epon blocks containing 2–3 tissue samples was analysed. For each mouse and atrium, at least two Epon blocks were evaluated.

For determination of sarcomere lengths, only sections were chosen which had been cut parallel to the longitudinal axis of the microfibril. Sarcomeres from myofibrils cut at obscure angles were excluded from the measurement. Starting from one field of view at the upper part of the grid, the camera was moved across the grid in a meandering manner from field of view to field of view, stopping at every field suitable for analysis. For sarcomere length measurements, a magnification of 12.000x was chosen. The final screen magnification was 43.576x.

2.11 Statistical analysis

All morphometric data are presented as mean values $\pm$ 95% confidence interval (C.I.). Data analysis was performed using SPSS for Windows or Excel including Student's T-Test calculations for unpaired data. Significance was considered at a *p* value <0.05 and high significance at a *p* value <0.01.

3 Results

The morphological characterization of hearts from transgenic mice is presented. These hearts constitutively express a cardiac troponin inhibitory subunit with a deletion at position 184 (cTnI$^{\Delta K184}$) in addition to the native protein. CTnI$^{\Delta K184}$ substitutes the native protein nearly completely (Line B, 98 %, line E 92 % of total cTnI, male adult mice 12 weeks of age). The corresponding mutation in the human cTnI sequence (cTnI$^{\Delta K183}$) is inherited by an autosomal-dominant trait and has been linked to familial hypertrophic cardiomyopathy (Kokado et al., 2000; Kimura et al., 1997; Shimizu et al., 2002 a).

To reduce effects of a varying genetic background, non-transgenic siblings served as controls in all experiments. Besides weight determinations, morphology and histology of hearts arrested and fixated at a defined heart phase, namely in diastole were analyzed. In addition, the *in vivo* morphology as assessed by magnetic resonance imaging (MRI) was determined. The ultrastructural investigation identified sarcomere disarray as the main characteristic of the cTnI$^{\Delta K184}$ mutant. Both ventricles *and* atria were investigated. The α-MHC promoter that controls cTnI$^{\Delta K184}$ is equally expressed in atria and ventricles. The altered hemodynamic and tissue organization thus serves as an experiment in itself.

3.1 Small hearts with enlarged atria

Transgenic (TG) cTnI$^{\Delta K184}$ mice had visibly smaller hearts than their non-transgenic (nTG) littermates. This difference was so striking that TG hearts were usually identifiable in blind tests. Fig. 3.1 shows representative nTG (A) and TG (B) hearts from 12 week old mice from line E. Particularly, ventricular width was reduced in TG animals, resulting in hearts of a pointed conical shape compared to the more rounded shape of hearts from nTG littermates. The reduction in overall heart size was consistently accompanied by an atrial enlargement. Especially left atria were oversized and occasionally, were even larger than the right atria.
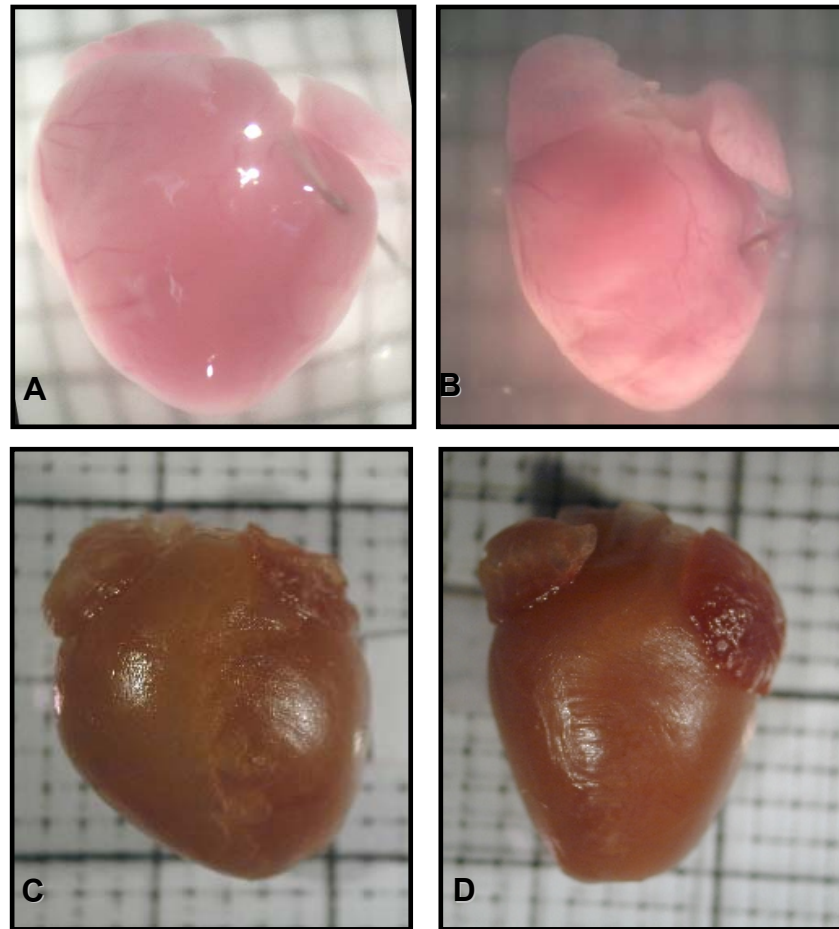
Fig. 3.1 Hearts from cTnI$^{\Delta K184}$ mice have smaller ventricles, but enlarged atria. Heart geometry is altered to a pointed conical shape compared to the rounded shape of hearts from non-transgenic mice. Top row: unfixed hearts (**A**) nTG and (**B**), TG, line E, respectively; bottom row: gross morphology of hearts was unchanged after perfusion fixation with formaldehyde/ glutaraldehyde (**C**) nTG and (**D**), TG.

To determine if the ventricular size reduction was accompanied by a reduction in ventricular and total heart mass, total hearts and separately, left and right ventricles were weighed. In addition, atrial weight was assessed to differentiate between a mere dilation and eccentric growth associated with an increase in atrial mass. The hearts were weighed after perfusion and post-fixation. This had the disadvantage of possible weight alterations due to the fixation, but these alterations should be similar in TG and nTG mice. This disadvantage was outweighed by the more precise preparation that was possible in fixated hearts. Especially delicate structures as the atria could be accurately dissected. In addition, it allowed to directly relate weight to morphological findings.

For comparability, all data are presented in ratios to body weight. However, body weights did not differ significantly between cTnI$^{\Delta K184}$ mice and their nTG littermates.

At the age of 12 weeks, total hearts from TG mice showed a drastic weight decrease (–15% compared to nTG siblings). The lower total heart weight in TG mice was due to a ventricular weight reduction that was proportional in the left and right ventricles (see table 3.1). Thus, the smaller ventricle size correlated with a lower ventricle weight.

Atria, by contrast, were consistently heavier in cTnI$^{\Delta K184}$ mice in animals of both ages (+34%). Atrial enlargement therefore, is not only a consequence of dilation but also of mass increase.

Table 3.1: Comparison of heart preparations from cTnI$^{\Delta K184}$ and nTG mice.

		nTG	TG
Heart weight [mg]	**MW**	**184.44**	**143.30**
	95% CI	10.48	7.23
	% difference		–22
	T-Test		0.0001
Body weight [g]	**MW**	**30.80**	**28.05**
	95% CI	1.80	2.07
	% difference		–9
	T-Test		0.079
Heart/body weight [mg/g]	**MW**	**6.00**	**5.09**
	95% CI	0.35	0.42
	% difference		–15
	T-Test		0.009
Left ventricle/ body weight [mg/g]	**MW**	**4.6**	**3.80**
	95% CI	0.13	0.24
	% difference		–17
	T-Test		0.000076
Right Ventricle/ body weight [mg/g]	**MW**	**1.07**	**0.94**
	95% CI	0.09	0.03
	% difference		–13
	T-Test		0.019
Left/right ventricle [%]	**MW**	**23.44**	**24.64**
	95% CI	2.55	1,53
	% difference		+5.13
	T-Test		0.45
Atria/body weight [mg/g]*	**MW**	**0.32**	**0.43**
	95% CI	0.04	0.06
	% difference		+34
	T-Test		0.017

NTG, n=6; TG, n=6; 12–14 weeks old mice.

3.2 Absence of regional wall thickness abnormalities

Hypertrophic cardiomyopathy patients who carry the $cTNI^{\Delta K183}$ mutation occasionally have regional wall thickness changes despite an overall normally sized heart. Apical hypertrophy and septal wall thinning have been reported (Kokado et al., 2000; Kimura et al., 1997) To investigate regional wall thickness changes due to the expression of the in $cTnI^{\Delta K184}$ transgene, serial cross sections (vibratome or paraffin sections) of hearts from mice 12 weeks of age were made (TG and nTG; line E or B), that had been arrested in diastole to ascertain comparability of wall thickness, and perfusion fixed with 4% PFA (*n*=6). None of the hearts showed global or regional wall thickening in the left ventricle, right ventricle, or septum. Fig. 3.2 shows representative cross sections.

Fig.: 3.2: Cross sections of ventricles from $cTNI^{\Delta K183*}$ (top row) and nTG mice (bottom row) from 2/3 of the ventricular length (**A** and **D**), 1/3 the ventricular length (**B** and **E**), and the heart base (**C** and **F**). Mice were from line E. Scale bar: 1mm.

3.3 Hyperdynamic contraction

More important than the static wall thickness is the wall thickness and circumference *change* during the heart cycle as it is a direct measure for contraction dynamics. Besides, it gives hints to the force that acts on the blood column in the ventricular cavity.

The *in vivo* left and right ventricular wall thickness in end-diastole and end-systole were measured in magnetic resonance images. As a measure for left ventricle dimension, the cavity and outer ventricle diameter were determined. Fig. 3.3 shows representative magnetic resonance images from TG and nTG animals. The first three optical slices proximal to the heart base were used in each case to ensure comparability (optical slice distance was 1 mm). Wall thickness was measured at three independent sites of each right ventricle, left ventricle, and septum.
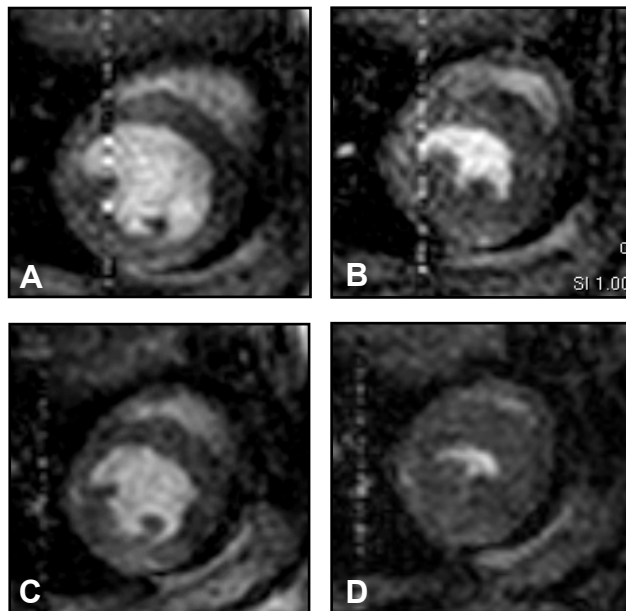

Fig. 3.3: Magnetic resonance images from from cTNI$^{\Delta K184}$ (top row) and nTG mice (bottom row) in diastole (**A** and **C**) and systole (**B** and **E**), respectively. Note the enormous wall thickness increase and cavity minimization in TG mice. MRI images by N. Blaudeck

As an approach to the true left ventricular cavity and outer diameter, the largest and smallest diameters were measured and averaged. As there were no statistical differences between septum and free LV wall thickness, the mean of all six values was calculated. Data are summarized in table 3.2.

Table 3.2: Comparison of wall thickness and cavity diameter from cTnI$^{\Delta K184}$ and nTG mice.

	LV wall thickness (mm)	RV wall thickness (mm)	LV/RV wall thickness	LV cavity Ø (mm)	LV Outer Ø (mm)	LV wall thickness/ LV cavity Ø
Diastole						
MW nTG	**0,92**	**0,4**	**2,39**	**3,62**	**5,73**	**0,26**
95% CI	0,09	0,04	0,51	0,39	0,41	0,03
MW TG	**0,92**	**0,34**	**2,75**	**2,94**	**5**	**0,32**
95% CI	0,08	0,06	0,56	0,57	0,46	0,07
T-Test	**0,852**	**0,043**	**0,186**	**0,01**	**0,003**	**0,031**
%TG/nTG	**-0,8**	**-13,6**	**15**	**-18,9**	**-12,7**	**25,8**
Systole						
MW nTG	**1,27**	**0,42**	**3,13**	**2,48**	**5,12**	**0,53**
95% CI	0,11	0,06	0,52	0,44	0,55	0,12
MW TG	**1,49**	**0,44**	**3,46**	**1,22**	**4,52**	**1,28**
95% CI	0,11	0,08	0,62	0,29	0,36	0,31
T-Test	**0,001**	0,562	0,265	**0**	**0,015**	**0**
%TG/nTG	**16,9**		**10,6**	**-50,8**	**-11,8**	**141,3**

Although absolute diastolic left ventricular wall thickness did not differ between TG and nTG mice, wall thickness to cavity diameter ratio was significantly increased already in diastole (fig. 3.4).
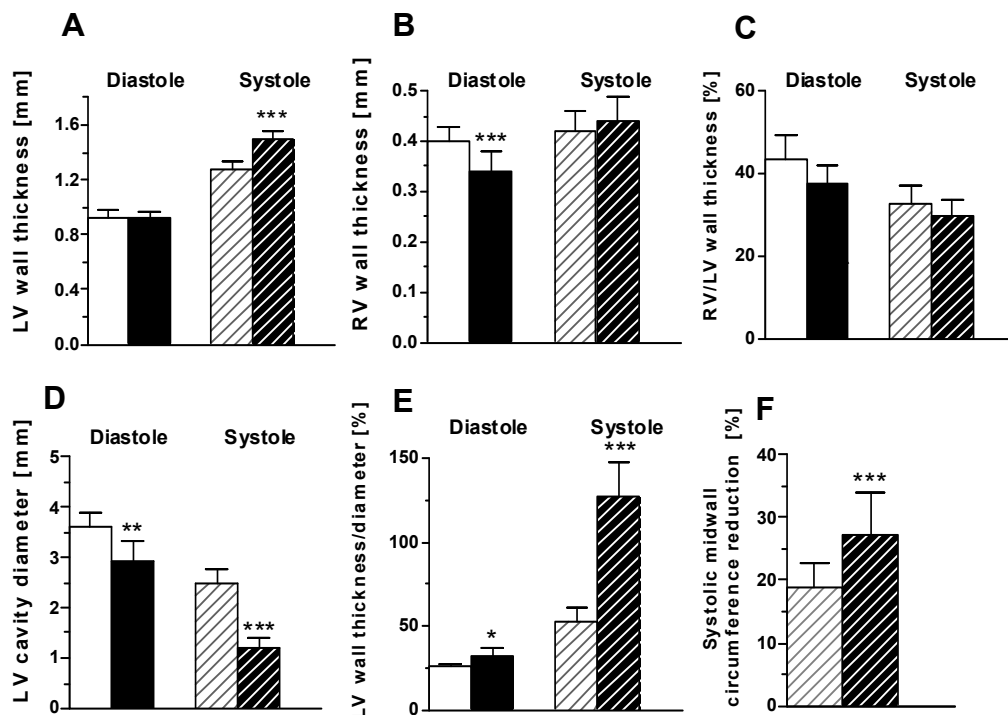

Fig. 3.4: *In vivo* wall thickness differences during diastole in systole. **A**, Left ventricular wall thickness; **B**, right ventricular wall thickness; **C**: right to left ventricle wall thickness ratio; **D**: left ventricular cavity diameter; **E**: left ventricular wall thickness to cavity diameter ratio; **F**: systolic left ventricular midwall circumference reduction. Data from diastole are represented by solid bars, from systole as striped bars. Light bars show data from nTG, dark bars from TG mice.

In systole, absolute wall thickness and wall thickness relative to ventricle cavity diameter were increased with highest statistical significance (17% and 141%, respectively). The right ventricle wall is significantly thinner in TG mice in diastole (−14%). In systole, however, the right ventricular wall thickness from $cTnI^{\Delta K184}$ mice is indifferent from nTG mice. Thus, the left and right ventricle walls from TG mice likewise, thicken to a greater extent than those from nTG mice, and the slightly decreased right to left ventricular wall thickness ratio of the TG mice persists throughout the heart cycle.

The enhanced wall thickening constitutes a gain of systolic function in the $cTNI^{\Delta K183}$ mutant that can be directly converted into sarcomere shortening: The middle layer of the left ventricular myocardium has a circular orientation. In approximation, the rod-shaped midwall cardiomyocytes (and sarcomeres) are arranged tangentially to the midwall circumference. Hence, midwall circumference changes are directly proportional to sarcomere length changes. The midwall circumference (c_m) is calculated as $c_m = 2\pi r_m$; $r_m = (r_o+r_i)/2$ (r_m = midwall radius, r_o = outer wall radius, r_i = inner wall radius). For nTG and TG mice, the following values result (table 3.3):

Table 3.3: Midwall circumference reduction in systole in $cTnI^{\Delta K184}$ and nTG mice.

	midwall circumference (c_m)		
	diastole	systole	% shortening
nTG	14.69 ± 1.4	11.95 ± 1.5	18.8 ± 3.9
TG	12.47± 1.8	9.02 ± 1.1	27. 2 ± 6.8
T-Test			0.007

For an estimated diastolic sarcomere length of L=2,2 µm which corresponds to maximal relaxation and sarcomere pre-stretching, the resulting mean systolic sarcomere length would be 1.78 µm for nTG mice, but only 1.6 µm for $cTNI^{\Delta K183}$ mice. For submaximal diastolic sarcomere lengths the resulting systolic sarcomere lengths would be even lower.

3.4 Absence of fibrosis

Fibrosis is one of the major hallmarks in many hypertrophy associated sarco-mere cardiomyopathies. It often appears in unison with a hypertrophic pheno-type, although independent cellular signalling may lead to either of these two. In mouse models, even a reduction in heart size coincided with ventricular tissue fibrosis (James, et al., 2000) However, none of the cTnI$^{\Delta K183}$ mice had any ven-tricular interstitial fibrosis or exhibited scarring. We dyed serial vibratome or pa-raffin cross sections with picrosirius red stain. Sirius red is more sensitive than other connective tissue dyes like Goldner stain, because it stains not only large collagen fibers but also reticular fibers (Van Kerckhoven et al., 2000; Ammar-guellat et al., 2001) These fibers are stained red, whereas cytoplasm is colored yellow.
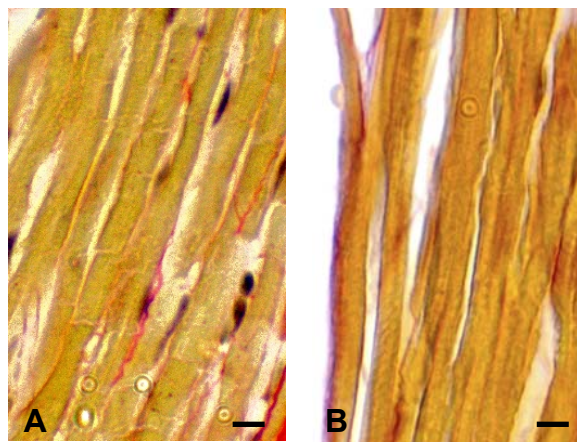

Fig. 3.5: Absence of left ventricular tissue fibro-sis in TG mice. A, nTG; B, TG. Scale bar: 10 µm.

3.5 Light and electron microscopic morphometry of ventricles

Heart muscle tissue is extremely anisotropic which means that, depending on the location within the tissue (e. g. in the subendocardial, midwall or subepicardi-al layer of heart muscle cells) but also depending on sectioning angle, its ap-pearance varies considerably. Therefore, a simple random sampling is insuffi-cient and produces unreliable results. Instead, we performed a random syste-matic sampling on all levels of tissue preparation and image analysis (Nyengaard & Gundersen, 2006; Gundersen, 1988; Elias, 1983). Because there were no vis-ible differences between larger blood vessels and other components of non-

contractile parts of the ventricular working myocardium e. g. veins, nerves, endo-card) the analysis focused on the contractile tissue. Male cTnI$^{\Delta K184}$ and nTG mice 12 weeks of age were analyzed (*n*=4).

3.5.1 Area fractions of contractile tissue components: Increased interstitial space

Ventricular contractile tissue mainly consists of cardiomyocytes and capillaries, which are connected to one another by a fine web of reticular connective tissue. The space harboring the connective tissue is called the interstitium, and may be enlarged due to interstitial fibrosis but also due to interstitial edema. Either of them have consequences on the efficiency of substance exchange between ca-pillaries and cardiomyocytes. Data are presented as area fractions (%) from the total contractile tissue and are summarized in fig. 3.6.
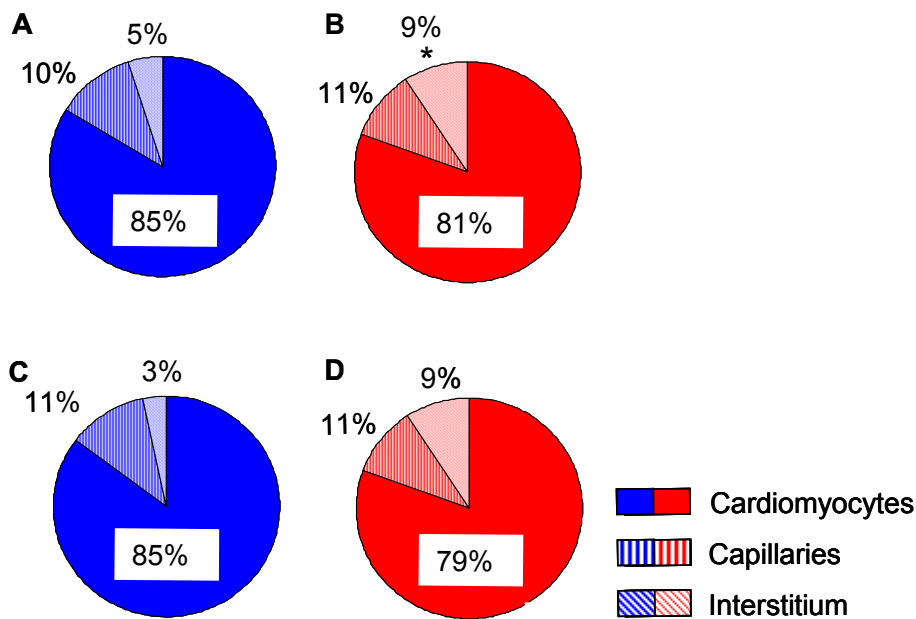

Fig. 3.6: Area fractions in the contractile tissue from the left and right ventricle. **Top row:** left ventricle; **bottom row:** right ventricle. **A, C**: nTG; **B, D**: cTnI$^{\Delta K184}$ mice.

In the left ventricle of TG mice, the interstitium was significantly increased (+71%), but the capillary space was reduced by 10%, while the cardiomyocyte fraction was slightly reduced by 5% (**left ventricle:** *interstitium*, nTG, 5.23 ± 2.27%; TG, 8.98 ± 1.36, *p*<0.05; *capillaries*, nTG, 10.25 ± 0.5%; TG, 11.43 ± 1.25%, *p*>0.05; *cardiomyocytes*, nTG, 84.8 ± 4.2%; TG, 80.78 ± 1.35%,

p>0.05). Fig. 3.8 shows representative micrographs of left ventricular contractile tissue.

In the right ventricle, the increase of mean interstitial area fraction is increased 3-fold in TG mice compared to nTG mice. The capillary area fraction was unchanged in the right ventricle from TG mice. The cardiomyocyte area fraction was slightly smaller by 6% and thus, equalled that from the left ventricle. (**right ventricle:** *interstitium*, nTG, 3.20 ± 2.03%; TG, 9.40 ± 6.42%; *p*>0.05; *capillaries*, nTG, 11.44 ± 3.34%; TG, 11.47 ± 3,18 %, *p*>0.05; *cardiomyocytes*, nTG, 84.45 ± 3.55%; TG, 79.03 ± 7.12%, *p*>0.05).

3.5.2 Heart weight reduction correlates with cardiomyocyte size only in the right, but not in the left ventricles

Cardiomyocytes make up ~70% of heart weight (Katz, 2006). Therefore, a decreased heart weight likely is the result of either a reduced cardiomyocyte size or a reduced cardiomyocyte number. To analyze which of the two was mainly responsible for the lighter hearts, cardiomyocyte cell area and number were determined on semithin sections that allowed for a reliable identification of cell borders, especially intercalated discs. Results are summarized in fig. 3.7A.

In the left ventricle, cardiomyocytes from cTnI$^{\Delta K184}$ mice had approximately the same size as those from their nTG brothers. By contrast, mean cardiomyocyte size in the right ventricle was decreased by 12% (**left ventricle:** nTG, 428.0 ± 60.5 μm^2; TG, 417.3 ± 12.7 μm^2 (– 2 %); *p*>0.05; **right ventricle:** nTG, 382.0 ± 31.3 μm^2; TG, 336.1 ± 38.4 μm^2; *p*>0.05).

In addition to this unbiased estimate of cellular size, cardiomyocyte diameter was determined, because in many pathological state, heart muscle cell length to width ratio is altered. In the left ventricle, cardiomyocyte diameter from cTnI$^{\Delta K184}$ mice almost equaled that from nTG littermates (**left ventricle:** nTG, 11.83 ± 0.78 μm; TG, 11.23 ± 0.15; (–5%; *p*>0.05). In the right ventricle however, cell diameter was reduced by 15% in TG mice (right ventricle: nTG, 11.98 ± 0.75; TG, 10.24 ± 1.27; *p*>0.05), correlating well with the overall size reduction.

As all hearts were arrested in diastole before perfusion fixation, it was assumed that the contractile status of TG and nTG mice would be equal, so that comparability of our cell size determination would be given. This assumption was con-

firmed by electron microscopic sarcomere length measurements carried out in left ventricular samples at a 12,000 x magnification. There were no statistically significant differences in sarcomere lengths from TG and nTG mice (nTG: 2036 ± 116 nm; TG: 2193 ± 222 nm, $p > 0{,}05$, fig. 3.7C).

In the right ventricle, the 12% smaller cardiomyocytes from cTnI$^{\Delta K183}$ mice coincided with a 13% reduced ventricle weight and a 14% reduced diastolic wall thickness. In the left ventricle, diastolic cardiomyocyte size was unchanged in TG mice as was diastolic wall thickness. However, left ventricular weight was reduced by 17% in TG mice 12 weeks of age. In other words, left ventricular cardiomyocyte size did not correlate with left ventricular weight reduction.
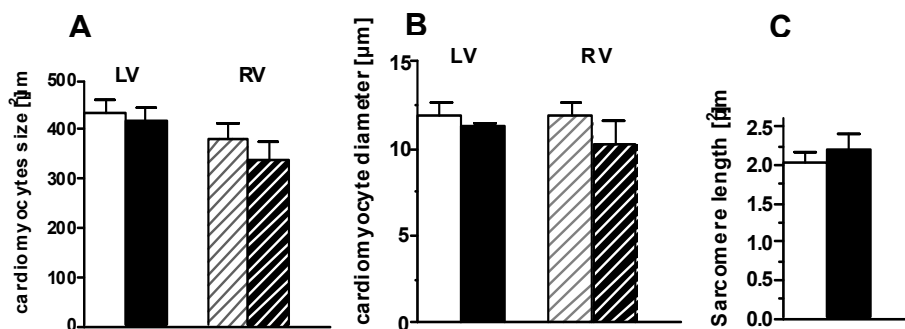

Fig. 3.7: (A) Cardiomyocyte size, **(B)** Cardiomyocyte diameter and **(C)**, sarcomere lengths in the left ventricle. LV, left ventricle, RV, right ventricle. Data from the left ventricle are represented by solid bars, from the left ventricle as striped bars. Light bars show data from nTG, dark bars from TG mice.

3.5.3 Blood supply

We calculated the ratio of capillary to cardiomyocyte number in order to get a first estimate for myocardial blood supply. The amount of capillaries per cardiomyocyte was indifferent between cTnI$^{\Delta K184}$ mice and their nTG littermates and was one capillary per cardiomyocyte on average both in the left and right ventricle (**left ventricle:** nTG 0.98 ± 0.05; TG: 0.98 ± 0.05; **right ventricle:** nTG 0.99 ± 0.10; TG: 0.99 ± 0.04; $p>0.05$; fig.3.8 A).

However, the intercapillary distance is a more meaningful index for oxygen supply, because it considers the *area* that is provided by the capillaries, corrected by capillary diameter. So if the intercapillary distance (or oxygen diffusion distance) is large, tissue oxygen (and nutrient supply) may be jeopardized. Assuming a hexagonal capillary array, we calculated the maximal diffusion dis-

tance, because it is more critical to aerobic metabolism than the average diffu-
sion distance. Nevertheless, diffusion distance was equally large or slightly
smaller in cTnI$^{\Delta K184}$ mice compared to their nTG littermates (**left ventricle:** nTG:
9.85 ± 0.35 µm; TG: 10.00 ± 0.92 µm, $p>0{,}05$; **right ventricle:** nTG: 9.85 ± 1.36
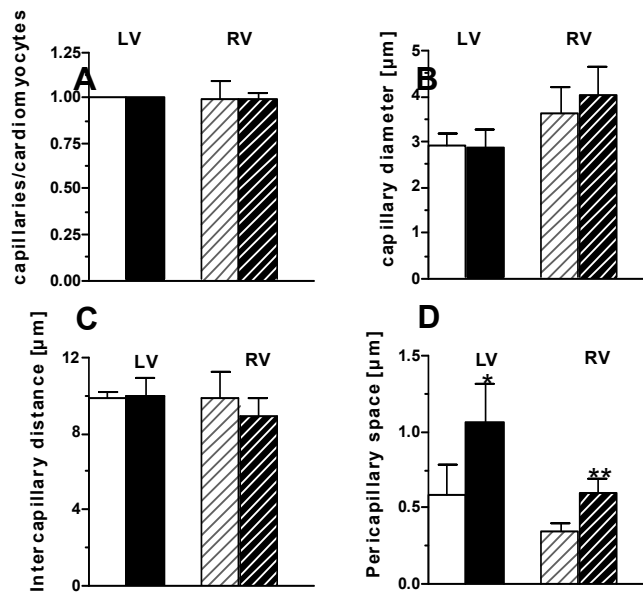µm; TG: 8.95 ± 0.94, $p>0{,}05$; see fig. 3.8).

Fig. 3.8: Parameters of oxygen supply and capillary edema.
Data from the left ventricle are represented by solid bars,
from the left ventricle as striped bars. Light bars show data
from nTG, dark bars from TG mice. (**A**) Capillary density; (**B**)
Capillary diameter; (**C**) intercapillary distance; (**D**) Pericapil-
lary space. Error bars: 95% CI $n=4$

Although the intercapillary distance was not altered in the TG mice, it was readily
visible on the photomicrographs that the increase in interstitial area fraction (see
above) was prominent especially in direct neighborhood of the capillaries. Peri-
capillary edemas do not hinder O_2 diffusion, they however have several adverse
effects on myocardium and contribute to cardiac dysfunction. Therefore, the
mean distance between capillaries and surrounding myocardium were deter-
mined. It showed that it was significantly increased both in the left and right ven-
tricle (fig. 3.8 C) (left ventricle: nTG, 0.58 ± 0.2 µm (+85%, $p<0.05$); TG, 1.06 ±
0.26 µm; right ventricle: nTG, 0.34 ± 0.06 µm; TG, 0.51 ± 0.09 µm (+77%,
$p<0.01$)).

3.6 Light and electron microscopic characterization of the ventricles

Left and right ventricular tissue from TG mice 12 weeks of age were analyzed in comparison with their nTG littermates to identify structural abnormalities associated with cTnI$^{\Delta K184}$ -based cardiomyopathy (n=4).

3.6.1 Histology

There are three classical histological hallmarks of hypertrophic cardiomyopathy, namely cardiomyocyte hypertrophy, interstitial fibrosis, and cellular disarray. Nevertheless, the more recent literature allows for absence of hypertrophy and fibrosis (Ho & Seidman, 2006), both now being considered as secondary effects of sarcomere cardiomyopathy. Whether this applies for cardiomyocyte disarray as well is currently not known.

The cTnI$^{\Delta K184}$ mutant showed neither hypertrophy nor fibrosis, but interstitial edema. Both in the left and right ventricle, cellular disarray was mild. Cardiomyocytes from TG mice showed only a mild, focal disarray fig. 3.9) but were more irregularly shaped (fig. 3.10).
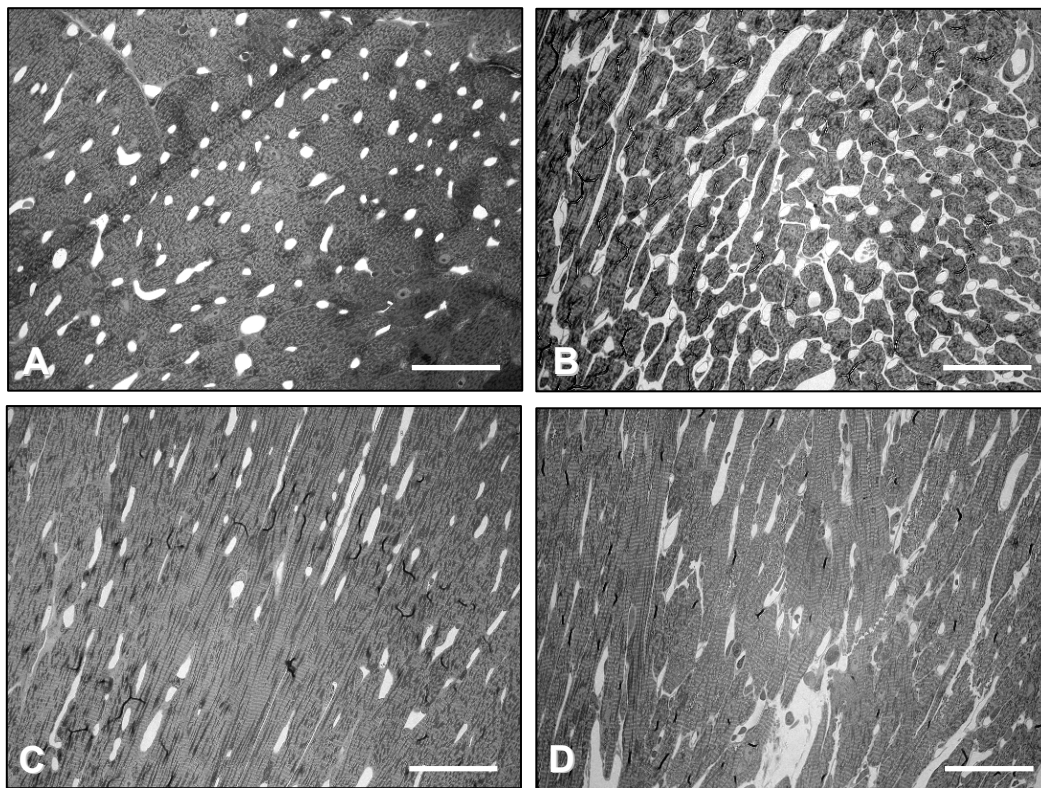
Fig. 3.9: Representative survey micrograph of left vetricular tissue from non-transgenic (A, C) and transgenic TnI$^{\Delta K184}$ mice **(B, D)** (semithin sections). **A**: cross-section. Cardiomyocytes are surrounded by ~ four capillaries each. Almost no extracellular space visible. **B:** By contrast, there is more extracellular space in tissue from TG mice. Cells have a more irregular shape and appear to be smaller. Capillary-to-cardiomyocyte-ratio appears to be unchanged. **C**: Longitudinal section (nTG). Cells are properly arrayed. **D**: Slight disarray of cardiomyocytes in longitudinal view. Irregular cell shapes, more interstitium. Scale bar 50 µm.

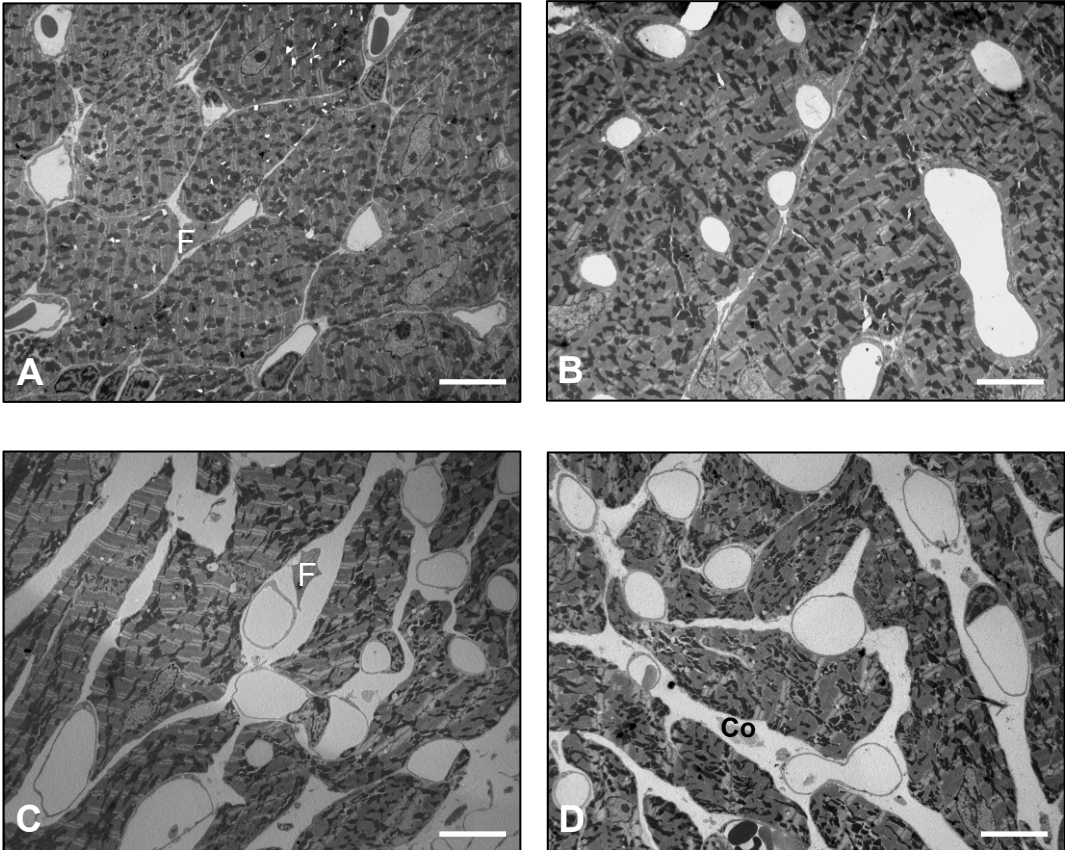**Fig. 3.10: Survey electron micrographs of oblique sections from left and right ventricular tissue. A**, left ventricle and **B**, right ventricle from nTG mice. Regularly shaped cardiomyocytes, little interstitium. **C**, left ventricle and **D**, right ventricle from TG mice. Cardiomyocytes are more irregularly shaped and interstitial space is increased. Arrow: cellular fold. Co, Collagen. Scale bar 10 µm

Besides, cardiomyocytes occasionally displayed plasma membrane foldings which did not occur in nTG mice (fig. 3.11]. **Interstitium** was enlarged and was electron-penetrable or electron-opaque with minor collagen fiber inclusions. Thus, interstitium increase is mainly due to an increase in watery ground substance instead of collagen and/or reticular fibers. This corroborates the notion of interstitial edema. **Fibroblast** number was not quantified, but it did not appear to be altered. Also, fibroblast size and appearance was unchanged in TG animals even in large magifications (not shown). **Capillaries** from TG mice usually did not differ from those from nTG mice as they had a regular shape and a round cross sectional area. There were no thickened endothelial cell basal laminae indicative of small vessel disease as have been reported for HCM that are based on other sarcomere protein mutations.

Non-contractile structures such as arteries, arterioles, veins, and lymphatic vessels were inconspicuous (not shown). In other words, there was no media and/or intima thickening of blood vessels occasionally associated with the HCM phenotype (Hughes, 2004; Maron, 1978) Besides, the endo- and ectocardium appeared similar in TG and nTG animals.

3.6.2 Cellular folds, buds and sarcomere disarray

Thus, the effects of cTnI$^{\Delta K184}$ mainly remained restricted to the location of their expression, the cardiomyocytes. On the fine structural level, several additional aberrations were visible that did not occur in nTG mice. These alterations were not visible in all cardiomyocytes but often enough to distinguish TG from nTG mice in blind tests. In addition to the already mentioned more irregular cell shape of cardiomyocytes, abnormal buds and invaginations were common (fig. 3.11). Cardiomyocytes from TG mice were rounded/folded in themselves and had so-called double-intercalated discs, as has been described as a common feature of HCM (Hughes, 2004].
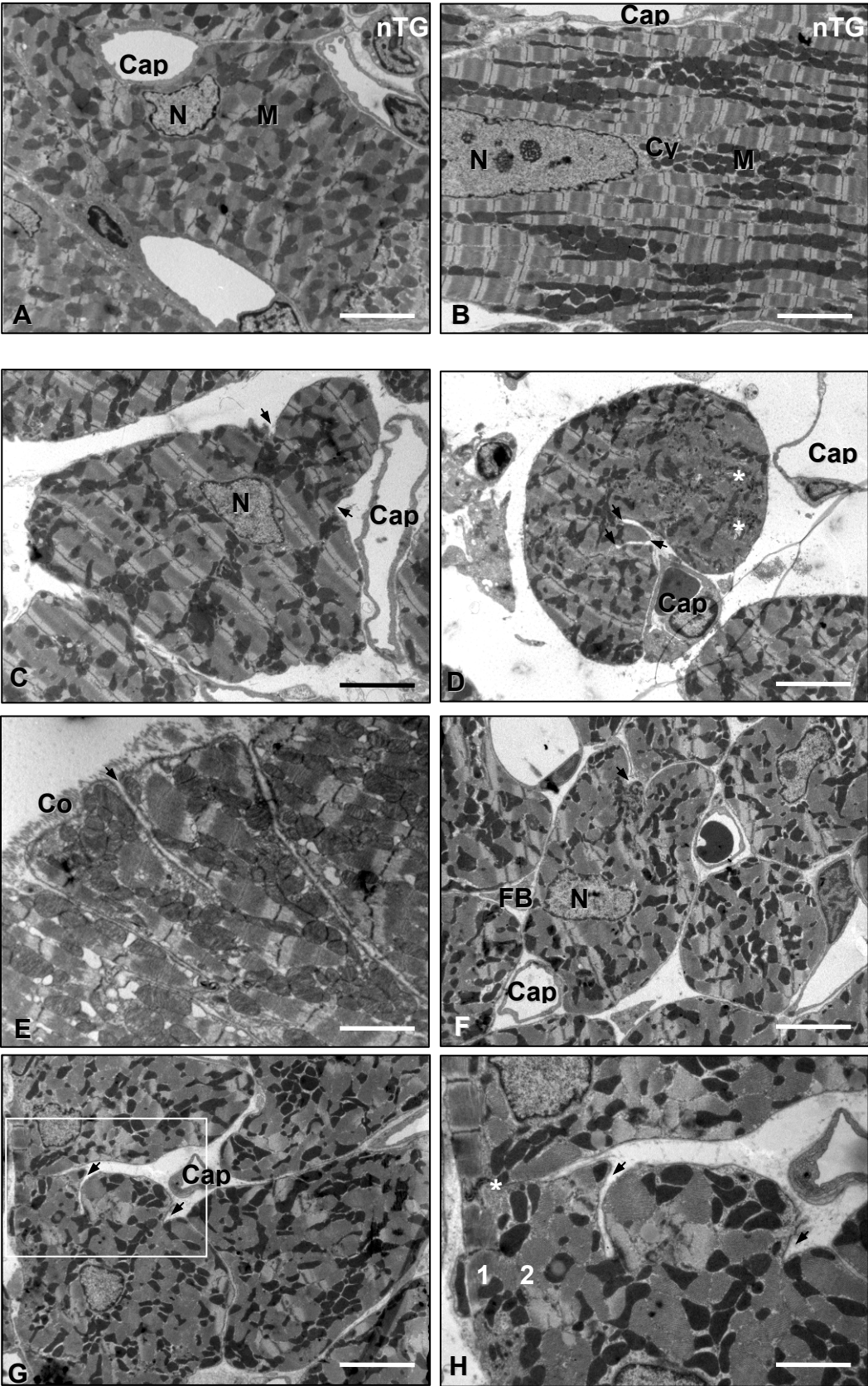
However, the most prominent feature of cTnI$^{\Delta K184}$ mice was myofibrillar disarray. Myofibrillar disarray may be defined as sarcomeres that are not arranged in the longitudinal direction of the cell but at obscure angles to the longitudinal axis of the cell and/or to each other. Those myofibrils are out of register. It is important to note that it does not mean a spatial shift of sarcomeres along the longitudinal axis of cells, as this is a common feature of wild type mice as well, but has been used by several groups to define FHC morphology. Fig. 3.12 shows representative electron micrographs of cardiomyocytes with disarrayed sarcomeres in addition to regular phase shifted sarcomeres in nTG and TG mice. In fig. 3.13, a high magnification of an extreme case of sarcomere disarray is presented with myofibrils arranged perpendicular to each other. Myofilament spacing is irregular as well. Note that single myofibrils are surrounded by network SR and dyads and that that they, too, are not arranged in a regular manner. In cells with sarcomere disarray, nuclear shape was rather angular as opposed to the rounded cigar shape of cardiomyocytes from nTG mice. This is explicable by the necessarily altered cytoskeletal structure. Besides, nuclei were generally located at the cell center as in nTG cardiomyocytes. To date, it is unknown how the shape of cells with sarcomere disarray changes during contraction. Sarcomere disarray was found in both in the right and left ventricle, as well as in both atria. By contrast to these observations, a smaller fraction of cells showed extremely wide myofibrils. In those cells, width-to length ratio appeared to be increased (or cells were folded/curved, so that they disappeared from focus) and here, nuclear shape was more angular, too (fig. 3.12 G–H).

Fig. 3.11: (previous page): Electron micrographs of abnormally formed cells in ventricular tissue from TG mice. **A** and **B**, nTG, typical regularly, rod-shaped cardiomyocytes from left ventricles from nTG mice: roughly ordered sarcomeres, mitochondria with electron-dense mitochondria, centrally located nucleus, and only very little sarcomere-free cytoplasm, mainly in close proximity to the nucleus. **C–H**: TG. C, irregularly shaped cardiomyocyte narrowing to a neck (arrow) and then, widening again. Cutting angle may not explain this shape. Sarcomere length and width are within the usual range. **D**, strongly arched cardiomyocyte with invaginations and protrusions (arrows), large, so-called double intercalated disc (asterisk), which connects cell with another cardiomyocyte. **E**, cardiomyocyte with large invagination (arrow), sarcomere array is regular. **F, G**: rounded cardiomyocytes with atypical invaginations and "buds". **H**, detail of rectangle in **G**, disarray of sarcomeres that are aligned perpendicular to each other (1, longitudinal; 2, cross section), asterisc: intercalated disc. Scale bar 5 µm.
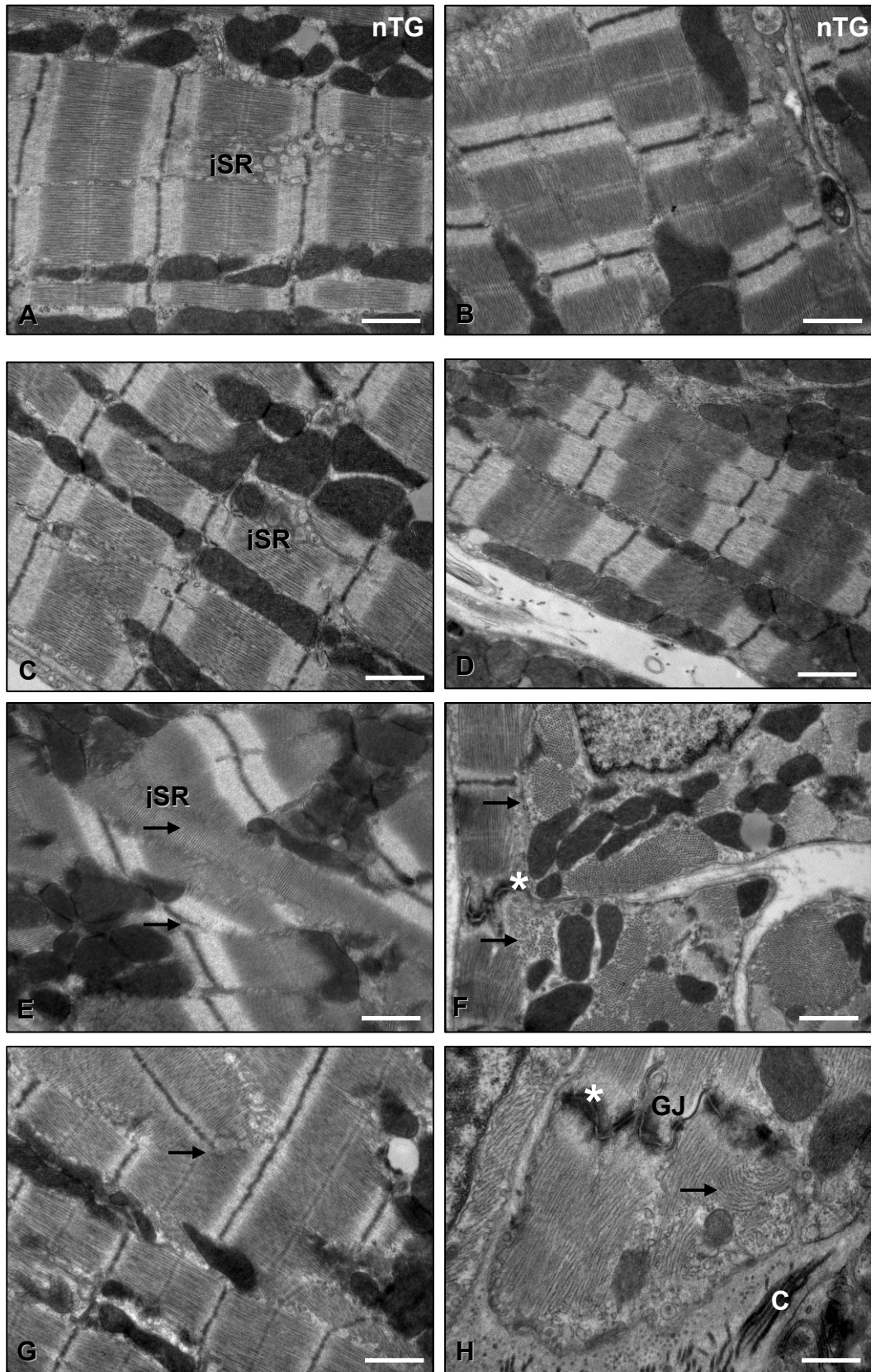
Fig. 3. 12: Sarcomere disarray. A, B: Typical sarcomeres from the left ventricle of an nTG mouse. **A**, parallel myofibrils in register, **B**, parallel myofibrils out of register, common. **C, D:** sarcomeres from the left ventricle of a TG mouse, C, parallel myofibrils in register, D, parallel myofibrils out of register. **E–H:** non-parallel myofilaments (TG mice) = sarcomere disarray (arrows). JSR, junctional SR. Asterisc, intercalated disc; GJ, gap junction. Scale bar 1 μm.
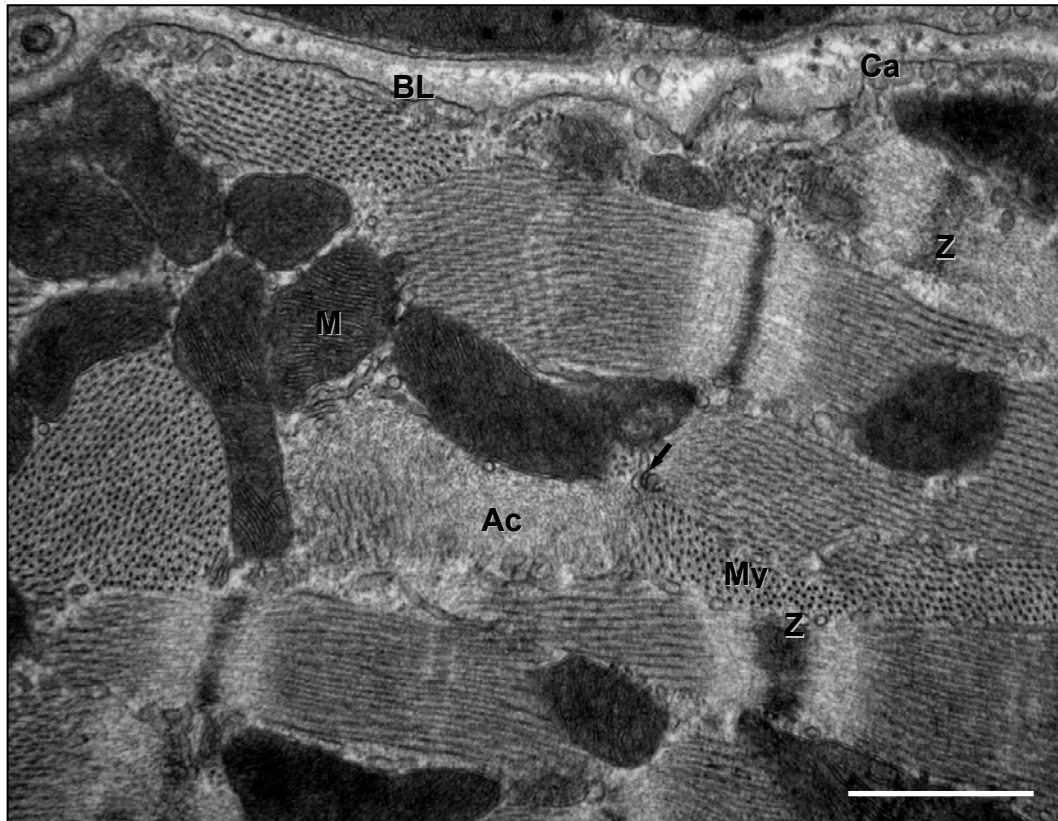
Fig. 3.13:Sarcomere disarray in a left ventricular cardiomyocyte from a TG TnI$^{\Delta K184}$ mouse. Myofibers are arranged perpendicular to each other. Thickened Z-disc in lower right corner. BL, basal lamina. M, mitochondrion. Ac, actin. My, myosin. Cav, caveolae. Arrow, SR with triad feet.

3.6.3 Sarcomere reconstruction

Sarcomere disposition is high during development when the myocardium is growing, but may be increased in mechanically stressed cells as well. In adult myocardium, sarcomere addition occurs during hypertrophic growth. To date, there exists no report on sarcomere turnover in cardiomyopathies, but it seems likely that it should be altered due to different protein-protein binding affinities and mechanic stability of the sarcomere. Besides, cardiomyocyte turnover might be altered, and the addition of new cardiomyocytes would require sarcomere disposition as well. Therefore, sarcomere reconstruction in the cTnI$^{\Delta K184}$ mouse model was investigated.

Exclusively in TG mice, evidence was found for sarcomere reconstruction, i.e. de novo synethesis and putatively intra-sarcomeric addition of myofilaments. Areas of sarcomere de novo synthesis were found both at the cell periphery and between already existing myofibrils. Such areas have been characterized mainly in cell culture systems and in whole embryonic chicken heart rudiments (Dabiri et al., 1997; Ehler & Perriard, 2000; Sanger et al., 2000). In early stages of myofi-

brillogenesis Z-bodies form, consisting of α-actinin, the Z-disc end (N-terminus) of titin and filamentous actin. Those premyofibrils (or I–Z–I–brushes, depending on the favored hypothesis) presumably detach from the plasma membrane upon tension generation and subsequently integrate the C-termini of titin and thick filaments (now named nascent myofibrils), which still
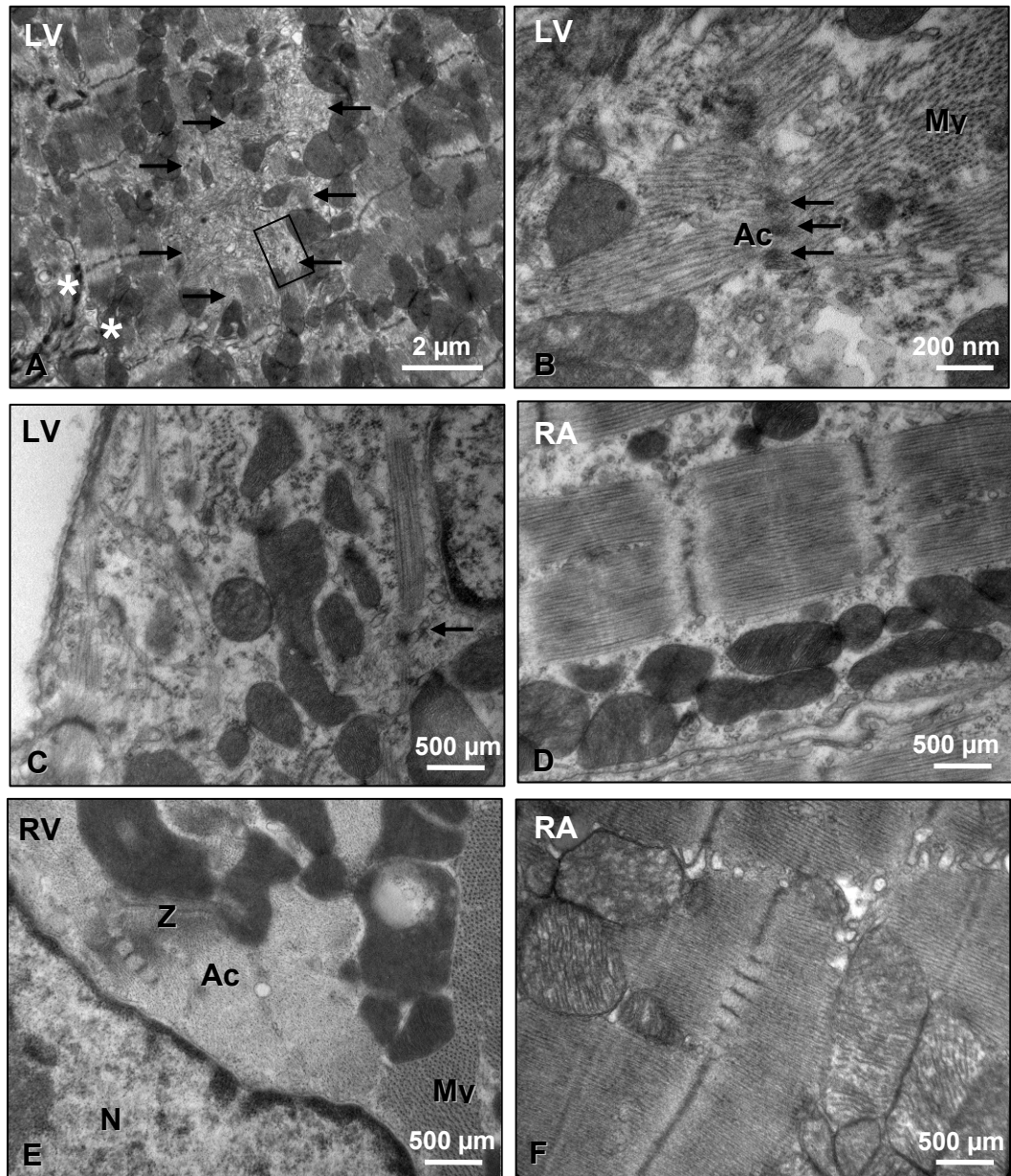
Fig. 3.14: Sarcomere reconstruction in hearts from TG TnI$^{\Delta K184}$mice. A, longitudinal section of a cardiomyocyte with an area of sarcomere regeneration (surrounded by arrows). In the left corner there is a double intercalated disc (asteriscs). **B,** high magnification of Z-Bodies (arrows) that are surrounded by thin filaments (pre-myofibrils) and thick filaments. **C,** addition of sarcomeres at the periphery of a cardiomyocyte. **D–F:** Later stages of myofibril development (nascent myofibrils) or addition of filaments to already existing sarcomeres. Neither of these structures has been found in nTG mice. Ac, actin. My, myosin. N, nucleus. Z, Z-Band. LV, left ventricle; RV, right ventricle; RA; right atrium

lack an uninterrupted Z-band. When the disposition of the Z-band is completed (i.e. when it consists of the typical, uninterrupted protein network) and contraction begins, myofibril maturity is reached.

In fig. 3.14, several stages of myofibrillogenesis are shown. In fig. 3.14 E, the regularly interrupted Z-band lies close to a nucleus, that is, at the cell center. This picture was interpreted as an addition of sarcomeres to already existing myofibrils. Myofibrillogenesis was not only found in ventricles, but also in atria from TG mice.

Besides myofibrillogenesis, otherwisely affected Z-bands (e.g. thickened, irregular) were found, as have been reported in cases of sarcomere degradation (Nepomnyashchikh, 2001; Moses & Claycomb, 1989), (fig. 3.13 and fig. 3.12 F).

3.6.4 Sarcoplasmic reticulum

Alteration in calcium cycling are common in sarcomere cardiomyopathies. For the cTnI$^{\Delta K183}$ mutation, it is currently unknown whether Ca^{2+} cycling is aberrant from healthy myocardium. Therefore, we investigated the structure of the major Ca^{2+}-compartment of the cardiomyocyte, the sarcoplasmic reticulum (SR).

SR was usually inconspicuous in TG mice. In some cardiomyocytes however, it showed a marked disorganization (fig. 3.15). In those cells, abundance and volume of either network SR (nSR) or corbular SR (cSR) or both was increased and the overall appearance was bullous, making it difficult to distinguish one from the other lest triad feet were detectable. These abnormalities were found both in ventricles and in atria.
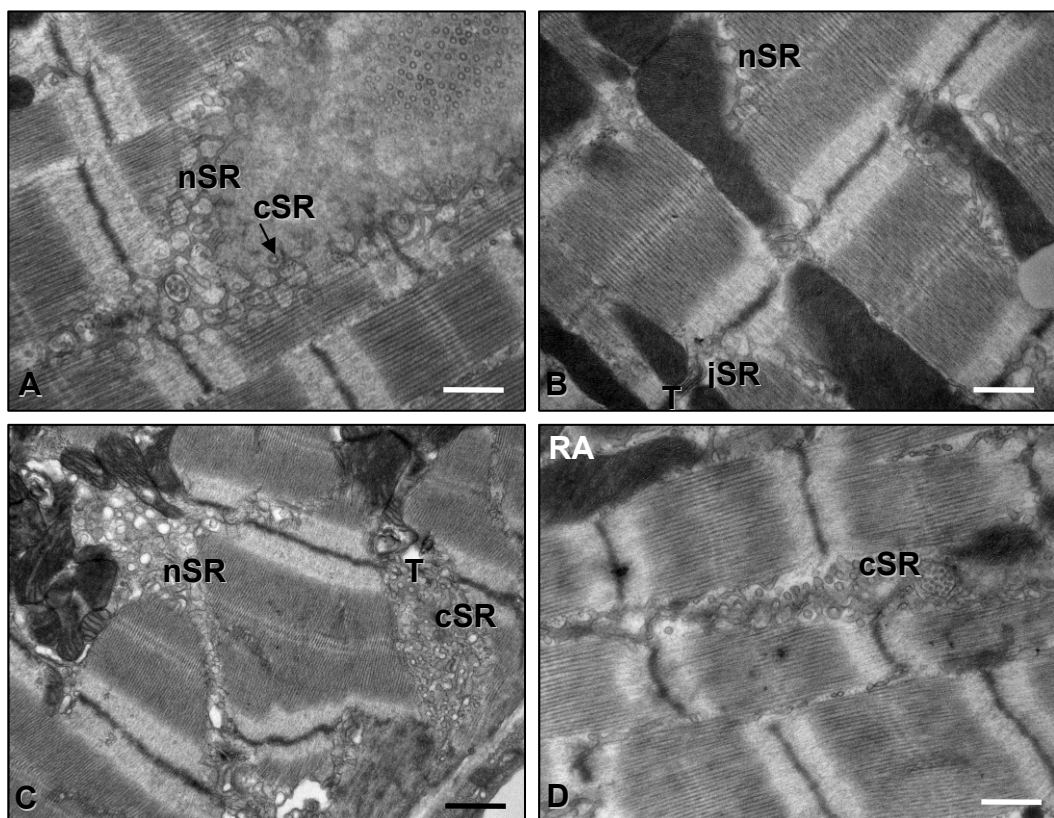
Fig. 3.15: Sarcoplasmic reticulum and cytoplasm. A, typical sarcomeres from an nTG mouse with surrounding network SR that is composed of nearly pentagonal and hexagonal meshes and corbular SR cisternae that protrude from the nSR (left ventricle). **B**, TG mouse, normally developped nSR (most cells). Left ventricle. Corbular SR invisible in this section. Junctional SR with T-tubule show typical location (close to Z-disc), arrangement and dimension. **C**. TG. Extremely pronounced nSR, disorganized and voluminous SR-cisternae. Diameter of T-tubules enlarged. Bullous and abundant cSR. Note sarcomere disarray (left ventricle). **D**, TG. A similar appearance of cSR is within the range of a healthy atrial cardiomyocyte. RA, right atrium. Scale bar 500 nm.

3.6.5 Myofilament spacing

Myofilament spacing appeared to be more irregular in TG compared to nTG mice as can be seen both in longitudinal as well as in cross sections of myofibrils at high magnifications (fig. 3.16 and 3. 17). This finding has yet to be validated by measurements of myofilament distances.
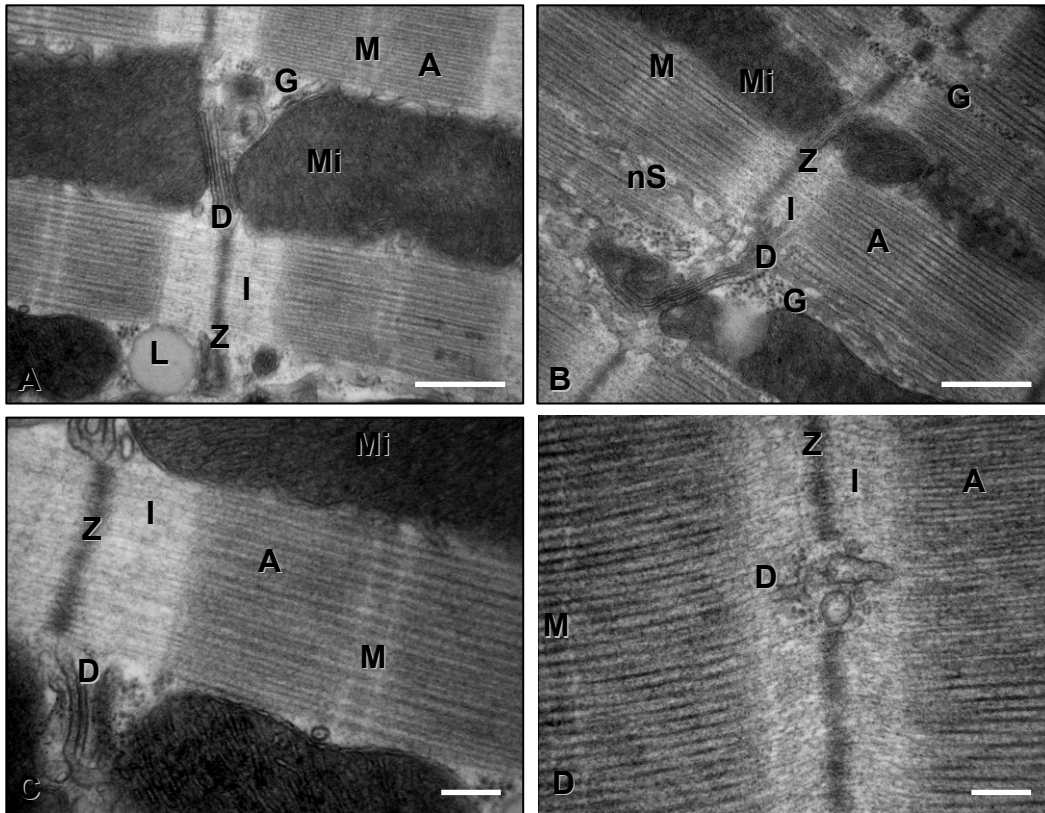
Fig. 3.16: Longitudinal sections of sarcomeres from nTG (left column) and TG TnI$^{\Delta K184}$ mice (right column). T-Tubles of nTG (**A, C**) and TG (**B, D**) mice are equally wide.Note that in **B** and **D**, filament spacing is slightly more irregular. Z, Z-band. A, A-band. I, I-band. M, M-band. Dy, dyad composed of T-tubule and junctional SR. nSR, network SR. Mi, mitochondrion. L, lipid droplet, G, glycogen. Scale bar in A, B 500 nm; in C, D 200 nm.
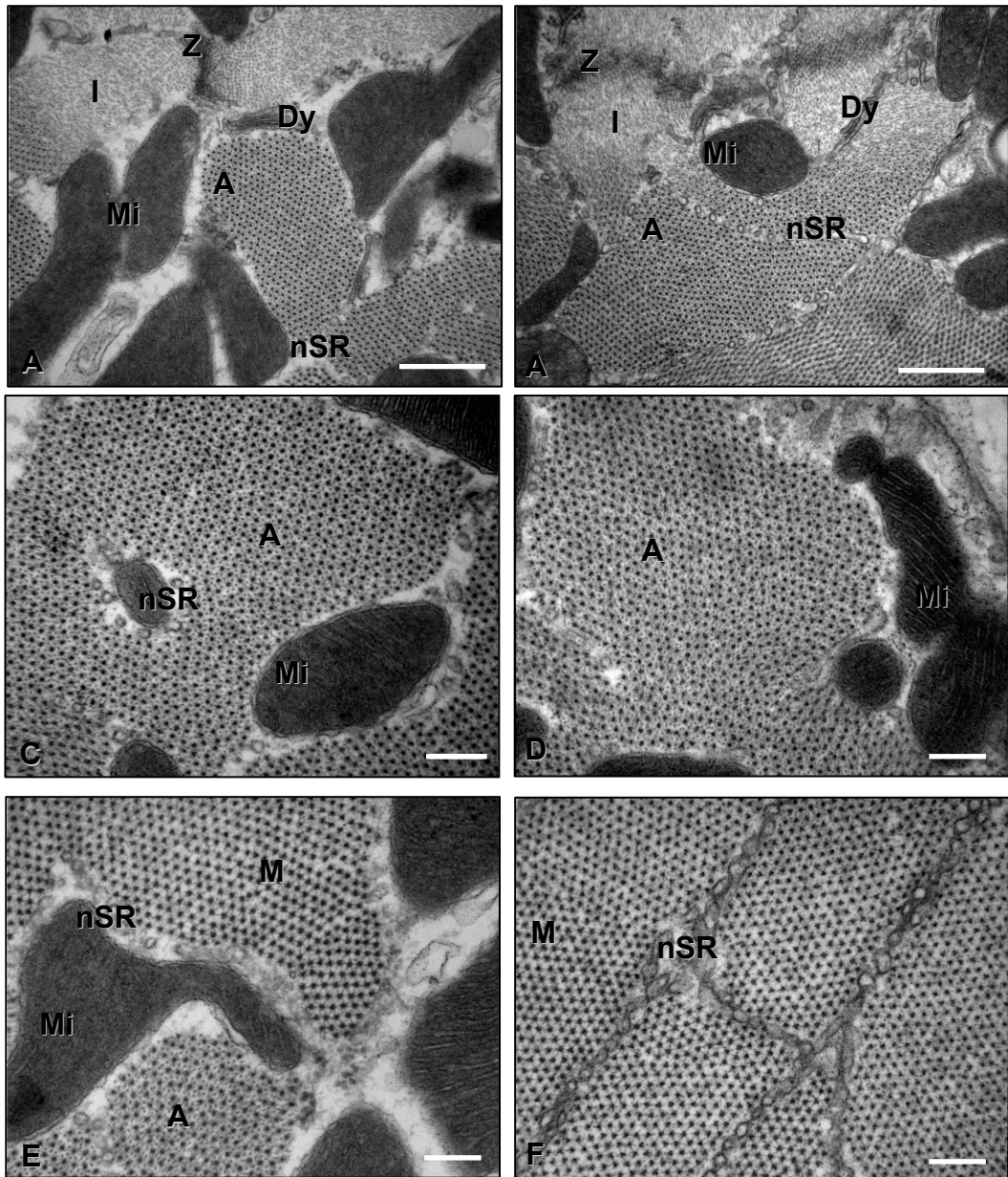
Fig. 3.17: Oblique/cross sections of sarcomeres from nTG (left column) and TG TnI$^{\Delta K184}$ mice (right column). A, B, survey micrograph showing Z-Band, I-Band (actin) and part of the A-Band where myosin and actin overlap. The distance between single filaments is more irregular in TG mice. C and D, cross section of A-Band, thick and thin filaments. Filament spacing is more irregular in TG mice. E and F, cross section at position of M-Band. Both nTG and TG mice have equally well ordered filament distances. Z, Z-band. A, A-band. I, I-band. M, M-band. Dy, dyad composed of T-tubule and junctional SR. nSR, network SR. Mi, mitochondrion.

3.6.6 Contraction bands and intercalated discs

In TG mice 10 months of age, a considerable amount of cells displaying contraction bands was found (not shown). In addition, over- and hypercontracted sarcomeres were common despite cardiac arrest in diastole (not shown). In mice 12 weeks of age, mean sarcomere lengths were not decreased.
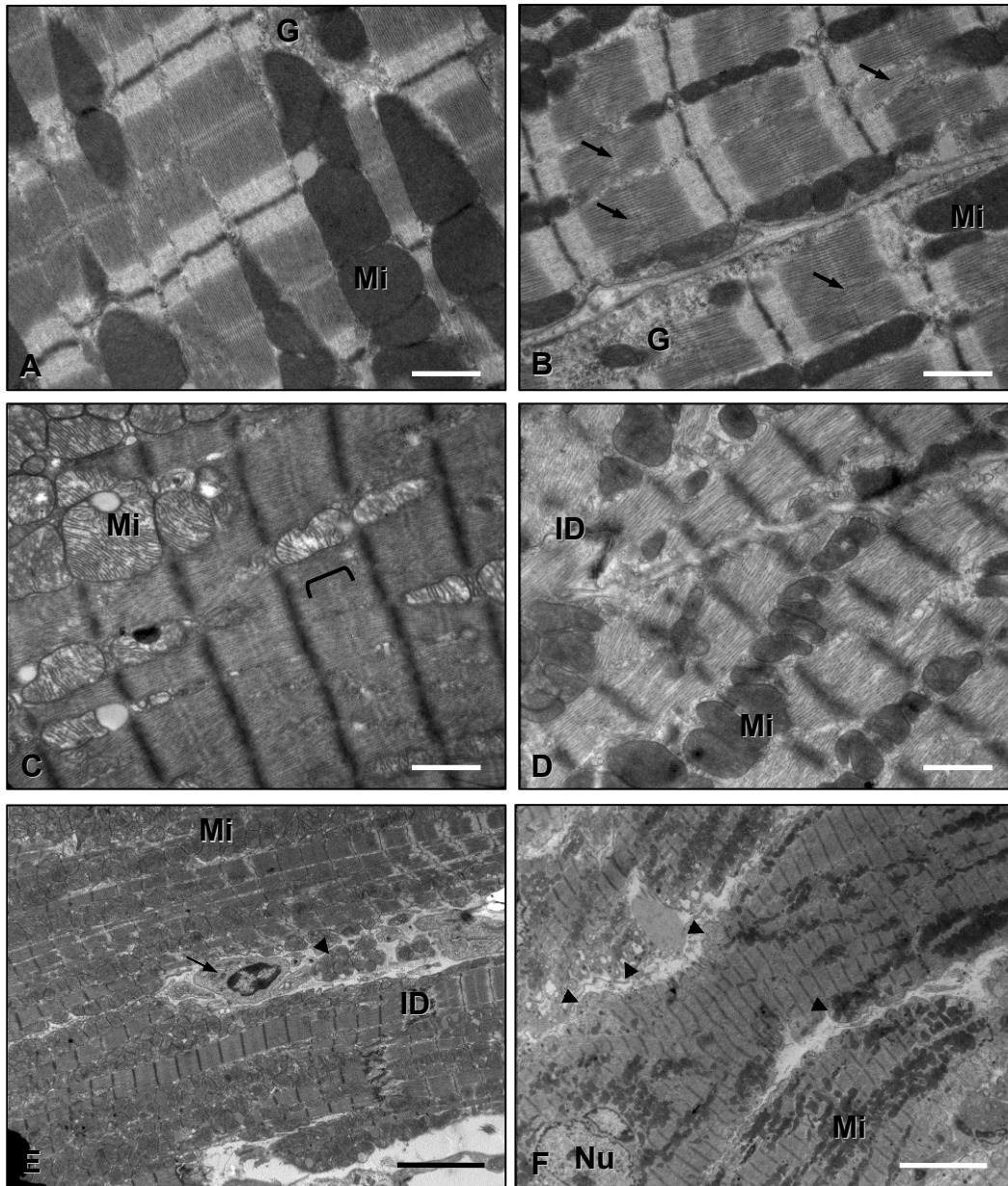
Fig. 3.18: Longitudinal section of sarcomeres from nTG (A) and TG TnI$^{\Delta K184}$ mice (B-F). A, accurately arranged sarcomeres in relaxed state, surrounded by mitochondria with tightly aligned cristae and dark matrix. **B**, equally well organized sarcomeres from TG mice. Nevertheless, not the slightly irregular filament spacing (arrows). **C**, overcontracted sarcomeres with invisible I-bands due to double overlap of actin and myosin (bracket). A-band may contact Z-band. Z-Band is thickened. Mitochondria have a light matrix and interrupted and widely spaced cristae. **D**, contraction bands, invisible I-Band, strongly shortened A-Band, disorganziation of myofilaments, hardly visible M-band, mitochondria are slightly lighter and have loosened cristae. Z-band is thickened and has a bushy appearance. **E** and **F,** survey micrograph of areas with overcontracted cells. Note the accumulation of swollen mitochondria and the collapsed capillary (arrow) in **E** and the packages of cyotoplasma with and without mitochondria forming buds at the cell periphery in **E** and **F** (arrowheads). Mi, mitochondria. Nu, nucleus of cardiomyocyte. G, Glycogen. ID, intercalated disc. Scale bars A–D 1 µm, E–F 5 µm.

Nevertheless, some cells displayed over- and hypercontracted cells not explicable by cutting edge effects.

In those cells, packages of cytoplasm filled with cell organelles formed buds at the cell periphery. Besides, swollen mitochondria with loosened cristae were present. In addition, intercalated discs that were inconspicuous in relaxed cells from TG mice, occasionally showed signs of tearing (fig. 3.19).

Fig. 3.19: Intercalated discs from nTG (A, C) and TG TnI$^{\Delta K184}$ mice (B, D, E). A and **B**, cross section, **C–E** longitudinal section of intercalated discs. There are no visible diff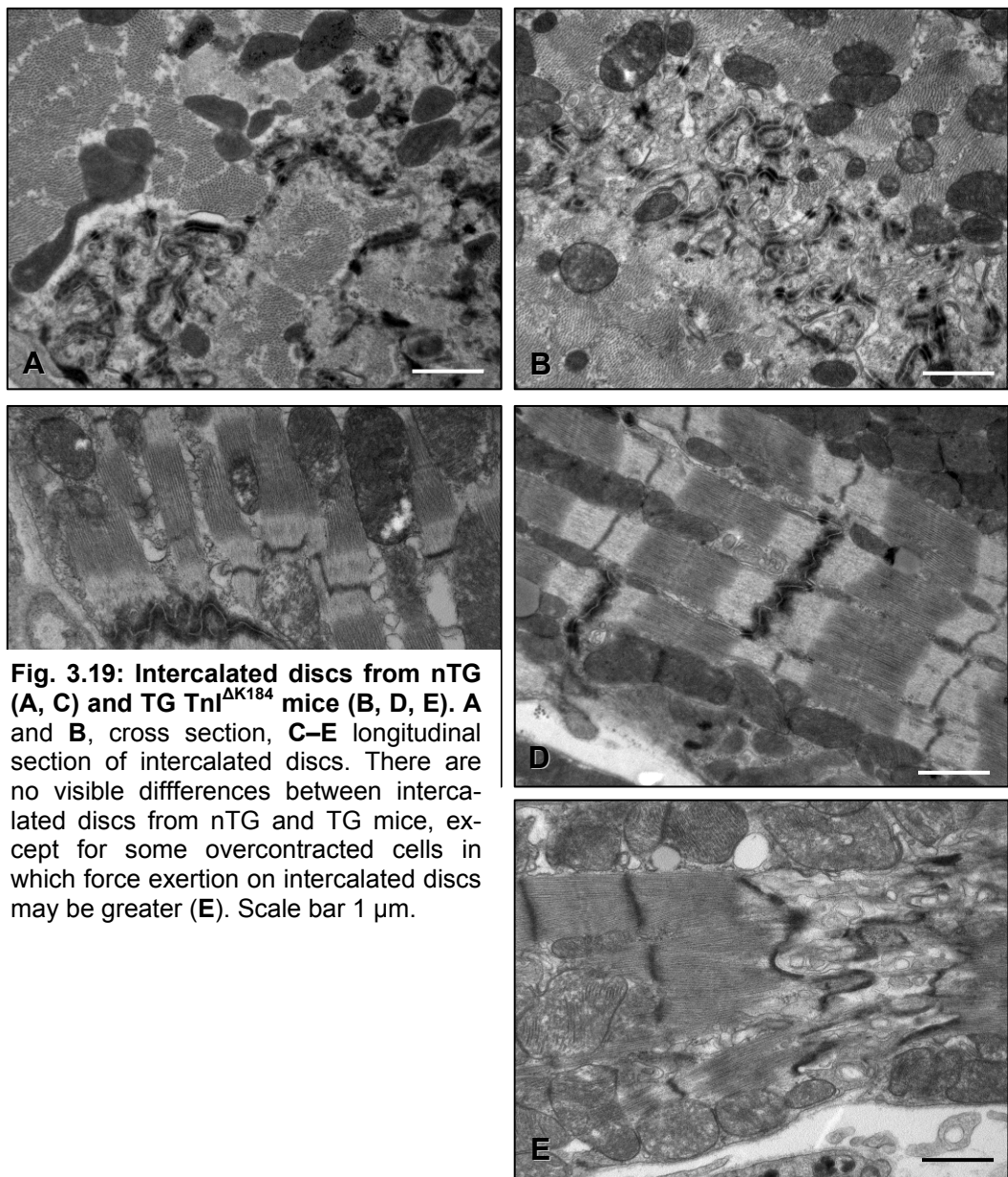ferences between intercalated discs from nTG and TG mice, except for some overcontracted cells in which force exertion on intercalated discs may be greater (**E**). Scale bar 1 µm.

3.7 Light and electron microscopic characterization of the atria

By contrast to the ventricles, atria were visibly enlarged in transgenic cTnI$^{\Delta K183}$ mice (fig. 3.20). In addition, atrial mass was increased by 26 % in 12 week old transgenic mice from line E, indicating that cellular or interstitial growth must have occured. Assessment of wall thickness was not readily achievable as it was highly variable due to the musculi pectinati that fortify parts of the free wall of both left and right atrium. Parts of atrial walls are rather thin (e. g. in gaps between Mm. pectinati) and others are thick (e. g. Mm. pectinati). Thus, the anisotropy of atria is even more pronounced than that of ventricles. Due to the small size of mice's atria, random systematic sampling is impossible, making quantitative (morphometric) statements questionable if not a large amount of animals are measured. Therefore, it was chosen to qualitatively compare the atria of TG and nTG mice. Paraffin sections in fig. 3.20 show the right and left atria from 12 week old TG and nTG mice stained with picrosirius red. To ensure comparability, longitudinal heart sections were made in position of the bicuspidal and aortic valves. Of note, both the atrial internal space as well as maximal atrial wall thickness was increased in transgenic mice in this position, which is a hint to an eccentric atrial growth.

As the increase in mass was more pronounced in the left atria than in the right atria, the thinnest, and thickest parts of the left atrial free walls of transgenic mice and their non-transgenic littermates were compared. Fig. 3.21 is a survey microphotograph of the most distal parts of the left auricles. The Mm. pectinati of transgenic mice were reinforced by more collagenous and/or reticular fibers (see arrows in fig. 3.21 B), and single ridges of the Mm. pectinati appeared to be thicker than those from non-transgenic littermates. In a higher magnification of a rather thin part of the left atrium (fig. 3.21), the increase in collagenous/reticular fortification of the Mm. pectinati was even more conspicuous (see arrows fig. 3.21 B, D). Besides, cardiomyocytes appeared to be enlarged. To confirm this impression atrial muscle cell diameter was measured both in transgenic and non-transgenic mice in (fig. 3.21 E, F) (n = 40 cells each) in a random systematic fashion.
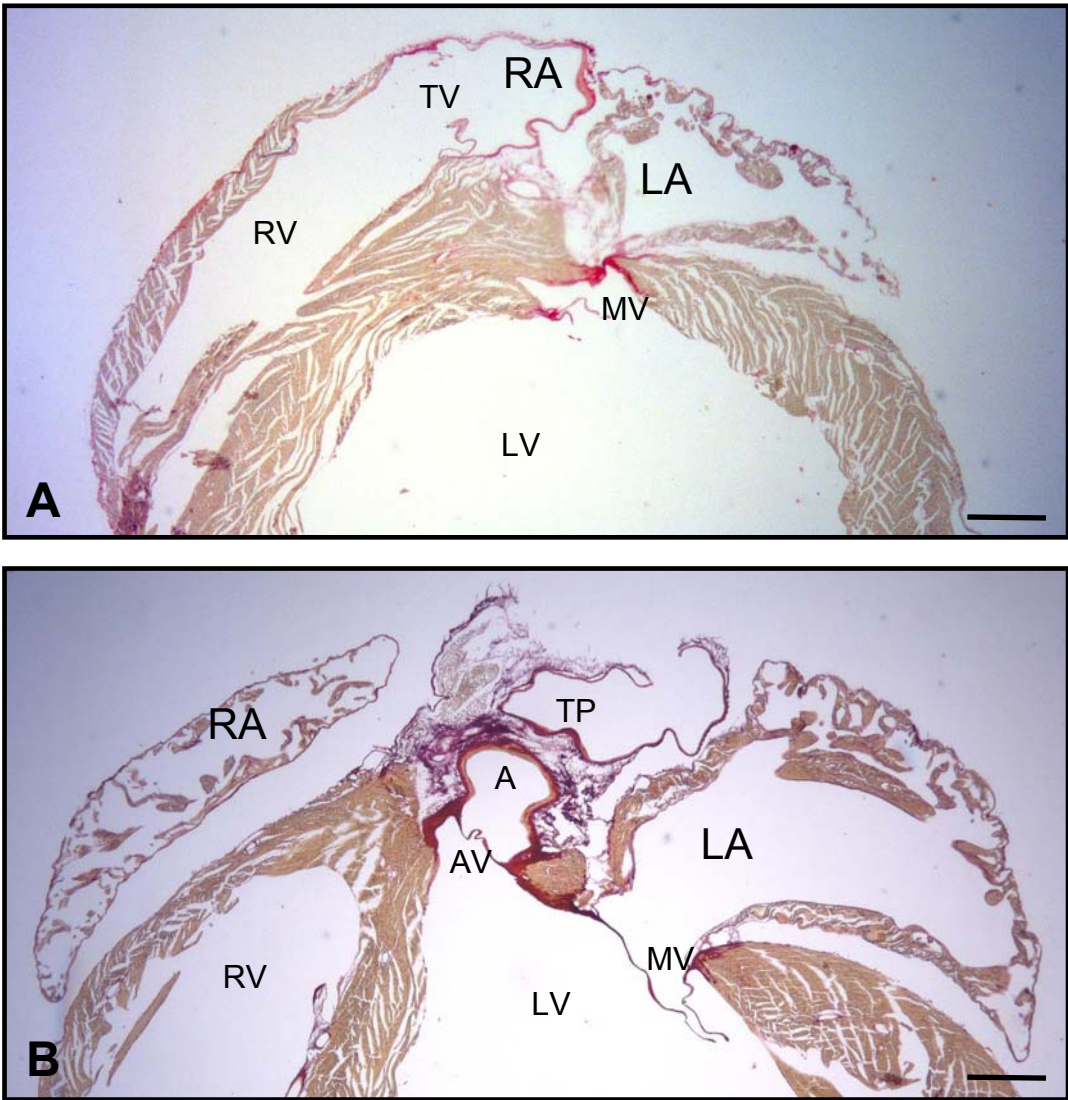
Fig. 3.20: Longitudinal paraffin sections (3 µm) of hearts from nTG (A) and TG (B) mice dyed with picrosirius red. The left atrium is increased. Note that the vetricular septum is not thickened in tg mice. LA: left atrium; RA, right atrium; LV: left ventricle; RV: right ventricle; TV: tricuspid valve; MV: mitral valve; AV: aortic valve; MV: mitral valve; A: Aorta; TP: Truncus pulmonalis. Scale bar 2 mm.
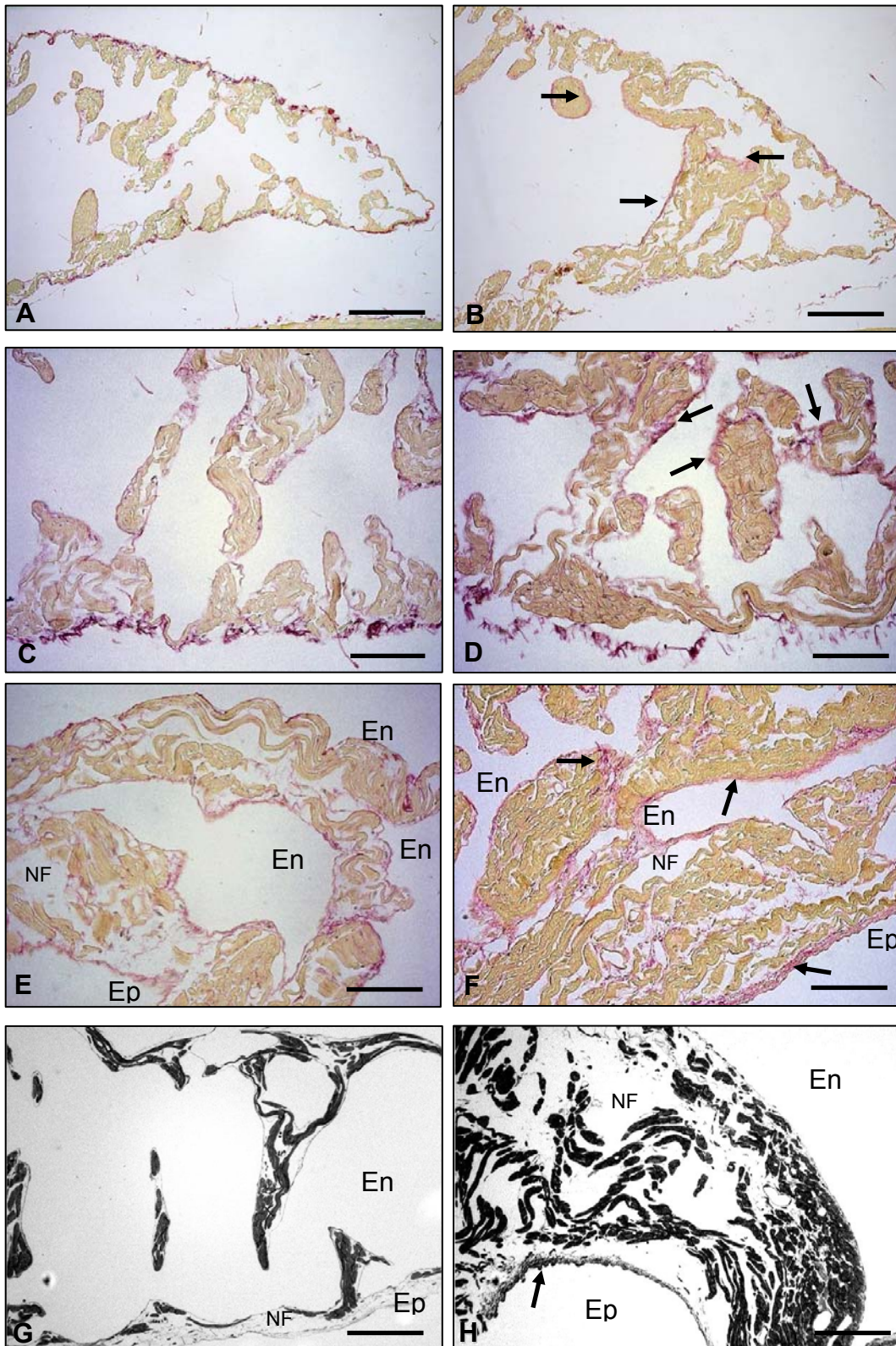
Fig. 3.21: Higher magnifications of left atria reveal increased cell size and increased amount of collagen and/or reticular fibers in TG mice. A–F: 3 µm paraffin sections, stained with picrosirius red. **A:** nTG; **B:** TG; Mm. pectinati account for differences in atrial wall thickness, so atrial walls from both nTG and TG mice have thinner and thicker areas. **C–F:** Comparison of each the thickest and thinnest wall parts from atria of nTG and TG mice at a higher magnification. **C-D:** areas of thin to medium wall thickness, **C:** nTG; D: TG; **E–F:** areas of greatest wall thickness. E: **nTG; F:** increased cell and interstitium size in TG mice. **G–H:** semithin sections (500 nm) of the thickest regions of left atrial walls. **G:** nTG; **H:** TG. Note the increase of non-fibrous extracellular matrix in addition to the fibrous meshwork. Arrows: increased fibrous material; En: inner atrial space (endocardial side); Ep: epicardial side, NF: non-fibrous extracellular matrix. Scale bars A–B 200 µm; C–H 50 µm.

The mean cellular diameter was 4.28 µm ± 0.38; in non-transgenic and 5.98 µm ± 0.49 in transgenic cTnI$^{\Delta K183}$ mice, that is a ~28 % increase in cardiomyocyte cell diameter. Of course, this measurement may not be considered representative and therefore only serves to assure a visual impression. Additionally, we have no information on atrial muscle cell length and thus, do not know if there is a change in length-width ratio in cardiomyocytes of the left atrium. However, the increase in extracellular fibrous material surrounding the Mm. pectinati is visible in fig. 3.21 F as well.

Fig. 3.21 G, H shows 500 nm semithin sections of left atria from 12 week old transgenic cTnI$^{\Delta K183}$ and non-transgenic mice fixed with PFA/glutaraldehyde dyed with methylene blue/azure. Here too, especially in the thick parts of the atrial wall an increase in reticular/collagen fibers surrounding the Mm. pectinati is visible. Furthermore, due to the difference in fixation it is conceivable from semithin sections that reticular fibers form a fine meshwork that lies in the extracellular matrix between single cardiomyocytes. As the extracellular space did not dye with methylene blue/azure, it probably mainly consists of water (jelly-like substance). This substance appears to be increased in transgenic animals (see fig. 3.21 C and D] in some parts of the atrial wall.

Electron microscopy revealed that the amount of elastic fibers underlying endocardial cells is considerably increased (fig. 3.22 A, B). Higher magnification of the subendocardial lamina propria showed that only the amount, but not the kind of fibers were altered (fig. 3.22 C, D). Also, endocardial cells appear thickened (fig. 3.22 B).
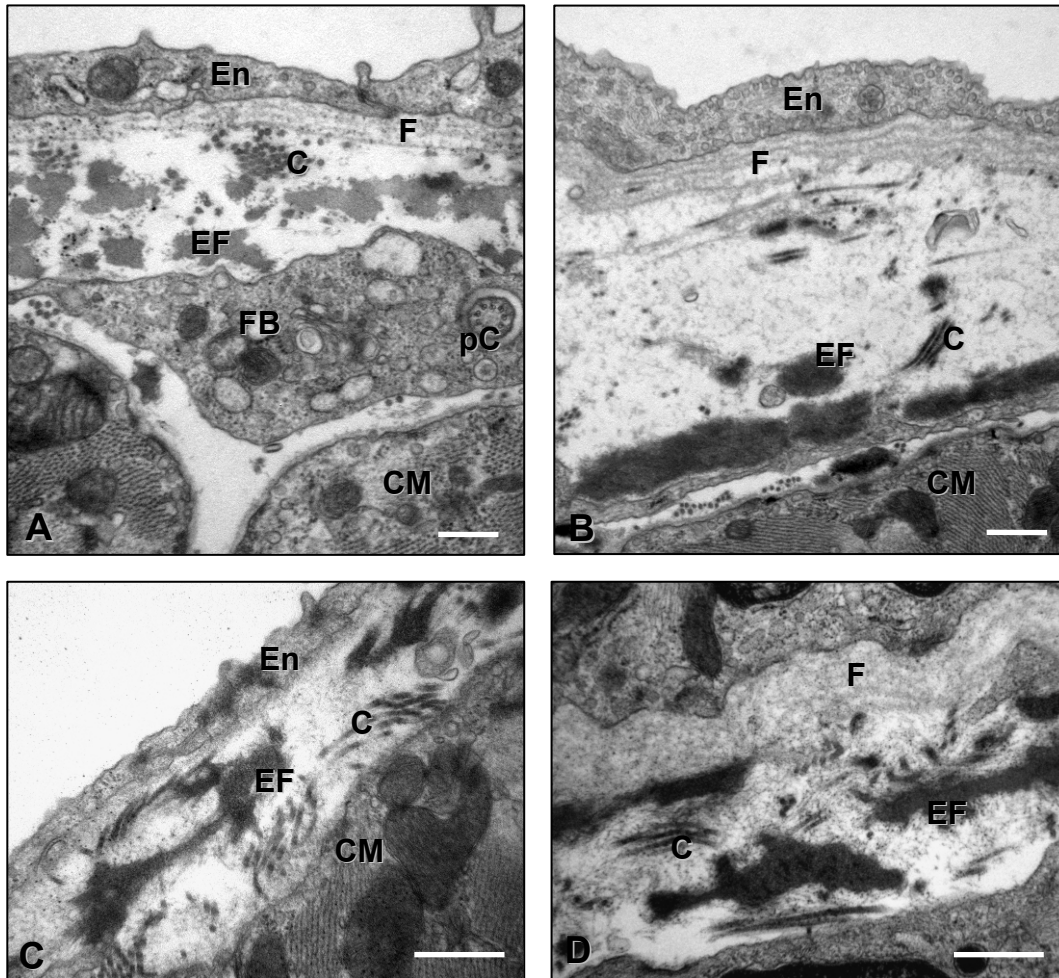
Fig. 3.22: Only the amount but not the kind of fibers is differerent in TG mice. A and **C**, nTG; **B** and **D**, TG. High magnification of extracellular matrix adjacent to atrial endocard. Directly under the endocardial cells there are 3 – 4 layers of non-collagenous, fibrous material, followed by an electron-penetrable fibroelastic layer containing a flocculent ground substance, collagen/reticular and elastic fibers. EF, elastic fibers. F, fibrous material. C, collagen fibers. pC, primary cilium. FB, fibroblast. CM, cardiomyocyte. En, endocardial cell. Scale bar 500 nm.

Atrial cardiomyocytes showed the same alterations that had been observed in ventricular heart muscle cells: folds, invaginations, irregular shape (fig. 3.23) sarcomere reconstruction (fig. 3.14 D, F, fig. 3.24 B), and most importantly, sarcomere disarray (fig. 3.24 B,), that was most pronounced in the right atria. We did not analyze filament spacing and intercalated discs. In summary, the major difference between cardiomyocytes from atria and from ventricles was their increased size relative to those from nTG littermates.
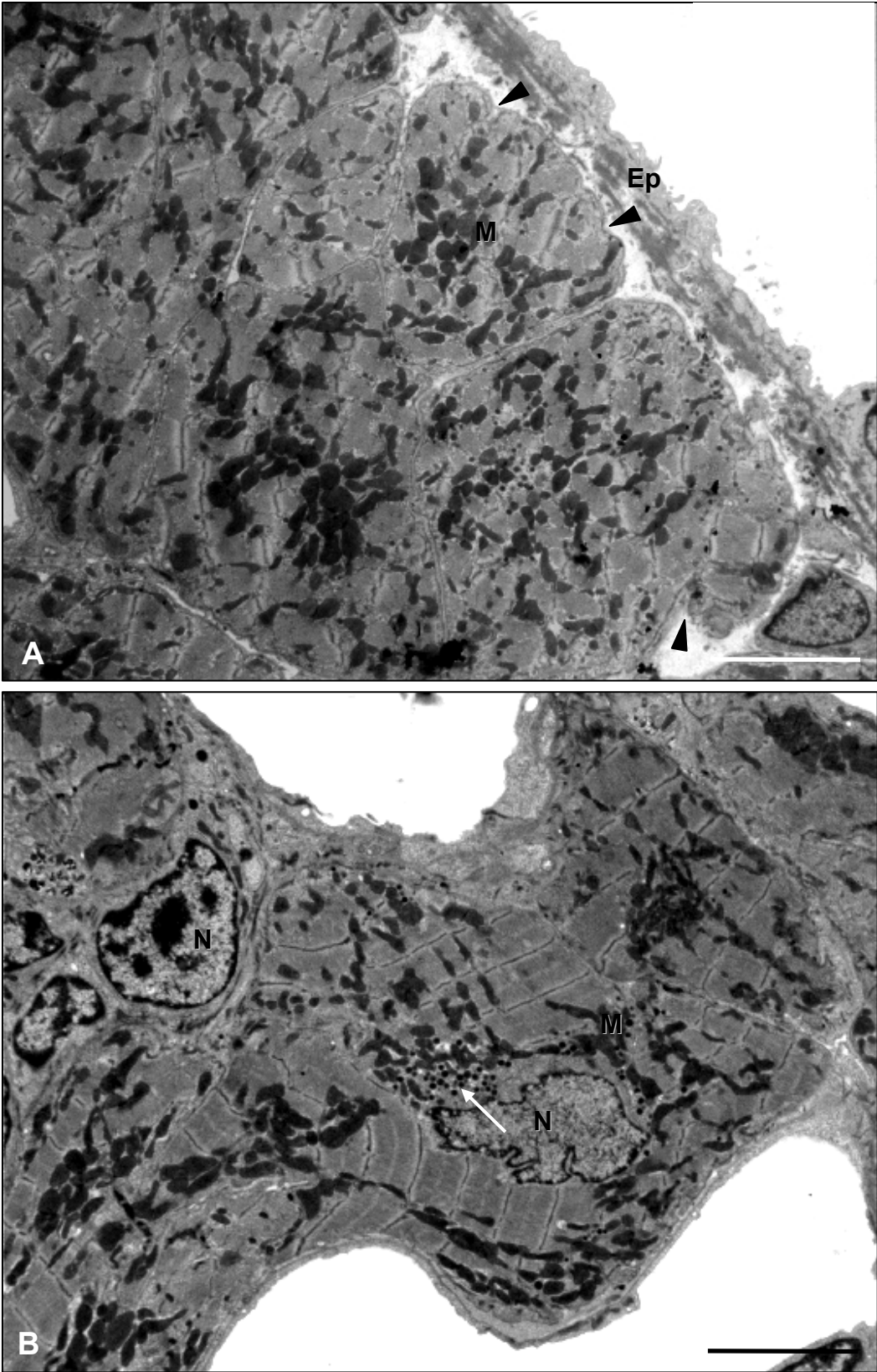
Fig. 3.23: Features of atrial cells from transgenic mice (1). A: cardiomyocytes with irregular surface. Invaginations and protrusions (arrowheads). Ep: epicardial cells; M: mitochondria; **B:** Large cardiomyocyte with sarcomere disarray. Contains inconspicous amounts of ANP-granula (Arrowhead) in perinuclear region. N: nucleus. Scale bars 5 μm.
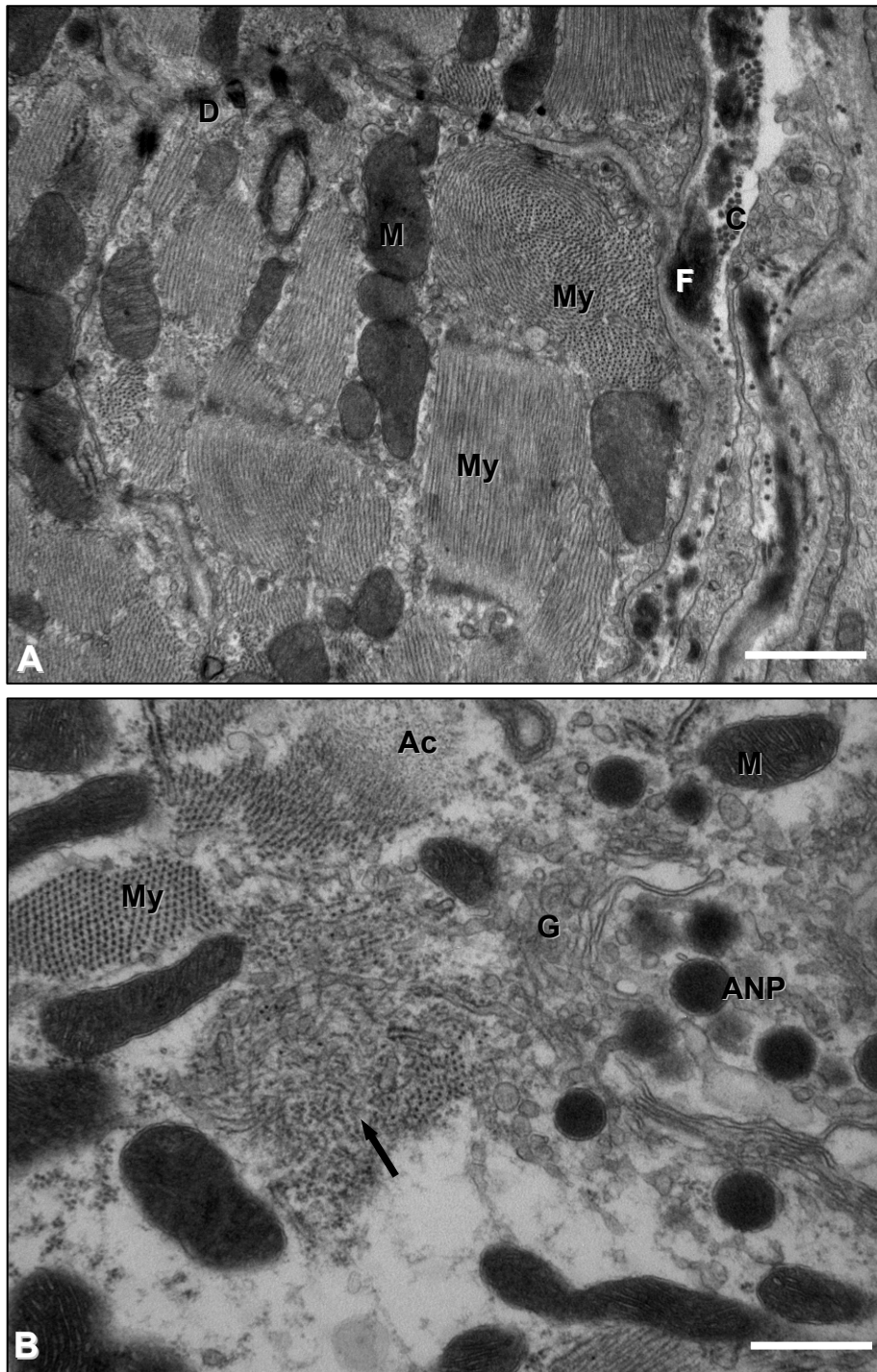
Fig. 3.24: Features of atrial cells from transgenic mice (2). A: Sarcomere disarray in an atrial cardiomyocyte from a transgenic TnI$^{\Delta K184}$ mouse. Myosin filaments are arranged perpedicular to each other. **B:** Reconstruction of sarcomeres in an atrial cardiomyocyte (arrow). D, desmosome. M, mitochondrion, My, myosin. Ac, actin. F, fibrous material. C, collagen fibers. G: golgi stacks. ZT, Z-tubule, ANP, granula containing atrial natriuretic peptide. Scale bar 1 μm.

4 Discussion

This is the first comprehensive morphological study on a cardiac troponin I mutation associated with hypertrophic cardiomyopathy, the lysine 183 deletion mutation (cTnI$^{\Delta K183}$), that lies in a mutational hotspot on Exon 7 of the *TNNI3* gene. Lysine 183 is located in a highly flexible C-terminal portion of cTnI required for full inhibitory function of actinomyosin interaction. This C-terminal portion toggles between actin and cTnC in dependance of the intracellular Ca^{2+}-concentration and thus is part of the molecular switch between diastole and systole. The scarcity of this nonetheless clinically most thoroughly investigated cTnI mutation makes it impossible to truly morphologically characterize it in humans. Therefore we resorted to a novel mouse model, cTnI$^{\Delta K184}$, kindly provided by the Institute of Vegetative Physiology, Cologne.

We ensured the comparability of hearts from nTG and TG mice by the following:

- usage of the same gender and age (male, 12 weeks of age)
- comparison of littermates (nTG and TG mice) to reduce the variability of the genetic background
- equal breeding conditions (free access to water and a standard normo-caloric diet, voluntary exercise without physical strain)
- heart arrest in diastole by perfusion with a Ca^{2+}-free Krebs-Henseleit solution containing procainhydrochloride
- adequate sampling procedure of heart probes (see below) used for morphometry
- morphometry was done without knowledge of the probe identity

Thus, it is assured that the observed morphological effects solely depend on the genotype and primary and secondary effects of the mutation.

Curiously, nearly all of the reported morpholological hallmarks for hypertrophic cardiomyopathy are missing in this mouse model, despite the unequivocal presence of gross morphological, tissue and fine structural heart abnormalities.

These heart abnormalities were found in all of the investigated TG mice and will be discussed in the following.

4.1 Small hearts or diastolic dysfunction?

The first striking abnormality of cTnI$^{\Delta K184}$ mice was the drastic reduction of heart size and weight (–22%). Body weight, by contrast, was only slightly decreased, and both TG and nTG mice had an otherwise healthy appearance.

The possible causes for these findings and the impact of the heart size reduction may have on the evaluation of the cTnI$^{\Delta K184}$ mouse model for hypertrophic cardiomyopathy will be discussed in later sections. Here, the focus lies on the impact the heart size reduction may have for the mouse as an organism and for the comparability of nTG and TG mice in physiological experiments.

The small hearts of the cTnI$^{\Delta K184}$ mice have a reduced filling volume (–19%, as determined by the *in vivo* diastolic left ventricular cavity diameter), but the ventricular wall thicknesses equal those from the normal sized hearts of nTG littermates, so that wall thickness to cavity diameter is greatly increased (+26%). This has two direct consequences:

1. The minimized cavity reduces the amount of blood that may *maximally* enter the ventricle during diastole (preload). Thus, also the amount of blood that may flow through the heart during each heart cycle is reduced, leading to a decrease in stroke volume.

2. Diastolic filling should be impeded, because the wall resistance to blood influx during diastole is greater in hearts with such a geometry, given that wall compliance (as predetermined by tissue composition, myofibrillar properties) is otherwise nearly equal.

With respect to the reduced cavity size and the increase of wall thickness to cavity diameter ratio, the hearts from cTnI$^{\Delta K184}$ mice in fact resemble those with a concentric hypertrophy. In hypertrophied hearts as can be often observed in HCM, left ventricular cavity size is often reduced as well, but the reason is mass increase instead of the mass decrease displayed by the cTnI$^{\Delta K184}$ mice (fig. 4.1). Diastolic dysfunction is one of the major physiological characteristics of individuals affected from HCM. A variety of recent studies provide evidence in support of alterations in the contractile apparatus itself as causative for diastolic dysfunction (summarized in LeWinter, 2005). Experiments with cardiac myofibrils isolated from cTnI$^{\Delta K184}$ mice point in the same direction: their passive stiffness is in-

creased. Besides, the time constant of force decay is significantly prolonged. This effect could be completely abrogated by administration of 2,3-butanedione monoxime, which prevents the formation of force-generating cross-bridges (B. Iorga, personal communication). However, it is currently unknown, how this relates to the much more complex system of the heart. It is nevertheless possible that the mutation potentiates the effect of a minimized heart. However, a diastolic dysfunction cannot be deduced if solely relying on the cavity size reduction and the increase in wall thickness to diameter ratio.

Concentric
hypertrophy

cTnI$^{\Delta K184}$
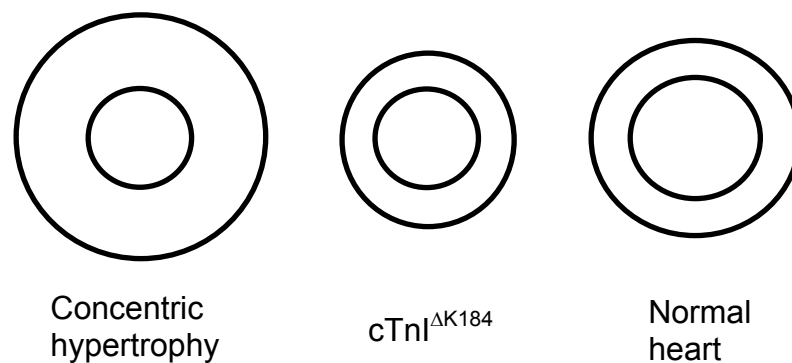
Normal
heart

Fig. 4.1: Schemes of left ventricular wall thickness and cavity diameter in concentric hypertrophy (as common in HCM), cTnI$^{\Delta K184}$ mice, and normal hearts.

In diastolic dysfunction, the decrease of preload is caused by a reduced ventricular compliance that countervails blood influx, leading to increased diastolic cavity pressures and to a ratio increase of early to late filling phase.

Thus, hard proof for a diastolic dysfunction could be only provided by left ventricular pressure measurements, either by insertion of a tip catheter in the left ventricle or alternatively, by Langendorff or whole heart experiments. To establish an altered ratio of early to late filling phase by non-invasive means, mouse doppler echocardiography would be the method of choice (Stypmann, 2007; Collins et al., 2003).

However, one gross anatomical feature of cTnI$^{\Delta K184}$ mice is a direct hint to blood afflux caused by stiffer left ventricles, the enlarged left atria. It is unlikely that the

atrial enlargement is a direct effect of the mutation (primary atrial hypertrophy), because in this case, both atria had to be enlarged. In any case, left atrial enlargement is a considerable health risk, because it promotes the formation of blood thrombi both directly and by promoting atrial fibrillation, and thereby, increases the risk for apoplexy. In recent literature, left atrial enlargement therefore is considered an important prognostic criterion (Abhayaratna et al., 2006).

Besides atrial enlargement, another aspect of the $cTnI^{\Delta K184}$ mice is the lower maximal cardiac output that follows from the small heart size, regardless of the degree of systolic function. It is not known whether other physiological parameters such as blood pressure or volume are affected by this. However, it is very likely that cardiac reserve is reduced, because other than heart weight, body weight is not altered in $cTnI^{\Delta K184}$ mice. With exercise experiments, this issue could be addressed. In addition, these investigations could clarify if with exercise, a secondary hypertrophy could be induced in $cTnI^{\Delta K184}$ mice or if the hearts show any pathological response as has been reported for other mouse models of HCM (Nguyen et al., 2007).

Eventually, the evaluation of any physiological experiment has to be taken with caution, because the different heart sizes may lead to diverging results that are not a direct consequence of the mutation.

4.2 Gain of systolic function

Also the systolic function is abnormal in $cTnI^{\Delta K184}$ mice, as it is drastically increased. This has been reported of in other mouse models for HCM as well as in humans affected by the disease (Iorga et al, 2008; Revera et al, 2008). This increase in systolic function is not caused by an increase of contractile elements due to cellular and heart mass gain, but again, heart geometry plays a part in it. According to the law of Laplace, the contractility resulting from a given wall tension is higher in hearts with a thicker wall to cavity diameter ratio. This should result in a higher pressure that acts on a smaller blood volume. So even if the contractility of the cardiomyocytes were not increased, this would result in an increased *organ* contractility, and even more so, as the heart has a more tapered shape. Indeed, the systolic wall thickening both in the left and in the right ventricle is strikingly increased. Additionally, the Ca^{2+}-sensitivity of force generation in isolated myofibrils and in skinned fibers is also higher in $cTnI^{\Delta K184}$ mice (B. Iorga

and I. Stehle, personal communication). This leads to fibril and fiber contraction at lower Ca^{2+}-concentrations. Given that other factors (such as Ca^{2+} cycling) are not altered, this could potentially lead to an earlier cellular contraction during systole. Thus, the small heart cavity, the relatively thicker walls and the direct effects of the mutation on contractility potentiate each other also in systole. This may be the case in both the left and right ventricles, as wall thickness gain is similar in both. The decreased cooperativity during contraction as determined with the skinned fiber studies (I. Stehle, personal communication) could however counteract blood ejection.

We have calculated the midwall circumference reduction during systole as a measure for contractility. In the $cTnI^{\Delta K184}$ mutant, circumference reduces by 27% from end-diastole to end-systole (compared to 19% in the nTG mice). This potentially has dramatic effects on sarcomere integrity: In the middle cardiomyocyte layer of left ventricular wall, cardiomyocytes are arranged nearly tangentially to cavity diameter. Therefore, circumference reduction can directly be converted into cellular and sarcomere shortening. If assuming maximally relaxed and pre-stretched sarcomeres during diastole (~2.1 µm), the resulting mean end-systolic sarcomeric length would be only 1.6 µm. At these values, sarcomeres are in a hypercontracted state which means that the thin filaments overlap with the thick filaments of the ipsilateral half-sarcomere and in addition, with the thick filaments of the contralateral half-sarcomere. That is, they cross the M-band at the center of the sarcomere. In addition, the thick filament approaches the ipsilateral Z-band. This overcontraction promotes the formation of contraction bands, irreversible protein agglutinations in the sarcomere.

At an increased work load, β-adrenergic stimulation, or under positive inotropic medication, all of which increase inotropy, cardiomyocytes from $cTnI^{\Delta K184}$ mice would overcontract with a greater probability than heart muscle cells from nTG mice. Cardiomyocytes with contraction bands, however, can neither contract nor relax, so they interfere both systolic and diastolic heart function. Besides, single cells or groups of cells could decay by contraction band necrosis or apoptosis. Such a cellular loss could contribute to heart minimization. However, the above values are only rough estimates for sarcomere length. For accurate measurements, it would be necessary e.g. to arrest the heart in systole and then, to directly measure sarcomere lengths. This has been done with dog's hearts in pio-

neer experiments (Sonnenblick et al., 1967; Ross et al., 1967], but will be difficult or impossible to adopt for the mouse due to its high heart rate. Other models such as heart contracture induced by barium chloride perfusion are difficult to evaluate because of the unnatural prolongation of contraction (Munch et al., 1980]. Alternatively, the correlation of Ca^{2+}-dependent force with sarcomere length could be determined by fixating skinned fibers at defined Ca^{2+}- concentrations. Some laboratories have isolated single adult cardiomyocytes and paced them by field stimulation. Cell and sarcomere lengths were measured by video edge detection with or without 2,3-butanedione monoxime (BDM) administration; sarcomere lengths were measured in white light video images (Tardiff et al., 2007).

These considerations do not include possible alternative explanations as fiber slippage (which is unlikely because of lateral cell contacts mediated by integrins), and altered fiber orientation during contraction compared to nTG mice

In summary, the observed hypercontractility has a variety of potentially adverse effects. The extremely reduced chamber size in systole itself is problematic, because it is the starting point of diastole. Especially the high frequency of the mouse heart beat could aggravate the situation because it may not give the sarcomeres enough time for full relaxation so that the diastolic tone could be raised.

4.3 Absence of classical morphological hallmarks for hypertrophic cardiomyopathy

For human myocardium affected by the $cTnI^{\Delta K183}$ mutation, there exist no light and electron microscopic studies, only macroscopic data that show a great variability up to a complete lack of a morphological phenotype in some carriers of the K183del mutation (Kokado et al, 2000). Therefore, the $cTnI^{\Delta K184}$ mouse model provides the first data on structural effects of the mutatation.

The $cTnI^{\Delta K184}$ mice lacked the classical morphological hallmarks for hypertrophic cardiomyopathy: cardiomyocyte hypertrophy, interstitial fibrosis, and cellular disarray. In considering these results it should however be kept in mind that most information on the phenotype is skewed by the patient selection of tertiary centers. These studies mostly refer only to patients who have a distinct phenotype, and to patients with the most common mutations. Indeed, mutations in 3 proteins (β-myosin heavy chain, myosin binding protein-C, and troponin T) make up the

majority of HCM cases, while the contribution of cTnI mutations amounts to only ~3%. This has been reported in several independent studies worldwide (Doolan et al., 2005; Wu et al., 2004, Mogensen et al., 2003). Therefore it remains questionable if the cTnI$^{\Delta K183}$ mutation, too, displays microscopic features in humans that have been identified for the obscure mixture of genotypes that the classical morphological studies on HCM naturally had to be based on (Maron, 1975; Maron, 1979).

A very recent and intriguing study analyzed the extent of a restrictive filling in HCM (Kubo et al., 2007). A total of ~1.5% of hearts with hypertrophic cardiomyopathy had a restrictive filling pattern. About half were caused by mutations in beta-myosin heavy chain, and half by mutations in TnI. In spite of the caution that has to be taken in interpreting such data resulting from a single study, compared to the total incidence of TnI mutations in HCM worldwide (see above), the TnI fraction of HCM-related RCM is considerable.

4.3.1 Cardiomyocyte size, number and heart weight

The first of the three classical hallmarks of hypertrophic cardiomyopathy that is missing in the cTnI$^{\Delta K184}$ mice is cardiomyocyte hypertrophy.

Since the discovery of sarcomere mutations as final causes for HCM it became evident that cardiomyocyte hypertrophy (transverse diameter of 20 – 70 μm) is not an essential attribute of the disease that is named after it (Tardiff, 2005). The analogous is known for morphological changes in dilated cardiomyopathy (Chang & Potter, 2005), which can be associated with some mutations in sarcomere proteins, among other causes. Besides, both hypertrophic and dilated phenotypes have been reported in restrictive cardiomyopathy (Angelini et al., 1997), which is characterized functionally by a pronounced diastolic dysfunction.

We determined cardiomyocyte size by two means: First, we determined cell area in systematically randomized semithin sections that allowed precise determination of cell boundaries including intercalated discs, which are difficult to identify in paraffin or cryo-sections. By systematic randomization on all levels of investigation (tissue sampling, photography, image analysis by the point counting/linear grid method), the division of the estimated total cardiomyocyte area by cell number results in an unbiased cardiomyocyte area. Second, we directly measured cell diameter at the level or close by the nucleus. Interestingly, we found a high

consistency of these results: In the left ventricle, cell area and diameter were not altered in mice carrying the mutation (–2% and –6%, respectively). However, in the right ventricle, both cardiomyocyte area and diameter were reduced (–12% and –15%, respectively). Thus it is likely that in the right ventricles, cell area reduction is caused by cell thinning rather than cell shortening, whereas in the left ventricles, cell length-to-width ratio is unchanged.

In the ventricle walls, cardiomyocyte minimal caliper diameters (as can be measured in cross, longitudinal and oblique sections) are arranged perpendicular to the wall tangentials, irrespective of the orientation of the cellular longitudinal axis. In this context, it is of interest that the *in vivo* diastolic left ventricular wall thickness is unaltered in the left ventricle (–0.8%), but decreased in the right ventricles (–14%). Again, these values match well the left and right ventricular cell diameter. So it could be hypothesized that in the right ventricles, cellular thinning leads to wall thinning, whereas in the left ventricles, the unaltered cell thickness sustains left ventricular wall thickness.

However, several other factors contribute to wall thickness: capillary number and diameter, interstitial area fraction, and cardiomycyte number.

These factors will be first discussed for the left ventricle: capillary number per cardiomyocyte and diameter are equal in TG and nTG mice. So if total cardiomyocyte numbers are equal, capillary number and diameter have no part in diastolic wall thickness change. Nevertheless, this is very likely not the case, because although in the left ventricle, cardiomyocyte size and diameter are unaltered, left ventricular weight is drastically reduced (–17%). As cardiomyocytes make up the majority of the ventricular mass, it is most likely that in the left ventricles of cTnI$^{\Delta K184}$ mice, there are *less* cardiomyocytes. As capillary per cardiomyocyte number equals one, though, capillary number must be reduced accordingly, and perhaps adaptationally.

The interstitium (or pericapillary edema, see below) contributes to the wall dimensions. In cTnI$^{\Delta K184}$ mice, it is significantly increased, though the extend is small (+4%). In effect, as cardiomyocyte size is unchanged, this makes it even more likely that cardiomyocyte loss occurs in the left ventricle.

In the right ventricle, capillary to cardiomyocyte ratio equals one, and capillary dimensions are not altered, so both can be neglected. Cellular size and diameter

are equally reduced. The right ventricular weight reduction nearly equals the reduction in cell size (–13%), while the interstitial space is nearly unaltered (–3%). As we have no direct measurements of cell number, we cannot exclude the loss of a small amount of cardiomyocytes in the right ventricle. However, cardiomyocyte size reduction should play the main part in right ventricular weight (and wall thickness) reduction.

The difference between the predominant cellular loss in the left ventricle and the size reduction in the right ventricle is somewhat difficult to explain. However, it is quite uncommon to even regard the right ventricle, which may have distinct pathomechanisms both due to the low pressures and to the altered hemodynamics. Being short of data on this issue, we are tempted to speculate: cardiomyocyte sizes of the right ventricles are reduced in comparison to the left ventricles both in mutation carriers *and* in nTG mice. As form follows function, this might be an expression of the comparatively decreased right ventricular pressure and afterload. Right ventricular cardiomyocyte size/diameter would in this sense, represent a physiological adaptation to its utilization. If the cardiomyocytes from TG mice indeed overcontract, as indicated by the *in vivo* measurements, they may exert a greater force *per se*, so that a further cell diameter reduction may be an adaptational response to counterbalance this. To a lesser extent, this effect can be also seen in nTG mice, where right ventricular cardiomyocytes are likewise smaller than those from the high pressure left ventricle. Another aspect concerns the differential transition of isoform expression of sarcomere proteins in the right and left ventricle. In mice, this transition occurs first in the left and only later, in the right ventricle (Zammit et al., 2000). This might also influence contractile efficiency, sarcomere stability and eventually, cell size.

In the left ventricle from cTnI$^{\Delta K184}$ mice, cell number appears to be reduced. The size of the remaining cardiomyocytes may simply be adaptational, too, i.e. just sufficient to exert the heart work needed to subsist the body under the given circumstances.

Causes for cardiomyocyte loss could lie in the greater torque, shear stress and/or pressure exerted especially on the subendocardial cardiomyocyte layer during (hyper-)contraction. Besides, sarcomere overcontraction may lead to contraction band necrosis.

To identify the cause(s) for this loss it would be important to first know the time frame of the highest rate of cellular demise. With this information it would be easier to identify the possible mechanisms.

In mice, cardiac troponin I substitutes the slow skeletal isoform within the first three weeks after birth (Siedner at al., 2003). Preliminary western blot experiments suggest equal substitution rates in cTnI$^{\Delta K184}$ mice, albeit the protein signal has not been quantified yet (N. Blaudeck, personal communication). So cellular loss in hearts from cTnI$^{\Delta K184}$ mice probably does not take place before birth but could start soon after the transgene expression has commenced. Very recent determinations of heart weights from mice three weeks of age indeed show already significantly reduced heart weights (N. Blaudeck, personal communication), but the weight reduction seems to continue thereafter with a lower rate.

There are several mechanisms by which the cellular loss could occur: oncosis is characterized by an early disruption of plasma membrane and is considered to be an "accidental" form of cellular decay that involves inflammation and phagocytosis by mononuclear phagocytes, macrophages and monocytes. From oncosis, necrosis usually follows that involves groups of cells and leads to substitution fibrosis (Jugdutt & Idiko, 2005). As fibrosis is not an attribute of cTnI$^{\Delta K184}$ mice it is unlikely that oncosis plays a major part in the cell demise of the left ventricle.

Instead, cells seem to vanish without trace, which is known for apoptosis and autophagy, both being forms of programmed cell death. In both apoptosis and autophagy, cell membranes stay intact. In apoptosis, the remains of the cell are phagocytosed by neighbouring cells such as other cardiomyocytes, fibroblasts, endothelial cells, and vascular smooth muscle cells. The whole process of apoptosis of a single cardiomyocyte may not take more than 1–3 hours (Gavrieli et al., 1992; Potten, 1996) which explains why it is important to first identify the developmental phase with the highest heart weight reduction. In our electron microscopic investigations, we indeed have found some apoptotic cardiomyocytes in cTnI$^{\Delta K184}$ mice (while in nTG mice we found none), but they appeared to be singular findings (not shown). However, it is possible that earlier in postnatal development, the apoptosis rate is much higher.

Autophagy represents a dysbalance between organelle synthesis and turnover and has been reported of in failing hearts (Schaper & Kostin, 2005, Kostin et al.,

2003) where it appears to be associated to the ubiquitin/proteasome system. However, to our knowledge it has not been determined yet for hypertrophic cardiomyopathy. Cellular material is packed into double membrane vacuoles that fuse with lysosomes to autophagic vacuoles. After protein degradation, autophagic vacuoles are then exocytosed.

There are several ways to determine both apoptosis and autophagy. The gold standard for apoptosis is electron microscopy which may identify all of its phases but it should be combined with methods that allow a higher sample throughput (e.g TUNEL, Caspase-3 immunohistochemistry) but have a lower sensitivity or specificity (for an overview on currently available methods see Rodriguez & Schaper, 2005).

State-of-the-art *in vivo* experiments for apoptosis detection make use of annexin-V labelled to fluorescent or technetium-99m and real-time imaging both in men and mice (Kietselaer et al., 2007; Kietselaer, 2003 a; 2003 b; Dumont et al., 2001; Dumont et al., 2000). The detection of biotin-labeled Annexin-V tissue in paraffin sections may also be used in combination with TUNEL (van den Eijnde et al., 1997).

By contrast, the left atria are increased and display hypertrophied cells. Left atrial weight is also increased (N. Blaudeck, personal communication). As stated above, this is indicative for an adaptation to an increased left ventricular diastolic pressure. The atria specific isoform expression of myosin light chains (MLC1A and MLC2A) (Schaub et al, 1998; Miyata et al, 2000; Reiser et al., 2001) might not contribute to this difference to the ventricles, because only the left atria are hypertrophied.

4.3.2 Lack of fibrosis

The second hallmark of hypertrophic cardiomyopathy is interstitial fibrosis which the cTnI$^{\Delta K184}$ mouse model likewise lacks. Notably, fibrosis is considered a secondary and rather unspecific effect in hypertrophic cardiomyopathy and besides, it is common in other diseases as well.

Interstitial fibrosis is an accumulation of collagen fibrils between cardiomyocytes and cardiomyocytes and capillaries. Collagen composition in HCM may have an altered collagen fiber morphology (Shirani et al., 2000) and an increase in colla-

gen may exacerbate small vessel disease that is common in HCM. Several stimuli promote interstitial fibrosis, i.e. angiotensin II or TNF-alpha, and the signaling pathways are shared to a certain extend with hypertrophic signaling. Nevertheless, independent fibrosis or hypertrophy may also occur independently.

Instead, the enlarged interstitial space in absence of collagen fibrils characterizes the cTnI$^{\Delta K184}$ mouse. This constitutes an interstitial edema, that may increase diffusion distances from capillaries to cardiomyocytes. Such edemas are rather known from dilated myocardium. In areas with massive edema, lateral cardiomyocyte contacts should be affected.

The augmentation of fibrous material in the atria that accompanies cardiomyocyte hypertrophy likely is a secondary adaptation to increased load.

4.3.3 Cardiomyocyte disarray

In HCM, cardiomyocytes are often bizarrely shaped, which means that they lack the regular rod-shaped structure but instead, have a rather stellate shape and sometimes large branches. In addition, cardiomyocytes are arranged obliquely or perpendicular to adjacent cells. This is called "cellular disarray". The percentage of disarray required to constitute an HCM-like appearance is ~5 – 10%, depending on the author (Maron & Roberts, 1979; Davies, 1984). Mostly, however, the extent is much higher (~30%) (Maron et al., 1992). Clearly, the very mild and focal disarray as exhibited by the cTnI$^{\Delta 184}$ mice is well below the reported fractions. While hypertrophy and interstitial fibrosis are known to occur in many heart diseases, cardiomyocyte disarray is usually referred to as highly suggestive of HCM and when absent, "diagnosis (of HCM) should be questioned" (Seidman, 2006) But what may be true for humans must not necessarily apply for mice. Then again, some patients diagnosed with RCM in the Mogensen study displayed the common morphological triad of HCM, i.e. cardiomyocyte disarray, hypertrophy, and interstitial fibrosis (Mogensen, 2003).

So either the diagnostic value of cellular disarray is lower than usually stated or cTnI mutation-based HCM and RCM are closer related to each other than cTnI-mutation based cardiomyopathy and HCM as currently defined. Clearly, more data e.g. as provided by research on animal models are needed for a secure classification.

We have no explanation for the lack of cardiomyocyte disarray in cTnI$^{\Delta K184}$ mice, but it should be kept in mind that there exist no data on the absence or presence of disarray in human cTnI$^{\Delta K183}$ carriers. Of the four other transgenic animal models that express cTnI mutations associated with hypertrophic or restrictive cardiomyopathy only the cTnI^{R203S} mouse displays disarray. Like the cTnI$^{\Delta K184}$ mouse, the cTnI^{R146G} mouse model does not show any cardiomyocyte disarray, if mice are held without physical strain (James et al., 2000). The analogous rabbit model likewise does not display myocyte disarray and fibrosis at a young age (Sanbe et al., 2005). Only rabbits advanced in age (18 months) do so, but even then disarray remains localized to the apex and some parts of the septum. The microscopic morphology of the R192H mutation has only been superficially investigated and the authors do not give any information on the absence or presence of disarray (Du et al., 2006). In summary, the cTnI$^{\Delta K184}$ mouse model is not the only one lacking cardiomyocyte disarray.

Both the causes and the consequences of cardiomyocyte disarray are unknown, although several proposals have been made. However, it seems likely that it should be closely related to sarcomere disarray (see below). The extensive cellular disarray in TnT mutation based cardiomyopathies coincides with the high incidence of sudden cardiac death, however (Varnava et al., 2001), which is why it has been related to ventricular arrhythmia. However, the extent of cardiomyocyte disarray does not correlate with wall thickness (Maron et al., 1979), so hypertrophy and disarray are probably induced differently.

4.4 Blood supply

We have not found any hints for a limited blood supply in the diastolic hearts. While the capillary diameters both in the right and left ventricles from cTnI$^{\Delta K184}$ mice equalled those from nTG littermates, the capillary to cardiomyocyte ratio was one. Thus, if in the left ventricles, the cardiomyocyte number were reduced, the capillary number must have abated accordingly. As the simple capillary to cardiomyocyte number is not sufficient to evaluate blood supply, we additionally determined the mean capillary density and calculated the mean diffusion distances in the myocardium therefrom. Here, we equally did not find any significant difference.

However, we found a significant pericapillary edema in cTnI$^{\Delta K184}$ mice, which we estimated as the mean capillary-to-cardiomyocyte distance. Pericapillary edema have adverse effects on myocardial functioning, e.g. contributes to substance leakage from the capillaries and alters ventricle compliance (Boyle et al., 2007).

4.5 Ultrastructural abormalities that characterize both ventricles and atria of cTnI$^{\Delta K184}$ mice

The ultrastructural abnormalities we found in cTnI$^{\Delta K184}$ mice may be separated in those that exclusively occur in the ventricles and those that are present both in the ventricles and the atria. It is reasonable to make such a distinction because ubiquitously present alterations are more likely to be direct effects of the mutation.

In cTnI$^{\Delta K184}$ mice, two features were present in both right and left heart chambers and atria. These alterations were situated at the location of the mutation, the sarcomeres, which further supports the idea of a direct effect of the mutation: sarcomere disarray and sarcomere reconstruction.

4.5.1 Sarcomere disarray: a consequence of altered stretch signaling?

We have not quantified the extend of sarcomere disarray, but it was not restricted to disarrayed cardiomyocytes. Hence it seems likely that sarcomere disarray precedes cellular disarray. The genesis of sarcomere disarray is still unknown, but several mechanisms are possible:

1. It could be a consequence of fallacious sarcomere construction or sarcomere instability (see below) that may lead to false anchoring of sarcomeres via the M-band and the Z-disc to costameres at the plasma membrane and via the Z-discs to the intercalated discs. Additionally or alternatively,

2. It could follow from tension or torque due to the increased heart contractility. It is known from cell culture experiments that cardiomyocytes align according to cyclic stretch signals (Simpson et al., 1996; Gopalan, 2003). If torque increases due to overcontraction, the force vector of tension rotates relative to the cell. This could lead to contradictory stretch signals during contraction, leading to a loss of cellular "sense of orientation" and to more misalignment of newly added sarcomeres during cardiomyocyte growth. Stretch in direction of the short axis of aligned cardiomyocytes in culture (intercalated discs were present) resulted in deterioration of sarcomeres not dissimilar to the disarrayed sarcomeres of a subpopulation of cardiomyocytes from cTnI$^{\Delta K184}$ mice (Simpson et al., 1999). Currently,

there is a vivid interest in how stretch changes are translated into hypertrophy signaling by structures containing stretch sensors such as the Z-disc, titin and the M-band (Linke, 2008; Cooper, 2006; Pyle und Solaro, 2004; Agarkova und Perriard, 2005; Frank et al., 2006) . It is possible that stretch links hypertrophy and disarray in some sarcomere cardiomyopathies.

4.5.2 Sarcomere reconstruction: decreased stability of the sarcomere?

We observed altererations in the Z-disc of sarcomeres that were highly suggestive for sarcomere reconstruction. Sarcomere genesis has been investigated in hypertrophic cells and from growing cardiomyocytes in culture. It begins by accumulation of Z-band material (Z-bodies), surrounded by thin filaments. Those I–Z–I- brushes or premyofibrils give rise to new sarcomeres (Dabiri et al., 1997; Ehler & Perriard, 2000; Sanger et al., 2000). As the new sarcomeres integrate, several Z-bodies with surrounding thin filaments combine to Z-bands. We have documented several phases of this gradual process. In developing cells, addition of new sarcomeres usually starts at the plasma membrane. During longitudinal growth, sarcomeres are added at the end of an existing myofibril, whereas during transversal growth, they are added on the side. It is not known how sarcomere repair takes place but such a repair mechanism should be economic for the cardiomyocyte.

The observed sarcomere reconstruction or repair may result from an altered stability of the sarcomere due to the lysine 184 deletion in cTnI. Lysine 184 lies in the second, flexible actin binding domain and its absence may alter the actin binding affinity of cTnI and besides, it might subtly change the configuration of the whole troponin complex, thereby altering its stability. This could have several consequences:

1. Troponin I is probably involved in actin configuration relative to myosin in a putative "closed state" of the crossbridge cycle. In the closed state actin is weakly bound to myosin without force generation (Gordon et al, 2000). The mutation could alter the stability of this state and/or the mechanical stability of the sarcomere, thereby increasing the probability of sarcomere damage or destruction. A decreased sarcomere stability could also contribute to the lowered cooperativity of contraction that has been observed

in skinned fiber experiments. The putatively more irregular filament spacing fits into this picture.

2. Second, it could alter the turnover rate of cTnI (and perhaps additional proteins of the sarcomere). The turnover rate of native cTnI is 3.2 days (Michele et al., 1999), but for cTnI$^{\Delta K184}$ it has not been determined. Turnover rates of sarcomere proteins depend on the mechanical stability. An example for such an effect is the troponin T affinity for tropomyosin, that is higher during rigor, thus slowing the exchange rate (Solaro & Rarick, 1998) When a sarcomere protein is released from the sarcomere, it may be degraded within minutes (Russell et al., 2000). Of course, any increase of protein turnover is energy-costly.

4.6 Other ultrastructural abnormalities

Sarcomere overcontraction

Sarcomere overcontraction has been reported in several studies on HCM. We have found sarcomere overcontraction, hypercontraction (and contraction bands) only in a small subpopulation of cells. However, as we have arrested the hearts in a relaxed state by transcardiac infusion of a cardioplegic solution this is not a surprise and rather reflects the reliability of the experimental setting.

As necessary to assure complete perfusion and maximum preservation of ultra-structure we applied the mean arteriolar pressure of mice (~80 mm Hg) on the hearts, which is tenfold higher than the physiological diastolic pressure. Besides, the perfusion with the relaxation solution had a duration of 45 sec instead of the milliseconds of physiological heart relaxation in mice.

In vivo, sarcomeres could however be shortened due to their impaired relaxation kinetics even at diastolic Ca^{2+}-concentrations. For possible experimental approaches to this issue please refer to section 4.2.

Multiple intercalated discs and cellular folds/buds

Multiple intercalated discs were present in ventricular cardiomyocytes from cTnI$^{\Delta K184}$ mice. Multiple intercalated discs are intercellular junctions that are separated by a maximum of ten continuous sarcomeres and form the boundaries of lateral processes of cardiac muscle cells. They are believed to be induced by localized mechanical tension and may serve to reinforce the connection between

adjacent layers of muscle cells, thus possibly preventing slippage (Maron & Ferrans, 1978). Their presence supports the idea of an increased mechanical stress or torque on cardiomyocytes from cTnI$^{\Delta K184}$ mice, as does the presence of cellular folds and buds.

4.7 The cTnI$^{\Delta K184}$ mouse as a model for hypertrophic cardiomyopathy

In the present study, we investigated the morphology and fine structure of hearts from a mouse strain expressing a deletion mutation of cardiac inhibitory troponin, cTnI$^{\Delta K184}$.

The finding that none of the mice had hypertrophied hearts was within the range of the expected: the analogous mutation in the human protein, cTnI$^{\Delta K183}$, has been associated to familial hypertrophic cardiomyopathy in a series of clinical studies (Kimura et al., 1997, Kokado et al., 2000; Shimizu et al., 2002a, 2002b), but disease presentation is highly variable. Especially hypertrophy is only a sporadic and variable phenomenon; apical hypertrophy, typical hypertrophy and complete absence of hypertrophy may even occur in the same family. So cTnI$^{\Delta K183}$ based cardiomyopathy obviously belongs to the "atypical" HCM diseases in which hypertrophy is not the cardinal symptom although the disease is named after it. In fact, the discovery of atypical forms (in a variety of protein mutations) has led to a shift in disease perception, so that currently, the existence of a disease causing sarcomere protein is of greater diagnostic relevance than the presence of heart hypertrophy. Hypertrophy itself is widely regarded a secondary effect regulated by a variety of factors.

However, there exists no report on human mutation carriers who have minimized hearts as we have consistently found in the cTnI$^{\Delta K184}$ mice and that has been found in another mouse model for HCM, the cTnT^{R92Q} mouse (Tardiff et al., 1999). This might either reflect that heart minimization does not occur at all in humans carrying the mutation, or that it has never been systematically investigated. In any case, heart size reduction is not a diagnostic criterion in HCM. In this context it might also be important that all the studies were carried out in Japan so that the patients who were included in the studies mostly had an Asian ethnicity. This might also explain the abundance of apical hypertrophy as it is much more common in oriental populations (Maron, 2002). In this respect it is of interest that so far, the cTnI$^{\Delta K183}$ mutation has been reported of in only one other

clinical study on HCM outside Japan with 3 affected individuals (Mogensen et al., 2004), although the incidence of TnI mutations appears to be equal (~ 3 %) in different countries (Doolan et al., 2005; Wu et al., 2004; Cheng, 2005; Mogensen et al., 2004). So the lack of hypertrophy and perhaps even a reduction of heart size might be more abundant in non-Japanese populations, thus leading to under-diagnosis/representation of the $cTnI^{\Delta K183}$ mutation. Ethnic (and gender) differences in phenotypic presentation are common in HCM (Maron et al, 2003), which makes this assumption more likely. Ethnicity and gender differences are but an expression of the sensitivity of the disease to genetic modifiers. After all, the hypertrophy sometimes identified in humans may be only one of many possible morphological phenotypes of the mutation.

So if the idea of what the original (human) morphological phenotype comprises has not been or cannot be clearly defined, the phenotype of the mouse must not surprise.

Mouse models of three other cardiomyopathy-related cTnI mutations $cTnI^{R145G}$, $cTnI^{G203S}$ and $cTnI^{R192H}$ have been generated (James et al., 2000; Tsoutsman et al., 2006; Du et al., 2006). The $cTnI^{R145G}$ and the $cTnI^{G203S}$ mutation have been related to hypertrophic cardiomyopathy by the *TNNI3* gene sequence analysis in 184 unrelated patients followed by family studies (Kimura et al., 1997). The resulting morphological information yielded by these tedious investigations are based on 5 ($cTnI^{R145G}$) and respectively, 3 individuals ($cTnI^{G203S}$): all patients with the R145G mutation belonged to one large Korean family and displayed a classical left ventricular hypertrophy, whereas all of the 3 patients who carried the G203S mutation had an apical hypertrophy that was accompanied by a Wolff-Parkinson-White syndrome. The association of the $cTnI^{R192H}$ mutation to restrictive cardiomyopathy is based on the data of only one patient (Mogensen et al., 2003), whose parents did not have the mutation, constituting a *de novo* mutation. Consequently, the co-segregation of the phenotype with this mutation has not been shown.

Therefore, the evaluation of how accurately the model resembles the original is impossible. The $cTnI^{R146G}$ mouse, for example, has a dose-dependent phenotype. The single mouse line that survived when heterogeneously expressing the mutated gene developed a morphological phenotype only in parous mice, but

even in these mice, hypertrophy remained absent. This led to the speculation that it was due to the mouse as a model not reflecting precisely enough the human conditions. Indeed, the altered protein composition of ventricular sarcomeres, cardiomyocyte Ca^{2+}-cycling and heart rate supports this opinion. However, the consecutively generated rabbit model also displayed only a mild hypertrophy in 1-2 year old animals, which was accompanied by fibrosis and focal cellular abnormalities (Sanbe et al., 2005). By contrast, the cTnI^{G203S} mutation does lead to a classical hypertrophy in mice, but the human counterparts developed apical hypertrophy and Wolff-Parkinson-White syndrome instead. Upon exercise at an age when the hypertrophy has not yet developed though, these mice *failed* to show a hypertrophic response (Nguyen et al., 2007).

The RCM-related cTnI^{R192H} mouse has not been extensively investigated. It does not exhibit hypertrophy, but heart weights are not presented. The authors interprete their ultrasound data as a diastolic dysfunction. If one critically re-evaluates the data presented for this mouse model it becomes obvious though, that this mouse, too, must have a reduced heart weight: wall thickness is unaltered and both systolic *and* diastolic cavity dimensions are reduced, just as in the cTnI$^{\Delta K184}$ mouse. From this it logically follows that total heart size must be reduced. As the authors only present end-systolic and end-diastolic cavity dimensions and not the ratio of early-to-late filling phase or alternatively, pressure development over time, their diagnosis of a diastlic dysfunction is questionable. Besides, it is doubtful if the degree of diastolic dysfunction or of diastolic ventricle pressures necessary to constitute a restrictive cardiomyopathy has ever been determined in mice.

In any case, hypertrophy and a restrictive filling pattern are not contradictory findings: in human RCM, normal cardiomyocyte size, and hypertrophied and dilated forms have been reported (Angelini et al., 1997). As RCM is an extremely rare disease and only currently, several TnI mutations have been identified that cause RCM (see above), no information on the specificity of the (ultra-) structural phenotype for sarcomere-based RCM exists.

In summary, the relationship between model and clinically scantly characterized original is weakly determined in all of the cTnI animal models so far. For this reason, the value of a model for a rare mutation cannot be based on the accuracy of

the reproduction. Instead, only the quality of the subsequent investigations on such a complex system as an animal model represents is decisive. Subsequent to the thorough investigation of the basic phenotype, the identification of genetic and environmental enhancers of adverse effects of the disease would be of clinical importance.

None of these mutations has been investigated in a different mouse strain. Besides being time and money costly to generate the mutation in several mouse strains for direct comparability, the expression rate of the different strains would have to match well because of the dose dependency of the effects. An alternative would be to cross in a different mouse strain. This has been done in a model where a transgenic tropomyosin (tm) mouse model (Tm^{E180G}) for hypertrophic cardiomyopathy was mated with a second transgenic mouse model expressing a chimeric alpha-/beta-TM protein that decreases calcium sensitivity in transgenic mouse cardiac myofilaments [Jagatheesan et al., 2007]

4.8 The state of the $cTnI^{\Delta K184}$ mouse

Like the other cTnI mouse models, the $cTnI^{\Delta K184}$ mice show a high reproducibility of their morphological and physiological phenotype. In other words, the phenotype seems to be stable, given that the genetic background, nutrition and physical strain are equal.

In comparison to humans carrying the $cTnI^{\Delta K184}$ mutation, the malignance of the disease appears to be reduced in mice. At least for the inbred mouse strain under investigation it may be stated that the disease represents itself not as malign as anticipated from the clinical studies in humans, as longevity does not seem to be reduced (N. Blaudeck, personal communication) and as the mice have an overall healthy appearance. However, we have identified several factors which indicate that the mice are in a compensated, albeit vulnerable physiological state:

1. The heart and chamber minimization signifies a reduced cardiac reserve

2. The increased ventricular circumference (and sarcomere) shortening may reduce the maximally possible relaxation during diastole and besides, lead to cellular decay due to greater probability of contraction band necrosis

3. Sarcomere disarray and reconstruction may constitute a reduced sar-
   comere stability and turnover

4. Cellular loss may decrease the regenerative capacity of hearts from
   cTnI$^{\Delta K184}$ mice

5. The pericapillary edema in the myocardium from cTnI$^{\Delta K184}$ mice may alter
   ventricular compliance and reduce the tissue integrity.

5 Summary

Familial hypertrophic cardiomyopathies (HCM) are highly variable in their clinical presentation. Classically, three morphological cardinal symptoms are mentioned: 1. ventricular hypertrophy, 2. interstitial fibrosis and 3. cardiomyocyte disarray. The mouse model investigated in the scope of this dissertation carries the $cTnI^{\Delta K184}$ mutation (deletion at amino acid position 184 of the cardiac isoform of the inhibitory troponin subunit), which has been related to the development of HCM as have > 450 other sarcomere protein mutations. However, $cTnI^{\Delta K184}$ mice did not show any of the three cardinal features although the expression of the mutated protein exceeded 90% of total cTnI.

On average, hearts from $cTnI^{\Delta K184}$-mice were 22% lighter than those from their non-transgenic (nTG) brothers although body weights were equal. Relative to the left ventricular (LV) inner diameter the LV wall from $cTnI^{\Delta K184}$ mice was ~26% thicker, which affects heart geometry and contractility. Analysis of magnetic resonance images from anesthetized mice revealed a stronger contraction of hearts from $cTnI^{\Delta K184}$ mice. In TG mice, the midwall wall circumference reduced by 27% during systole, whereas in nTG mice it reduced only by 19%. Consequently, systolic shortening of sarcomeres should be in the same range, as sarcomere length is directly proportional to midwall diameter. From this follows a regular maximal contraction of sarcomeres even at physical rest which cannot be further augmented under physical strain.

To investigate the underlying cause for heart weight reduction the ventricles were morphometrically investigated. There was no difference in LV cardiomyocyte size between $cTnI^{\Delta K184}$ and nTG mice. Thus, cellular size reduction could be excluded as cause for the minimized ventricles. Cellular loss remains as an alternative explanation.

Ultrastructurally, exclusively $cTnI^{\Delta K184}$-mice displayed typical aberrations: 1. irregular cell shapes such as folds, buds etc., 2. sarcomere disarray and 3. sarcomere reconstruction. Especially the sarcomere disarray and the sarcomere reconstruction point to an impaired sarcomere stability which might follow from the cTnI mutation. Interestingly, these aberrations consistently occurred in the ventricles as well as in the atria, which greatly differ e.g. in pressure conditions. Currently, it is unknown if these aberrations occur in human $cTnI^{\Delta K183}$ mutation carriers as well as from these, histological and ultrastructural data are completely lacking. The above mentioned classical features of HCM are missing in several other mouse models as well and often even in humans. Thus, it is possible that hypertrophy, fibrosis and cardiomyocyte disarray develop later in a long-term degenerative process which begins in a subclinical phase with more subtle (ultra-) structural aberrations.

6 Zusammenfassung

Die familiäre hypertrophe Kardiomyopathie (HCM) ist in ihrer klinischen Präsentation hoch variabel. Klassischerweise werden drei morphologische Leitsymptome genannt: 1. ventrikuläre Hypertrophie, 2. interstitielle Fibrose und 3. eine charakteristische Fehlstellung der Herzmuskelzellen, der Kardiomyozyten-Disarray. Das in dieser Dissertation untersuchte Mausmodell trägt eine Deletion an Aminosäureposition 184 der kardialen Isoform der inhibitorischen Troponin-Untereinheit (cTnI$^{\Delta K184}$), das wie weitere > 450 Sarkomerprotein-Mutationen mit der Genese familiärer hypertropher Kardiomyopathien in Verbindung steht. CTnI$^{\Delta K184}$-Mäuse zeigten jedoch keines der drei genannten Hauptmerkmale, obwohl der Anteil des Proteins bei über 90% vom gesamten cTnI lag.

Die Herzen der cTnI$^{\Delta K184}$-Mäuse (TG) waren bei gleichem Körpergewicht durchschnittlich um 22% leichter als die ihrer nicht-transgenen (nTG) Brüder. Im Verhältnis zum Herzinnendurchmesser war die Wand des linken Ventrikels (LV) der cTnI$^{\Delta K184}$-Mäuse allerdings um ~26% dicker, was Auswirkungen auf die Herzgeometrie und -kontraktilität hat. Die Analyse von MRI-Bildern anästhesierter Mäuse ergab eine stärkere Kontraktion der cTnI$^{\Delta K184}$- Herzen. Der mittlere Wandumfang nahm bei cTnI$^{\Delta K184}$-Mäusen um 27% ab, bei nTG Mäusen nur um 19%. Folglich müsste auch die systolische Verkürzung der Sarkomere um etwa den gleichen Betrag stärker sein, da die Sarkomerlänge direkt proportional zum mittleren Wandumfang ist. Dies bedeutet eine regelmäßige maximale Kontraktion der Sarkomere im körperlichen Ruhezustand, die unter körperlicher Belastung nicht weiter steigerbar ist.

Zur Bestimmung der Ursache für die Herzverkleinerung wurden die Ventrikel der Herzen an systematisch randomisierten Proben morphometrisch untersucht. Im LV gab es keine Unterschiede in der Kardiomyozytengröße von cTnI$^{\Delta K184}$ und nTG Mäusen. Somit konnte eine zelluläre Größenreduktion als Ursache für die verkleinerten Ventrikel ausgeschlossen werden. Als alternative Erklärung bleibt ein Zellverlust.

Ultrastrukturell zeigten ausschließlich die cTnI$^{\Delta K184}$-Mäuse typische Aberrationen 1. unregelmäßige Zellformen wie Einfaltungen, Knospen usw., 2. Sarkomer-Disarray und 3. Neu- und Umbildung von Sarkomeren (Sarkomer-Rekonstruktion). Insbesondere der Sarkomer-Disarray und die Sarkomer-Rekonstruktion sind Hinweise für eine verminderte Sarkomer-Stabilität, möglicherweise als direkter Folge der cTnI-Mutation. Interessanterweise traten diese Aberrationen konsistent sowohl in den Ventrikeln als auch in den Atrien auf, die sich u.a. hinsichtlich der Druckverhältnisse unterscheiden. Ob diese Veränderungen auch bei menschlichen Trägern der cTnI$^{\Delta K183}$-Mutation vorkommen, ist wegen fehlender histologischer und ultrastruktureller Daten bisher unbekannt. Die o.g. klassischen Merkmale fehlen auch bei einigen anderen Mausmodellen für hypertrophe Kardiomyopathie und oftmals auch beim Menschen. Ausprägungen wie Hypertrophie, Fibrose und Kardiomyozyten-Disarray könnten erst am Ende eines längerfristigen Degenerationsprozesses stehen, der in der subklinischen Phase der Erkrankung mit subtileren (ultra-) strukturellen Veränderungen beginnt.

7 References

1. Abhayaratna WP, Seward JB, Appleton CP, Douglas PS, Oh JK, Tajik AJ, Tsang TS. Left atrial size: physiologic determinants and clinical applications. J Am Coll Cardiol. 2006 Jun 20;47(12):2357-63

2. Agarkova I, Perriard JC. The M-band: an elastic web that crosslinks thick filaments in the center of the sarcomere. Trends Cell Biol. 2005 Sep;15(9):477-85.

3. Ahmad F, Seidman JG, Seidman CE. The genetic basis for cardiac remodeling. Annu Rev Genomics Hum Genet. 2005;6:185-216

4. Akella AB, Ding XL, Cheng R, Gulati J. Diminished Ca2+ sensitivity of skinned cardiac muscle contractility coincident with troponin T-band shifts in the diabetic rat. Circ Res. 1995 Apr;76(4):600-6.

5. Allen DG, Kentish JC: The cellular basis of the length-tension relation in cardiac muscle. J Mol Cell Cardiol. 1985 Sep;17(9):821-40

6. Ammarguellat F, Larouche I, Schiffrin EL: Myocardial Fibrosis in DOCA-Salt Hypertensive Rats: Effect of Endothelin ETA Receptor Antagonism. Circulation 2001 103: 319 - 324

7. Angelini A, Calzolari V, Thiene G, Boffa GM, Valente M, Daliento L, Basso C, Calabrese F, Razzolini R, Livi U, Chioin R: Morphologic spectrum of primary restrictive cardiomyopathy. Am J Cardiol. 1997 Oct 15;80(8):1046-50

8. Arteaga GM, Palmiter KA, Leiden JM, Solaro RJ. Attenuation of length dependence of calcium activation in myofilaments of transgenic mouse hearts expressing slow skeletal troponin I. J Physiol. 2000 Aug 1;526 Pt 3:541-9

9. Ashrafian H, Frenneaux MP, Opie LH. : Metabolic mechanisms in heart failure. Circulation. 2007 Jul 24;116(4):434-48

10. Ashrafian H, Redwood C, Blair E, Watkins H.: Hypertrophic cardiomyopathy: a paradigm for myocardial energy depletion. Trends Genet. 2003 May;19(5):263-8

11. Bhavsar PK, Dhoot GK, Cumming DV, Butler-Browne GS, Yacoub MH, Barton PJ: Developmental expression of troponin I isoforms in fetal human heart. FEBS Lett. 1991 Nov 4;292(1-2):5-8

12. Bilchick KC, Duncan JG, Ravi R, Takimoto E, Champion HC, Gao WD, Stull LB, Kass DA, Murphy AM. Heart failure-associated alterations in troponin I phosphorylation impair ventricular relaxation-afterload and force-frequency responses and systolic function. Am J Physiol Heart Circ Physiol. 2007 Jan;292(1):H318-25.

13. Binder J, Ommen SR, Gersh BJ, Van Driest SL, Tajik AJ, Nishimura RA, Ackerman MJ: Echocardiography-guided genetic testing in hypertrophic cardiomyopathy: septal morphological features predict the presence of myofilament mutations. Mayo Clin Proc. 2006 Apr;81(4):459-67

14. Bogoyevitch MA, Parker PJ, Sugden PH. Characterization of protein kinase C isotype expression in adult rat heart. Protein kinase C-epsilon is a major isotype present, and it is activated by phorbol esters, epinephrine, and endothelin. Circ Res. 1993 Apr;72(4):757-67.

15. Bowling, N, Walsh RA, Song G, Estridge T, Sandusky GE, Fouts RL, Mintze K, Pickard T, Roden R, Bristow MR, Sabbah HN, Mizrahi JL, Gromo G, King GL, and Vlahos CJ. Increased protein kinase C activity and expression of Ca2+-sensitive isoforms in the failing human heart. Circulation 99: 384-391, 1999

16. Boyle A, Maurer MS, Sobotka PA: Myocellular and interstitial edema and circulating volume expansion as a cause of morbidity and mortality in heart failure. J Card Fail. 2007 Mar;13(2):133-6

17. Burkart EM, Sumandea MP, Kobayashi T, Nili M, Martin AF, Homsher E, Solaro RJ. Phosphorylation or glutamic acid substitution at protein kinase C sites on cardiac troponin I differentially depress myofilament tension and shortening velocity. J Biol Chem. 2003 Mar 28;278(13):11265-72.

18. Casiero D, Frishman WH: Cardiovascular complications of eating disorders. Cardiol Rev. 2006 Sep-Oct;14(5):227-31

19. Chalovich JM, Eisenberg E. Inhibition of actomyosin ATPase activity by troponin-tropomyosin without blocking the binding of myosin to actin. J Biol Chem. 1982 Mar 10;257(5):2432-7

20. Chalovich JM. Regulation of striated muscle contraction: a discussion. J Muscle Res Cell Motil. 2002;23(4):353-61.

21. Chandra M, Dong WJ, Pan BS, Cheung HC, Solaro RJ. Effects of protein kinase A phosphorylation on signaling between cardiac troponin I and the N-terminal domain of cardiac troponin C. Biochemistry. 1997 Oct 28;36(43):13305-11.

22. Chandra M, Rundell VL, Tardiff JC, Leinwand LA, De Tombe PP, Solaro RJ. Ca(2+) activation of myofilaments from transgenic mouse hearts expressing R92Q mutant cardiac troponin T. Am J Physiol Heart Circ Physiol. 2001 Feb;280(2):H705-13

23. Chang AN, Potter JD. Sarcomeric protein mutations in dilated cardiomyopathy. Heart Fail Rev. 2005 Sep;10(3):225-35.

24. Charron P, Dubourg O, Desnos M, Bennaceur M, Carrier L, Camproux AC, Isnard R, Hagege A, Langlard JM, Bonne G, Richard P, Hainque B, Bouhour JB, Schwartz K, Komajda M: Clinical features and prognostic implications of familial hypertrophic cardiomyopathy related to the cardiac myosin-binding protein C gene. Circulation. 1998 Jun 9;97(22):2230-6

25. Cheng TO. Frequency of cardiac troponin I mutations in families with hyper-trophic cardiomyopathy in China. J Am Coll Cardiol. 2005 Jul 5;46(1):180-1;

26. Collins KA, Korcarz CE, Lang RM. Use of echocardiography for the pheno-typic assessment of genetically altered mice. Physiol Genomics. 2003 May 13;13(3):227-39

27. Cooper G 4th. Cytoskeletal networks and the regulation of cardiac contrac-tility: microtubules, hypertrophy, and cardiac dysfunction. Am J Physiol Heart Circ Physiol. 2006 Sep;291(3):H1003-14.

28. Crilley JG, Boehm EA, Blair E, Rajagopalan B, Blamire AM, Styles P, McKenna WJ, Ostman-Smith I, Clarke K, Watkins H: Hypertrophic car-diomyopathy due to sarcomeric gene mutations is characterized by im-paired energy metabolism irrespective of the degree of hypertrophy J Am Coll Cardiol. 2003 May 21;41(10):1776-82

29. Dabiri GA, Turnacioglu KK, Sanger JM, Sanger JW: Myofibrillogenesis visualized in living embryonic cardiomyocytes. Proc Natl Acad Sci U S A. 1997 Aug 19;94(17):9493-8.

30. Davies MJ. The current status of myocardial disarray in hypertrophic car-diomyopathy. Br Heart J. 1984 Apr;51(4):361-3.

31. Dhoot GK, Gell PG, Perry SV: The localization of the different forms of tro-ponin I in skeletal and cardiac muscle cells Exp Cell Res. 1978 Dec;117(2):357-70

32. Dhoot GK, Perry SV: Distribution of polymorphic forms of troponin compo-nents and tropomyosin in skeletal muscle. Nature. 1979 Apr 19;278(5706):714-8.

33. Dong WJ, Chandra M, Xing J, Solaro RJ, Cheung HC: Conformation of the N-terminal segment of a monocysteine mutant of troponin I from cardiac muscle. Biochemistry. 1997 Jun 3;36(22):6745-53

34. Doolan A, Tebo M, Ingles J, Nguyen L, Tsoutsman T, Lam L, Chiu C, Chung J, Weintraub RG, Semsarian C.: Cardiac troponin I mutations in Australian families with hypertrophic cardiomyopathy: clinical, genetic and functional consequences. J Mol Cell Cardiol. 2005 Feb;38(2):387-93

35. Du J, Zhang C, Liu J, Sidky C, Huang XP. A point mutation (R192H) in the C-terminus of human cardiac troponin I causes diastolic dysfunction in transgenic mice.Arch Biochem Biophys. 2006 Dec 15;456(2):143-50.

36. Dumont EA, Hofstra L, van Heerde WL, van den Eijnde S, Doevendans PA, DeMuinck E, Daemen MA, Smits JF, Frederik P, Wellens HJ, Daemen MJ, Reutelingsperger CP.: Cardiomyocyte death induced by myocardial ische-mia and reperfusion: measurement with recombinant human annexin-V in a mouse model. Circulation. 2000 Sep 26;102(13):1564-8.

37. Dumont EA, Reutelingsperger CP, Smits JF, Daemen MJ, Doevendans PA, Wellens HJ, Hofstra L.: Real-time imaging of apoptotic cell-membrane changes at the single-cell level in the beating murine heart. Nat Med. 2001 Dec;7(12):1352-5.

38. Ehler E, Perriard JC. Cardiomyocyte cytoskeleton and myofibrillogenesis in healthy and diseased heart. Heart Fail Rev. 2000 Oct;5(3):259-69.

39. Elias, H and Hyde, DM: A guide to practical stereology, Karger, Basel [u.a.], 1983

40. Elliott PM, Sharma S, Varnava A, Poloniecki J, Rowland E, McKenna WJ: Survival after cardiac arrest or sustained ventricular tachycardia in patients with hypertrophic cardiomyopathy. J Am Coll Cardiol. 1999 May;33(6):1596-601.

41. Erdbrügger W, Keffel J, Knocks M, Otto T, Philipp T, Michel MC. Protein kinase C isoenzymes in rat and human cardiovascular tissues. Br J Pharmacol. 1997 Jan;120(2):177-86.

42. Feld S, Caspi A: Familial cardiomyopathy with variable hypertrophic and restrictive features and common HLA haplotype. Isr J Med Sci. 1992 May;28(5):277-80.

43. Fentzke RC, Buck SH, Patel JR, Lin H, Wolska BM, Stojanovic MO, Martin AF, Solaro RJ, Moss RL, Leiden JM: Impaired cardiomyocyte relaxation and diastolic function in transgenic mice expressing slow skeletal troponin I in the heart. J Physiol. 1999 May 15;517 (Pt 1):143-57.

44. Flicker PF, Phillips GN Jr, Cohen C   Troponin and its interactions with tropomyosin: An electron microscope study. J Mol Biol. 1982 Dec 5;162(2):495-501.

45. Forissier JF, Carrier L, Farza H, Bonne G, Bercovici J, Richard P, Hainque B, Townsend PJ, Yacoub MH, Faure S, Dubourg O, Millaire A, Hagege AA, Desnos M, Komajda M, Schwartz K: Codon 102 of the cardiac troponin T gene is a putative hot spot for mutations in familial hypertrophic cardiomyopathy. Circulation. 1996 Dec 15;94(12):3069-73

46. Frank D, Kuhn C, Katus HA, Frey N. The sarcomeric Z-disc: a nodal point in signalling and disease. J Mol Med. 2006 Jun;84(6):446-68.

47. Franzini-Armstrong C, Protasi F, Tijskens P: The assembly of calcium release units in cardiac muscle. Ann N Y Acad Sci. 2005 Jun;1047:76-85

48. Gavrieli Y, Sherman Y, Ben-Sasson SA.: Identification of programmed cell death in situ via specific labeling of nuclear DNA fragmentation. J Cell Biol. 1992 Nov;119(3):493-501

49. Geisterfer-Lowrance AA, Kass S, Tanigawa G, Vosberg HP, McKenna W, Seidman CE, Seidman JG: A molecular basis for familial hypertrophic cardiomyopathy: a beta cardiac myosin heavy chain gene missense mutation. Cell. 1990 Sep 7;62(5):999-1006

50. Gomes AV, Potter JD: Cellular and molecular aspects of familial hypertrophic cardiomyopathy caused by mutations in the cardiac troponin I gene. Mol Cell Biochem. 2004 Aug;263(1-2):99-114.

51. Gopalan SM, Flaim C, Bhatia SN, Hoshijima M, Knoell R, Chien KR, Omens JH, McCulloch AD: Anisotropic stretch-induced hypertrophy in neonatal ventricular myocytes micropatterned on deformable elastomers. Biotechnol Bioeng. 2003 Mar 5;81(5):578-87.

52. Gordon AM, Homsher E, Regnier M. Regulation of contraction in striated muscle. Physiol Rev. 2000 Apr;80(2):853-924.

53. Greaser ML, Gergely J, Han MH, Benson ES: Lack of identity of tropocalcin with troponin components. Biochem Biophys Res Commun. 1972 Jul 25;48(2):358-61.

54. Greaser ML, Gergely J: Purification and properties of the components from troponin. J Biol Chem. 1973 Mar 25;248(6):2125-33.

55. Greaser ML, Gergely J: Reconstitution of troponin activity from three protein components. J Biol Chem 1971 Jul 10;246(13): 4226-33

56. Gundersen H: Notes of the estimation of the numerical density of arbitrary profiles, J Microsc 1977; 111:219-223

57. Gundersen HJ, Bagger P, Bendtsen TF, Evans SM, Korbo L, Marcussen N, Moller A, Nielsen K, Nyengaard JR, Pakkenberg B, et al.: The new stereological tools: disector, fractionator, nucleator and point sampled intercepts and their use in pathological research and diagnosis. APMIS. 1988 Oct;96(10):857-81.

58. Haim TE, Dowell C, Diamanti T, Scheuer J, Tardiff JC. Independent FHC-related cardiac troponin T mutations exhibit specific alterations in myocellular contractility and calcium kinetics. J Mol Cell Cardiol. 2007 Jun;42(6):1098-110.

59. Hamlin SK, Villars PS, Kanusky JT, Shaw AD: Role of diastole in left ventricular function, II: diagnosis and treatment. Am J Crit Care. 2004 Nov;13(6):453-66; quiz 467-8.

60. Heineke J, Molkentin JD. Regulation of cardiac hypertrophy by intracellular signalling pathways.at Rev Mol Cell Biol. 2006 Aug;7(8):589-600.

61. Ho CY, Seidman CE: A contemporary approach to hypertrophic cardiomyopathy. Circulation 2006 Jun 20;113(24):e858-62

62. Huang X, Pi Y, Lee KJ, Henkel AS, Gregg RG, Powers PA, Walker JW: Cardiac troponin I gene knockout: a mouse model of myocardial troponin I deficiency. Circ Res. 1999 Jan 8-22;84(1):1-8.

63. Huang XP, Du JF: Troponin I, cardiac diastolic dysfunction and restrictive cardiomyopathy. Acta Pharmacol Sin. 2004 Dec;25(12):1569-75

64. Hughes SE. The pathology of hypertrophic cardiomyopathy. Histopathology. 2004 May;44(5):412-27

65. Hunkeler NM, Kullman J, Murphy AM. Troponin I isoform expression in human heart. Circ Res. 1991 Nov;69(5):1409-14

66. Ingwall JS, Weiss RG. Is the failing heart energy starved? On using chemical energy to support cardiac function. Circ Res. 2004 Jul 23;95(2):135-45.

67. Iorga B, Blaudeck N, Solzin J, Neulen A, Stehle I, Lopez Davila AJ, Pfitzer G, Stehle R. Lys184 deletion in troponin I impairs relaxation kinetics and induces hypercontractility in murine cardiac myofibrils. Cardiovasc Res. 2008 Mar 1;77(4):676-86.

68. Itoh S, Ding B, Bains CP, Wang N, Takeishi Y, Jalili T, King GL, Walsh RA, Yan C, Abe J: Role of p90 ribosomal S6 kinase (p90RSK) in reactive oxygen species and protein kinase C beta (PKC-beta)-mediated cardiac troponin I phosphorylation. J Biol Chem. 2005 Jun 24;280(25):24135-42.

69. James J, Zhang Y, Osinska H, Sanbe A, Klevitsky R, Hewett TE, Robbins J. Transgenic modeling of a cardiac troponin I mutation linked to familial hypertrophic cardiomyopathy. Circ Res. 2000 Oct 27;87(9):805-11.

70. Jugdutt BI, Idikio HA.: Apoptosis and oncosis in acute coronary syndromes: assessment and implications. Mol Cell Biochem. 2005 Feb;270(1-2):177-200.

71. Jung WI, Sieverding L, Breuer J, Schmidt O, Widmaier S, Bunse M, van Erckelens F, Apitz J, Dietze GJ, Lutz O. Detection of phosphomonoester signals in proton-decoupled 31P NMR spectra of the myocardium of patients with myocardial hypertrophy. J Magn Reson. 1998 Jul;133(1):232-5.

72. Kalsi KK, Smolenski RT, Pritchard RD, Khaghani A, Seymour AM, Yacoub MH. Energetics and function of the failing human heart with dilated or hypertrophic cardiomyopathy. Eur J Clin Invest. 1999 Jun;29(6):469-77.

73. Kandabashi T, Shimokawa H, Miyata K, Kunihiro I, Kawano Y, Fukata Y, Higo T, Egashira K, Takahashi S, Kaibuchi K, Takeshita A. Inhibition of myosin phosphatase by upregulated rho-kinase plays a key role for coronary artery spasm in a porcine model with interleukin-1beta. Circulation. 2000 Mar 21;101(11):1319-23

74. Katz, AM: Physiology of the heart, 4th edition, Lippincott Williams & Wilkins, Philadelphia, Baltimore, New York, London, Buenos Aires, Hong Kong, Sydney, Tokyo

75. Kietselaer BL, Hofstra L, Dumont EA, Reutelingsperger CP, Heidendal GA: The role of labeled Annexin A5 in imaging of programmed cell death. From animal to clinical imaging. Q J Nucl Med. 2003 Dec;47(4):349-61.

76. Kietselaer BL, Reutelingsperger CP, Boersma HH, Heidendal GA, Liem IH, Crijns HJ, Narula J, Hofstra L. Noninvasive detection of programmed cell loss with 99mTc-labeled annexin A5 in heart failure. J Nucl Med. 2007 Apr;48(4):562-7.

77. Kimura A, Harada H, Park JE, Nishi H, Satoh M, Takahashi M, Hiroi S, Sasaoka T, Ohbuchi N, Nakamura T, Koyanagi T, Hwang TH, Choo JA, Chung KS, Hasegawa A, Nagai R, Okazaki O, Nakamura H, Matsuzaki M, Sakamoto T, Toshima H, Koga Y, Imaizumi T, Sasazuki T. Mutations in the cardiac troponin I gene associated with hypertrophic cardiomyopathy. Nat Genet. 1997 Aug;16(4):379-82.

78. Kokado H, Shimizu M, Yoshio H, Ino H, Okeie K, Emoto Y, Matsuyama T, Yamaguchi M, Yasuda T, Fujino N, Ito H, Mabuchi H. Clinical features of hypertrophic cardiomyopathy caused by a Lys183 deletion mutation in the cardiac troponin I gene. Circulation. 2000 Aug 8;102(6):663-9.

79. Konhilas JP, Irving TC, de Tombe PP. Frank-Starling law of the heart and the cellular mechanisms of length-dependent activation. Pflugers Arch. 2002 Dec;445(3):305-10.

80. Kostin S, Pool L, Elsasser A, Hein S, Drexler HC, Arnon E, Hayakawa Y, Zimmermann R, Bauer E, Klovekorn WP, Schaper J.: Myocytes die by multiple mechanisms in failing human hearts. Circ Res. 2003 Apr 18;92(7):715-24.

81. Kubo T, Gimeno JR, Bahl A, Steffensen U, Steffensen M, Osman E, Thaman R, Mogensen J, Elliott PM, Doi Y, McKenna WJ. : Prevalence, clinical significance, and genetic basis of hypertrophic cardiomyopathy with restrictive phenotype. J Am Coll Cardiol. 2007 Jun 26;49(25):2419-26.

82. Kushwaha SS, Fallon JT, Fuster V.: Restrictive cardiomyopathy. N Engl J Med. 1997 Jan 23;336(4):267-76.

83. LeWinter MM. Functional consequences of sarcomeric protein abnormalities in failing myocardium. Heart Fail Rev. 2005 Sep;10(3):249-57.

84. Li MX, Wang X, Sykes BD: Structural based insights into the role of troponin in cardiac muscle pathophysiology. J Muscle Res Cell Motil. 2004;25(7):559-79.

85. Liberthson RR: Sudden death from cardiac causes in children and young adults. N Engl J Med. 1996 Apr 18;334(16):1039-44

86. Linke WA. Sense and stretchability: the role of titin and titin-associated proteins in myocardial stress-sensing and mechanical dysfunction. Cardiovasc Res. 2008 Mar 1;77(4):637-48.

87. Marian AJ: Modifier genes for hypertrophic cardiomyopathy. Curr Opin Cardiol. 2002 May;17(3):242-52.

88. Marian AJ: Pathogenesis of diverse clinical and pathological phenotypes in hypertrophic cardiomyopathy. Lancet. 2000; 355:58-60

89. Maron BJ, Carney KP, Lever HM, Lewis JF, Barac I, Casey SA, Sherrid MV. Relationship of race to sudden cardiac death in competitive athletes with hypertrophic cardiomyopathy. J Am Coll Cardiol. 2003 Mar 19;41(6):974-80

90. Maron BJ, Ferrans VJ, Roberts WC: Ultrastructural features of degenerated cardiac muscle cells in patients with cardiac hypertrophy. Am J Pathol. 1975 Jun;79(3):387-434.

91. Maron BJ, Ferrans VJ: Ultrastructural features of hypertrophied human ventricular myocardium. Prog Cardiovasc Dis. 1978 Nov-Dec;21(3):207-38

92. Maron BJ, Gardin JM, Flack JM, Gidding SS: Bild DE HCM in the general population. Circulation. 1996 Aug 1;94(3):588-9.

93. Maron BJ, McKenna WJ, Danielson GK, Kappenberger LJ, Kuhn HJ, Seidman CE, Shah PM, Spencer WH 3rd, Spirito P, Ten Cate FJ, Wigle ED: American College of Cardiology Foundation Task Force on Clinical Expert Consensus Documents; European Society of Cardiology Committee for Practice Guidelines. American College of Cardiology/European Society of Cardiology Clinical Expert Consensus Document on Hypertrophic Cardiomyopathy.   A report of the American College of Cardiology Foundation Task Force on Clinical Expert Consensus Documents and the European Society of Cardiology Committee for Practice Guidelines. Eur Heart J. 2003 Nov;24(21):1965-91.

94. Maron BJ, Roberts WC: Quantitative analysis of cardiac muscle cell disorganization in the ventricular septum of patients with hypertrophic cardiomyopathy. Circulation. 1979 Apr;59(4):689-706.

95. Maron BJ, Towbin JA, Thiene G, Antzelevitch C, Corrado D, Arnett D, Moss AJ, Seidman CE, Young JB, American Heart Association; Council on Clinical Cardiology, Heart Failure and Transplantation Committee; Quality of Care and Outcomes Research and Functional Genomics and Translational Biology Interdisciplinary Working Groups; Council on Epidemiology and Prevention: Contemporary definitions and classification of the cardiomyopathies: an American Heart Association Scientific Statement from the Council on Clinical Cardiology, Heart Failure and Transplantation Committee; Quality of Care and Outcomes Research and Functional Genomics and Translational Biology Interdisciplinary Working Groups; and Council on Epidemiology and Prevention. Circulation. 2006 Apr 11;113(14):1807-16.

96. Maron BJ, Wolfson JK, Roberts WC. Relation between extent of cardiac muscle cell disorganization and left ventricular wall thickness in hypertrophic cardiomyopathy. Am J Cardiol. 1992 Sep 15;70(7):785-90

97. Maron BJ: Hypertrophic cardiomyopathy: a systematic review. JAMA. 2002 Mar 13;287(10):1308-20.

98. Maron MS, Olivotto I, Zenovich AG, Link MS, Pandian NG, Kuvin JT, Nistri S, Cecchi F, Udelson JE, Maron BJ: Hypertrophic cardiomyopathy is predominantly a disease of left ventricular outflow tract obstruction. Circulation. 2006 Nov 21;114(21):2232-9.

99. Maughan DW.: Kinetics and energetics of the crossbridge cycle. Heart Fail Rev. 2005 Sep;10(3):175-85.

100. McKillop DF, Geeves MA. Regulation of the interaction between actin and myosin subfragment 1: evidence for three states of the thin filament. Biophys J. 1993 Aug;65(2):693-701.

101. Messer AE, Jacques AM, Marston SB. Troponin phosphorylation and regulatory function in human heart muscle: dephosphorylation of Ser23/24 on troponin I could account for the contractile defect in end-stage heart failure. J Mol Cell Cardiol. 2007 Jan;42(1):247-59.

102. Metzger JM, Michele DE, Rust EM, Borton AR, Westfall MV: Sarcomere thin filament regulatory isoforms. Evidence of a dominant effect of slow skeletal troponin I on cardiac contraction. J Biol Chem. 2003 Apr 11;278(15):13118-23.

103. Metzger JM, Westfall MV. Covalent and noncovalent modification of thin filament action: the essential role of troponin in cardiac muscle regulation.Circ Res. 2004 Feb 6;94(2):146-58.

104. Michele DE, Albayya FP, Metzger JM.: Thin filament protein dynamics in fully differentiated adult cardiac myocytes: toward a model of sarcomere maintenance. J Cell Biol. 1999 Jun 28;145(7):1483-95.

105. Mogensen J, Kubo T, Duque M, Uribe W, Shaw A, Murphy R, Gimeno JR, Elliott P, McKenna WJ: Idiopathic restrictive cardiomyopathy is part of the clinical expression of cardiac troponin I mutations. J Clin Invest. 2003 Jan;111(2):209-16.

106. Mogensen J, Murphy RT, Kubo T, Bahl A, Moon JC, Klausen IC, Elliott PM, McKenna WJ. Frequency and clinical expression of cardiac troponin I mutations in 748 consecutive families with hypertrophic cardiomyopathy. J Am Coll Cardiol. 2004 Dec 21;44(12):2315-25.

107. Moolman JC, Corfield VA, Posen B, Ngumbela K, Seidman C, Brink PA, Watkins H: Sudden death due to troponin T mutations. J Am Coll Cardiol. 1997 Mar 1;29(3):549-55.

108. Moses RL, Claycomb WC.: Differentiated membrane specializations and myofibrillar breakdown and recovery in cultured adult cardiac myocytes treated with TPA and diacylglycerol. J Cell Sci. 1989 May;93 (Pt 1):95-105.

109. Munch DF, Comer HT, Downey JM: Barium contracture: a model for systole. Am J Physiol. 1980 Sep;239(3):H438-42.

110. Murphy RT, Mogensen J, Shaw A, Kubo T, Hughes S, McKenna WJ. Novel mutation in cardiac troponin I in recessive idiopathic dilated cardiomyopathy. Lancet. 2004 Jan 31;363(9406):371-2.

111. Nakajima-Taniguchi C, Matsui H, Eguchi N, Nagata S, Kishimoto T, Yamauchi-Takihara K: A novel deletion mutation in the beta-myosin heavy chain gene found in Japanese patients with hypertrophic cardiomyopathy. J Mol Cell Cardiol. 1995 Dec;27(12):2607-12.

112. Nepomnyashchikh LM.: Regenerative and plastic insufficiency of cardiomyocytes during impairment of protein synthesis. Bull Exp Biol Med. 2001 Jan;131(1):6-14.

113. Neubauer S, Horn M, Cramer M, Harre K, Newell JB, Peters W, Pabst T, Ertl G, Hahn D, Ingwall JS, Kochsiek K. Myocardial phosphocreatine-to-ATP ratio is a predictor of mortality in patients with dilated cardiomyopathy. Circulation. 1997 Oct 7;96(7):2190-6.

114. Nguyen L, Chung J, Lam L, Tsoutsman T, Semsarian C. Abnormal cardiac response to exercise in a murine model of familial hypertrophic cardiomyopathy. Int J Cardiol. 2007 Jul 10;119(2):245-8.

115. Nguyen L, Chung J, Lam L, Tsoutsman T. Abnormal cardiac response to exercise in a murine model of familial hypertrophic cardiomyopathy. Semsarian C.Int J Cardiol. 2007 Jul 10;119(2):245-8

116. Niimura H, Bachinski LL, Sangwatanaroj S, Watkins H, Chudley AE, McKenna W, Kristinsson A, Roberts R, Sole M, Maron BJ, Seidman JG, Seidman CE: Mutations in the gene for cardiac myosin-binding protein C and late-onset familial hypertrophic cardiomyopathy.N Engl J Med. 1998 Apr 30;338(18):1248-57.

117. Niimura H, Patton KK, McKenna WJ, Soults J, Maron BJ, Seidman JG, Seidman CE: Sarcomere protein gene mutations in hypertrophic cardiomyopathy of the elderly. Circulation. 2002 Jan 29;105(4):446-51

118. Noland TA Jr, Raynor RL, Jideama NM, Guo X, Kazanietz MG, Blumberg PM, Solaro RJ, Kuo JF: Differential regulation of cardiac actomyosin S-1 MgATPase by protein kinase C isozyme-specific phosphorylation of specific sites in cardiac troponin I and its phosphorylation site mutants. Biochemistry. 1996 Nov 26;35(47):14923-31

119. Nyengaard JR, Gundersen HJ: Direct and efficient stereological estimation of total cell quantities using electron microscopy. J Microsc. 2006 Jun;222(Pt 3):182-7.

120. Parmacek MS, Solaro RJ: Biology of the troponin complex in cardiac myocytes. Prog Cardiovasc Dis. 2004 Nov-Dec;47(3):159-76

121. Perry SV: Troponin I: inhibitor or facilitator. Mol Cell Biochem. 1999 Jan;190(1-2):9-32.

122. Perry SV: Troponin T: genetics, properties and function. J Muscle Res Cell Motil. 1998 Aug;19(6):575-602

123. Petersen SE, Jerosch-Herold M, Hudsmith LE, Robson MD, Francis JM, Doll HA, Selvanayagam JB, Neubauer S, Watkins H: Evidence for Microvascular Dysfunction in Hypertrophic Cardiomyopathy. New Insights From Multiparametric Magnetic Resonance Imaging. Circulation. 2007 Apr 23

124. Potten CS. What is an apoptotic index measuring? A commentary. Br J Cancer 1996; 74: 1743-1748

125. Pyle WG, Solaro RJ. At the crossroads of myocardial signaling: the role of Z-discs in intracellular signaling and cardiac function. Circ Res. 2004 Feb 20;94(3):296-305

126. Rakusan K, Korecky B, Sarkar K, Turek Z.: Merits and pitfalls in morphological assessment of cardiac growth. Fed Proc. 1986 Oct;45(11):2580-4.

127. Rarick HM, Tang HP, Guo XD, Martin AF, Solaro RJ. Interactions at the NH2-terminal interface of cardiac troponin I modulate myofilament activation. J Mol Cell Cardiol. 1999 Feb;31(2):363-75.

128. Reiffert SU, Jaquet K, Heilmeyer LM Jr, Herberg FW: Stepwise subunit interaction changes by mono- and bisphosphorylation of cardiac troponin I. Biochemistry. 1998 Sep 29;37(39):13516-25.

129. Reiser PJ, Portman MA, Ning XH, Schomisch Moravec C. Human cardiac myosin heavy chain isoforms in fetal and failing adult atria and ventricles. Am J Physiol Heart Circ Physiol. 2001 Apr;280(4):H1814-20

130. Revera M, van der Merwe L, Heradien M, Goosen A, Corfield VA, Brink PA, Moolman-Smook JC.Troponin T and beta-myosin mutations have distinct cardiac functional effects in hypertrophic cardiomyopathy patients without hypertrophy. Cardiovasc Res. 2008 Mar 1;77(4):687-94.

131. Richard P, Villard E, Charron P, Isnard R: The genetic bases of cardiomyopathies. J Am Coll Cardiol. 2006 Nov 7;48(9 Suppl):A79-89.

132. Richardson P, McKenna W, Bristow M, Maisch B, Mautner B, O'Connell J, Olsen E, Thiene G, Goodwin J, Gyarfas I, Martin I, Nordet P: Report of the 1995 World Health Organization/International Society and Federation of Cardiology Task Force on the Definition and Classification of cardiomyopathies. Circulation. 1996 Mar 1;93(5):841-2.

133. Rodriguez M, Schaper J. Apoptosis: measurement and technical issues. J Mol Cell Cardiol. 2005 Jan;38(1):15-2

134. Ross J Jr, Sonnenblick EH, Covell JW, Kaiser G, Spiro D. The architecture of the heart in systole and diastole. Technique of rapid fixation and analysis of left ventricular geometry. Circ Res. 1967 Oct;21(4):409-21

135. Rouet-Benzineb P, Mohammadi K, Pérennec J, Poyard M, Bouanani Nel-H , Crozatier B. Protein kinase C isoform expression in normal and failing rabbit hearts.Circ Res. 1996 Aug;79(2):153-61.

136. Russell B, Motlagh D, Ashley WW. Form follows function: how muscle shape is regulated by work. J Appl Physiol. 2000 Mar;88(3):1127-32.

137. Sage MD, Gavin JB: Morphological identification of functional capillaries in the myocardium. Anat Rec. 1984 Feb;208(2):283-9.

138. Sakthivel S, Finley NL, Rosevear PR, Lorenz JN, Gulick J, Kim S, VanBuren P, Martin LA, Robbins J: In vivo and in vitro analysis of cardiac troponin I phosphorylation. J Biol Chem. 2005 Jan 7;280(1):703-14.

139. Sanbe A, James J, Tuzcu V, Nas S, Martin L, Gulick J, Osinska H, Sakthivel S, Klevitsky R, Ginsburg KS, Bers DM, Zinman B, Lakatta EG, Robbins J: Transgenic rabbit model for human troponin I-based hypertrophic cardiomyopathy. Circulation. 2005 May 10;111(18):2330-8

140. Sanbe A, James J, Tuzcu V, Nas S, Martin L, Gulick J, Osinska H, Sakthivel S, Klevitsky R, Ginsburg KS, Bers DM, Zinman B, Lakatta EG, Robbins J.: Transgenic rabbit model for human troponin I-based hypertrophic cardiomyopathy. Circulation. 2005 May 10;111(18):2330-8

141. Sanger JW, Ayoob JC, Chowrashi P, Zurawski D, Sanger JM.: Assembly of myofibrils in cardiac muscle cells. Adv Exp Med Biol. 2000;481:89-102;

142. Sasse S, Brand NJ, Kyprianou P, Dhoot GK, Wade R, Arai M, Periasamy M, Yacoub MH, Barton PJ: Troponin I gene expression during human cardiac development and in end-stage heart failure. Circ Res. 1993 May;72(5):932-8.

143. Schaper J, Kostin S.: Cell death and adenosine triphosphate: the paradox. J Mol Cell Cardiol. 2005 Jan;38(1):15-20.

144. Schaub MC, Hefti MA, Zuellig RA, Morano I. Modulation of contractility in human cardiac hypertrophy by myosin essential light chain isoforms. Cardiovasc Res. 1998 Feb;37(2):381-404.

145. Schreiber KL, Paquet L, Allen BG, Rindt H. Protein kinase C isoform expression and activity in the mouse heart. Am J Physiol Heart Circ Physiol. 2001 Nov;281(5):H2062-71

146. Sepp R, Severs NJ, Gourdie RG: Altered patterns of cardiac intercellular junction distribution in hypertrophic cardiomyopathy. Circulation. 2001 Sep 18;104(12):1380-4

147. Shimizu M, Ino H, Okeie K, Yamaguchi M, Hayashi K, Nagata M, Itoh H, Iwaki T, Oe K, Konno T, Mabuchi H. Septal wall thinning and systolic dysfunction in patients with hypertrophic cardiomyopathy caused by a cardiac troponin I gene mutation. Am Heart J. 2002 Apr;143(4):690-5.

148. Shimizu M, Ino H, Yamaguchi M, Terai H, Hayashi K, Kiyama M, Sakata K, Hayashi T, Inoue M, Kaneda T, Mabuchi H. Chronologic electrocardiographic changes in patients with hypertrophic cardiomyopathy associated with cardiac troponin 1 mutation. Am Heart J. 2002 Feb;143(2):289-93

149. Shirani J, Pick R, Roberts WC, Maron BJ: Morphology and significance of the left ventricular collagen network in young patients with hypertrophic cardiomyopathy and sudden cardiac death. J Am Coll Cardiol. 2000 Jan;35(1):36-44

150. Siedner S, Kruger M, Schroeter M, Metzler D, Roell W, Fleischmann BK, Hescheler J, Pfitzer G, Stehle R: Developmental changes in contractility and sarcomeric proteins from the early embryonic to the adult stage in the mouse heart. J Physiol. 2003 Apr 15;548(Pt 2):493-505.

151. Simpson DG, Majeski M, Borg TK, Terracio L. Regulation of cardiac myocyte protein turnover and myofibrillar structure in vitro by specific directions of stretch. Circ Res. 1999 Nov 12;85(10):e59-69

152. Simpson DG, Sharp WW, Borg TK, Price RL, Terracio L, Samarel AM. Mechanical regulation of cardiac myocyte protein turnover and myofibrillar structure. Am J Physiol. 1996 Apr;270(4 Pt 1):C1075-87.

153. Solaro RJ, Lee JA, Kentish JC, Allen DG: Effects of acidosis on ventricular muscle from adult and neonatal rats. Circ Res. 1988 Oct;63(4):779-87

154. Solaro RJ, Rarick HM.: Troponin and tropomyosin: proteins that switch on and tune in the activity of cardiac myofilaments. Circ Res. 1998 Sep 7;83(5):471-80

155. Solaro RJ. The special structure and function of troponin I in regulation of cardiac contraction and relaxation. Adv Exp Med Biol. 2003;538:389-401

156. Sonnenblick EH, Ross J Jr, Covell JW, Spotnitz HM, Spiro D. The ultrastructure of the heart in systole and diastole. Chantes in sarcomere length. Circ Res. 1967 Oct;21(4):423-31. N

157. Spindler M, Saupe KW, Tian R, Ahmed S, Matlib MA, Ingwall JS. Altered creatine kinase enzyme kinetics in diabetic cardiomyopathy. A(31)P NMR magnetization transfer study of the intact beating rat heart. J Mol Cell Cardiol. 1999 Dec;31(12):2175-89.

158. Steinberg SF, Goldberg M, Rybin VO: Protein kinase C isoform diversity in the heart. J Mol Cell Cardiol. 1995 Jan;27(1):141-53.

159. Stypmann J. Doppler ultrasound in mice. Echocardiography. 2007 Jan;24(1):97-112.

160. Sweeney HL, Feng HS, Yang Z, Watkins H. Functional analyses of troponin T mutations that cause hypertrophic cardiomyopathy: insights into disease pathogenesis and troponin function. Proc Natl Acad Sci U S A. 1998 Nov 24;95(24):14406-10

161. Tagarakis CV, Bloch W, Hartmann G, Hollmann W, Addicks K. Testosterone-propionate impairs the response of the cardiac capillary bed to exercise. Med Sci Sports Exerc. 2000 May;32(5):946-53

162. Tagarakis CV, Bloch W, Hartmann G, Hollmann W, Addicks K. Anabolic steroids impair the exercise-induced growth of the cardiac capillary bed. Int J Sports Med. 2000 Aug;21(6):412-8.

163. Takeda N. Cardiomyopathy: molecular and immunological aspects (review). Int J Mol Med. 2003 Jan;11(1):13-6

164. Takeda S, Yamashita A, Maeda K, Maéda Y. Structure of the core domain of human cardiac troponin in the Ca(2+)-saturated form. Nature. 2003 Jul 3;424 (6944):35-41

165. Takeishi, Y, Chu G, Kirkpatrick DM, Li Z, Wakasaki H, Kranias EG, King GL, and Walsh RA. In vivo phosphorylation of cardiac troponin I by protein kinase C 2 decreases cardiomyocyte calcium responsiveness and contractility in transgenic mouse hearts. J Clin Invest 102: 72-78, 1998

166. Tanaka H, Kawanishi T, Shigenobu K: Optical bioimaging: from living tissue to a single molecule: atrio-ventricular difference in myocardial excitation-contraction coupling – sequential versus simultaneous activation of SR Ca2+ release units. J Pharmacol Sci. 2003 Nov;93(3):248-52.

167. Tardiff JC, Hewett TE, Palmer BM, Olsson C, Factor SM, Moore RL, Robbins J, Leinwand LA: Cardiac troponin T mutations result in allele-specific phenotypes in a mouse model for hypertrophic cardiomyopathy. J Clin Invest. 1999 Aug;104(4):469-81

168. Tardiff JC: Sarcomeric proteins and familial hypertrophic cardiomyopathy: linking mutations in structural proteins to complex cardiovascular phenotypes. Heart Fail Rev. 2005 Sep;10(3):237-48.

169. Toyota N, Shimada Y: Differentiation of troponin in cardiac and skeletal muscles in chicken embryos as studied by immunofluorescence microscopy. J Cell Biol. 1981 Nov;91(2 Pt 1):497-504

170. Tripet B, Van Eyk JE, Hodges RS. Mapping of a second actin-tropomyosin and a second troponin C binding site within the C terminus of troponin I, and their importance in the Ca2+-dependent regulation of muscle contraction. J Mol Biol. 1997 Sep 5;271(5):728-50.

171. Tsoutsman T, Chung J, Doolan A, Nguyen L, Williams IA, Tu E, Lam L, Bailey CG, Rasko JE, Allen DG, Semsarian C. Molecular insights from a novel cardiac troponin I mouse model of familial hypertrophic cardiomyopathy. J Mol Cell Cardiol. 2006 Oct;41(4):623-32.

172. Van den Eijnde SM, Luijsterburg AJ, Boshart L, De Zeeuw CI, van Dierendonck JH, Reutelingsperger CP, Vermeij-Keers C. In situ detection of apoptosis during embryogenesis with annexin V: from whole mount to ultrastructure.Cytometry. 1997 Dec 1;29(4):313-20.

173. Van Kerckhoven R, Kalkman EA, Saxena PR, Schoemaker RG: Altered cardiac collagen and associated changes in diastolic function of infarcted rat hearts. Cardiovasc Res. 2000 May;46(2):316-23.

174. Varnava AM, Elliott PM, Baboonian C, Davison F, Davies MJ, McKenna WJ: Hypertrophic cardiomyopathy: histopathological features of sudden death in cardiac troponin T disease. J Am Coll Cardiol. 2000 Jan;35(1):36-44

175. Varnava AM, Elliott PM, Baboonian C, Davison F, Davies MJ, McKenna WJ. Hypertrophic cardiomyopathy: histopathological features of sudden death in cardiac troponin T disease. Circulation. 2001 Sep 18;104(12):1380-4.

176. Venkatraman G, Gomes AV, Kerrick WG, Potter JD.: Characterization of troponin T dilated cardiomyopathy mutations in the fetal troponin isoform.J Biol Chem. 2005 May 6;280(18):17584-92.

177. Venkatraman G, Harada K, Gomes AV, Kerrick WG, Potter JD. Different functional properties of troponin T mutants that cause dilated cardiomyopathy. J Biol Chem. 2003 Oct 24;278(43):41670-6.

178. Villars PS, Hamlin SK, Shaw AD, Kanusky JT: Role of diastole in left ventricular function, I: Biochemical and biomechanical events. Am J Crit Care. 2004 Sep;13(5):394-403; quiz 404-5.

179. Vinogradova MV, Stone DB, Malanina GG, Karatzaferi C, Cooke R, Mendelson RA, Fletterick RJ: Ca(2+)-regulated structural changes in troponin. Proc Natl Acad Sci U S A. 2005 Apr 5;102(14):5038-43.

180. Wakasaki, H, Koya D, Schoen FJ, Jirousek MR, Ways DK, Hoit BD, Walsh RA, and King GL. Targeted overexpression of protein kinase C 2 isoform in myocardium causes cardiomyopathy. Proc Natl Acad Sci USA 94: 9320-9325, 1997

181. Wallis J, Lygate CA, Fischer A, ten Hove M, Schneider JE, Sebag-Montefiore L, Dawson D, Hulbert K, Zhang W, Zhang MH, Watkins H, Clarke K, Neubauer S.: Supranormal myocardial creatine and phosphocreatine concentrations lead to cardiac hypertrophy and heart failure: insights from creatine transporter-overexpressing transgenic mice. Circulation. 2005 Nov 15;112(20):3131-9.

182. Watkins H, McKenna WJ, Thierfelder L, Suk HJ, Anan R, O'Donoghue A, Spirito P, Matsumori A, Moravec CS, Seidman JG, et al: Mutations in the genes for cardiac troponin T and alpha-tropomyosin in hypertrophic cardiomyopathy. N Engl J Med. 1995 Apr 20;332(16):1058-64.

183. Watkins H, Rosenzweig A, Hwang DS, Levi T, McKenna W, Seidman CE, Seidman JG. Characteristics and prognostic implications of myosin missense mutations in familial hypertrophic cardiomyopathy. N Engl J Med. 1992 Apr 23;326(17):1108-14

184. Westfall MV, Lee AM, Robinson DA: Differential contribution of troponin I phosphorylation sites to the endothelin-modulated contractile response. J Biol Chem. 2005 Dec 16;280(50):41324-31.

185. Westfall MV, Metzger JM. Troponin I isoforms and chimeras: tuning the molecular switch of cardiac contraction. News Physiol Sci. 2001 Dec;16:278-8

186. Westfall MV, Rust EM, Metzger JM: Slow skeletal troponin I gene transfer, expression, and myofilament incorporation enhances adult cardiac myocyte contractile function. Proc Natl Acad Sci U S A. 1997 May 13;94(10):5444-9.

187. Wolf CM, Moskowitz IP, Arno S, Branco DM, Semsarian C, Bernstein SA, Peterson M, Maida M, Morley GE, Fishman G, Berul CI, Seidman CE, Seidman JG: Somatic events modify hypertrophic cardiomyopathy pathology and link hypertrophy to arrhythmia. Proc Natl Acad Sci U S A. 2005 Dec 13;102(50):18123-8.

188. Wu H, Wan W, Yang D, Zhang J: Cardiac troponin I mutations in 71 patients with hypertrophic cardiomyopathy. Clin Cardiol 2004, 27 Suppl VI:VI81

189. Yumoto F, Lu QW, Morimoto S, Tanaka H, Kono N, Nagata K, Ojima T, Takahashi-Yanaga F, Miwa Y, Sasaguri T, Nishita K, Tanokura M, Ohtsuki I. Drastic Ca2+ sensitization of myofilament associated with a small structural change in troponin I in inherited restrictive cardiomyopathy. Biochem Biophys Res Commun. 2005 Dec 23;338(3):1519-26.

190. Zakhary DR, Moravec CS, Stewart RW, Bond M. Protein kinase A (PKA)-dependent troponin-I phosphorylation and PKA regulatory subunits are decreased in human dilated cardiomyopathy. Circulation. 1999 Feb 2;99(4):505-10.

191. Zammit PS, Kelly RG, Franco D, Brown N, Moorman AF, Buckingham ME. Suppression of atrial myosin gene expression occurs independently in the left and right ventricles of the developing mouse heart. Dev Dyn. 2000 Jan;217(1):75-

8 Lebenslauf

Persönliche Daten

Name: Jutta Biskup geb. Reher

Geburtstag: 14.12.1972

Geburtsort: Salzgitter

Familie: Ehemann Bernhard Biskup, Diplom-Biologe/Softwareentwickler am Forschungszentrum Jülich

Kinder: Annika Biskup (*2000) und Lilith Biskup (*2002)

Beruflicher und akademischer Werdegang

Seit 06/08: Projektleiterin Medical Writing

bei der IMMEDIS GmbH, Königswinter

12/07 – 05/08: Weiterbildung Klinische Forschung

am mibeg-Institut Medizin, Köln und dem Profil Institut für Stoffwechselforschung, Neuss

03/04 – 10/07: Wissenschaftliche Mitarbeiterin/Doktorandin

am Institut I für Anatomie der Medizinischen Einrichtungen der Universität zu Köln (Direktor: Prof. Dr. med. K. Addicks)

04/99 – 09/05: Gebietsleiterin Vertrieb Home Care (Klinikreferentin)

bei der Caremark Deutschland GmbH, Neufahrn (heute Fresenius Kabi Compounding GmbH), individuell auf den Patienten zugeschnittene parenterale Ernährung und Medikation; aktiv: 04/99–09/00, Elternzeit: 10/00–09/05

1998 und 2006: freiberufliche Übersetzerin vom Englischen ins Deutsche

mehrerer Kapitel des Lehrbuchs „Biology of Plants", Raven, Evert, Eichhorn, 6th and 7th edition, Freeman and Company Publishers, New York

Deutsche Ausgabe: Biologie der Pflanzen, deGruyter-Verlag Berlin, New York

10/92 – 02/99: Studium der Biologie

an der Universität Hannover und der Georg-August-Universität Göttingen,

Titel der Diplomarbeit: „Molekularbiologische Charakterisierung der schweren Clathrinkette aus *Arabidopsis thaliana*" unter der Leitung von Prof. Dr. D. G. Robinson.

Auslandsaufenthalt

08/91 – 07/92: Pasadena City College, Kalifornien, USA

Schulbildung

1984 – 1991: Christian-von-Dohm-Gymnasium Goslar
Abschluss: Abitur

Fremdsprachen

Englisch: verhandlungssicher in Wort und Schrift
Französisch: Schulkenntnisse (7 Jahre)

Softwarekenntnisse

MS Office (Word, Excel, Power Point, Access)
GraphPad
SAS, SPSS (Statistik)
ITEM, ImageJ (morphometrische Bildanalyse)
Data Retrieval Programme (z. B. BLAST, FASTA u. a.)

Eigene Projekte

01/2004 – 06/2004: zur Ermöglichung der Doktorarbeit während der Elternzeit Leitung einer Elterninitiative zur Betreuung von Kindern unter 3 Jahren

Seit 05/06: Aufbau des Fördervereins der kath. Kindertagesstätte St. Vitalis in Köln (Fundraising, Öffentlichkeitsarbeit, soziale und interkulturelle Integration) seit Beginn Vorstandsmitglied